TOTAL SYNTHESIS OF 6,7-DIMETHYL-N-METHYL AZIRIDINOMITOSENE

by

Thaaer N. Muhammed

A thesis

submitted in partial fulfillment

of the requirements for the degree of

Master of Science in Chemistry

Boise State University

May 2018

BOISE STATE UNIVERSITY GRADUATE COLLEGE

DEFENSE COMMITTEE AND FINAL READING APPROVALS

of the thesis submitted by

Thaaer N. Muhammed

Thesis Title: Total Synthesis of 6,7-Dimethyl-N-Methyl Aziridinomitosene

Date of Final Oral Examination: 09 March 2018

The following individuals read and discussed the thesis submitted by student Thaaer N. Muhammed, and they evaluated his presentation and response to questions during the final oral examination. They found that the student passed the final oral examination.

Don Warner, Ph.D.	Chair, Supervisory Committee
Kenneth A. Cornell, Ph.D.	Member, Supervisory Committee
Eric Brown, Ph.D.	Member, Supervisory Committee

The final reading approval of the thesis was granted by Don Warner, Ph.D., Chair of the Supervisory Committee. The thesis was approved by the Graduate College.

DEDICATION

I dedicate this work to my daughter (Zainab) and my family and friends. To all of you that give me hope, encourage, and support. Thanks for always being there for me. I will always appreciate all that you have done.

ACKNOWLEDGEMENTS

I would like to express the deepest appreciation to my committee chair, Dr. Don L. Warner for his time, help, understanding, wisdom, and the opportunity to work on his research project. I would also like to thank the members of my committee, Dr. Ken Cornell and Dr. Eric Brown for their time and support. Further, I would like to thank all of my lab mates for their understanding and constant efforts to help me. I would like to thank all the staff and faculty of the Department of Chemistry and Biochemistry at Boise State University for their constant encouragement and support. Lastly, I would like to thank all my family and my friends, here in Boise, and in Iraq for love and support.

ABSTRACT

Mitomycin C (MC) is a naturally occurring antitumor agent isolated from a soil bacterium. MC is effective against solid hypoxic tumors that respond poorly to radiotherapy, such as colorectal, gastric, and lung tumors. Also, it has a role in the treatment of bladder, head and neck, and non-small cell lung cancers in combination with other chemotherapeutic.

MC and other members of the mitomycin family of antitumor agents fight cancer by forming DNA interstrand crosslinks (ICLs), which leads to apoptosis. In order to form ICLs, MC requires a reductive activation step that produces reactive oxygen species. This activation step is proposed to lead to adverse side effects, such as myelosuppression and hemolytic uremic syndrome. Aziridinomitosenes (AZMs) are structurally related to MC and are believed to form during in vivo reduction of MC. AZMs are relatively stable but are more sensitive than the parent mitomycins due to an activated aziridine ring. Consequently, AZMs do not require the reductive activation step in order to alkylate DNA.

The purpose of this work is to synthesize and study an AZM that is substituted with methyl groups at two potential electrophilic sites. It is hypothesized that certain synthetic AZMs crosslink DNA under non-reductive conditions as a result of a nucleophilic activation sequence involving the quinone ring. To test this hypothesis, analogs were prepared that would either reduce the rate of the activation step or prevent it from occurring. The synthetic route starts with commercially available reagents to form an oxazole, followed by the addition of a protected aldehyde that is converted to the required aziridine

ring via a Mitsunobu reaction. Once the aziridine ring is formed, all of the reaction conditions must be conducted using mild conditions in order to prevent ring-opening.

The completion of the synthesis and formation of the tetracyclic core was achieved by performing an oxazolium salt/azomethine ylide [3+2] cycloaddition sequence. This sequence was conducted multiple times, and the highest yield obtained was 44%. The final steps were the most challenging, requiring several transformations to accomplish a deprotection and oxidation to give a diketone that was oxidized to a quinone. Finally, the carbamate was attached in two steps using FmocNCO to yield the desired AZM product in an overall yield of 0.04% from the starting diol over the 22 step reaction sequence. The stability of the AZM was tested in buffered methanolic solutions, and the results were compared to other aziridinomitosenes. While unsubstituted AZMs decompose in basic solutions, the C6/C7 dimethyl AZM showed high stability under these conditions.

TABLE OF CONTENTS

DEDICATION iv

ACKNOWLEDGEMENTS v

ABSTRACT vi

TABLE OF CONTENTS viii

LIST OF TABLES x

LIST OF FIGURES xi

LIST OF ABBREVIATIONS xvii

CHAPTER ONE: MITOMYCIN C: ISOLATION AND ANTICANCER PROPERTIES 1

Clinical Use of Mitomycin C 2

Mitomycin C and DNA Adducts 3

Proposed Mechanism of DNA Alkylation: Path 1 to ICLs 5

Proposed Mechanism: Path 2 to Form DNA Monoadducts 7

Introduction to Aziridinomitosenes 9

Total Synthesis of Mitomycins and Aziridinomitosenes 11

The Solvolytic Stability of Synthetic Aziridinomitosenes 12

Reactivity and Cytotoxicity of Synthetic Aziridinomitosenes 13

References 18

CHAPTER TWO: TOTAL SYNTHESIS OF A 6,7-DIMETHYL-N-METHYL AZIRIDINOMITOSENE 22

Introduction 22

Previous Syntheses of Aziridinomitosenes 23

Enantiocontrolled Synthesis of Aziridinomitosenes 26

Results and Discussion 29

The Solvolytic Stability of a 6,7-Dimethyl Aziridinomitosene 40

Conclusions 42

Experimental 43

References 65

APPENDIX A 68

^{1}H, ^{13}C NMR Spectra 69

APPENDIX B 110

UV Spectra 111

LIST OF TABLES

Table 2.1. Methanolysis of Aziridinomitosene 1, 3, and 55, at 20 °C. 40

LIST OF FIGURES

Figure 1.1 Structures of Mitomycin C and Poriformycin. 1

Figure 1.2 Structures of DNA adducts resulting from MC treatment. 4

Figure 1.3 Monoalkylated MC-DNA adduct with proposed hydrogen bonding. The monoalkylated [MC] dG adduct involves a covalent bond between C-1 and an amino group on guanine and an intermolecular hydrogen bond between the ester oxygen attached to C-10 and the amino group of another guanine base (G= guanine, C= cytosine). 5

Figure 1.4 Resonance forms of MC in the natural oxidation state. Resonance from B depicts partial withdrawal of electrons from N-4 into the quinone ring. 5

Figure 1.5 Proposed Mechanism of DNA Alkylation: Path 1 to ICLs. Reduction of MC and loss of methanol generates a leuco-aziridinomitosene that bis-alkylates DNA.[17,18] 7

Figure 1.6 Proposed Mechanism of DNA Alkylation: Path 2 to DNA Monoadducts. Oxidation of the leuco-aziridinomitosene generates an AZM that monoalkylates DNA. 8

Figure 1.7 Formation of an AZM from an mitomycin. Hydrogenation of a mitomycin over platinum catalyst at and reoxidation results in an aziridinomitosene.[28] 10

Figure 1.8 Danishefsky's synthesis of an AZM and leuco-aziridinomitosene..... 11

Figure 1.9 Structures of AZMs synthesized and studied by Vedejs. 12

Figure 1.10 Methanolysis of the aziridinomitosenes 19 and 21. 13

Figure 1.11 Proposed mechanism of AZM ICL formation: Path A. Acidic activation of 20 results in aziridine ring-opening and carbamate departure to form an ICL. 16

Figure 1.12 Proposed mechanism of AZM ICL formation: Path B. Nucleophilic addition, by a protein or cellular nucleophile, activates the quinone ring for carbamate departure and ICL or DPC formation. 17

Figure 1.13 The C-6/C-7 dimethyl AZM 35, designed to test the nucleophilic addition mechanism. 18

Figure 2.1 Structures of Synthetic AZMs and MC. AZM 1 is unsubstituted at C-6 and C-7, while 2 has a methyl group at C-6. AZM 3 is the focus of this thesis project. 22

Figure 2.2 AZMs prepared by Rapoport and Edstrom. In both methods, the reduction of the carbonyl at C-10 was problematic. 24

Figure 2.3 The Jimenez and Dong racemic synthesis of an AZM. The first synthesis of an AZM (20) required 16 steps from 2,5-dimethylanisole and gave the final product in 3.4% overall yield. 25

Figure 2.4. Vedejs synthesis of oxazole 22 and amino alcohol 24. 27

Figure 2.5 Vedejs synthesis of tetracyclic precursor. 27

Figure 2.6 Mechanism of the oxazolium salt/azomethine ylide cycloaddition. 28

Figure 2.7 Formation of aziridinomitosene 2. 28

Figure 2.8 Synthesis of oxazole intermediate 35. The compound 35 was prepared in 15% yield over 5 steps from the starting diol. 30

Figure 2.9 Nucleophile addition to aldehyde 38. The amino alcohol 39 is formed in 80% yield as a mixture of six diastereomers in a 6:6:6:1:1:1 ratio..... 32

Figure 2.10 Formation of the deutoro-oxazole to confirm the formation of the intermediate 37..... 33

Figure 2.11 Synthesis of aldehyde 38 from N-Trityl-L-serine methyl ester. 33

Figure 2.12 Synthesis of the cycloaddition precursor 48 in 2.8% overall yield. The sequence required 15 steps from 1,3-propanediol and 10 steps from oxazole 39 (and 19% overall yield). 34

Figure 2.13 Oxazolium salt/azomethine ylide cycloaddition mechanism. 36

Figure 2.14 Oxazolium salt formation process monitored by ^{1}H NMR. The peaks under the blue star, corresponding to the aromatic proton on C-4 (δ=6.89 ppm), started to disappear over the time. The peaks under the red star, corresponding to a new peak at δ=7.46 ppm, began to appear and increase over the reaction time..... 37

Figure 2.15 Formation of diketone 51 in two steps and 48% yield..... 38

Figure 2.16 Final four steps to produce C-6/C-7 dimethyl AZM 3. 39

Figure 2.17 Methanolysis and azridine ring opening of AZMs 1, 3, and 55 in buffered methanol solutions. 41

Figure A1. ^{1}H NMR spectrum of 4-(tert-Butyldimethylsilyloxy)-2, 3-dimethyl-2-butenoic acid ethyl ester (33). 72

Figure A2. ^{13}C NMR of 4-(tert-Butyldimethylsilyloxy)-2, 3-dimethyl-2-butenoic acid ethyl ester (33). 73

Figure A3. ^{1}H NMR spectrum of 4-(tert-Butyldimethylsilyloxy)-2, 3-dimethyl-butyric acid ethyl ester (34). 74

Figure A4. ^{13}C NMR spectrum of 4-(tert-Butyldimethylsilyloxy)-2, 3-dimethyl-butyric acid ethyl ester (34). 75

Figure A5. ^{1}H NMR spectrum of 5-[3-(tert-Butyldimethylsilyloxy)-1,2-dimethylpropyl]-oxazole (35). 76

Figure A6. ^{13}C NMR of 5-[3-(tert-Butyldimethylsilyloxy)-1,2-dimethylpropyl]-oxazole (35). 77

Figure A7. 1H NMR spectrum of 2-[(lR,2S) and (lS,2S)-3-Allyloxy-l-hydroxy-2-tritylaminopropyl)-5-[(1R) and (1S) , (2R) and (2S)- tert-butyldimethylsilyloxy-1,2-dimethylpropyl]oxazole (39) 78

Figure A8. 13C NMR spectrum of 2-[(lR,2S) and (lS,2S)-3-Allyloxy-l-hydroxy-2-tritylaminopropyl)-5-[(1R) and (1S) , (2R) and (2S)- tert-butyldimethylsilyloxy-1,2-dimethylpropyl]oxazole (39) 79

Figure A9. 1H NMR spectrum of 2-[(2S,3R)-3-Allyloxymethyl-1-trityl-aziridin-2-yl]-5-[(1R) and (1S) , (2R) and (2S)- tert-butyldimethylsilyloxy-1,2-dimethylpropyl]oxazole (40) 80

Figure A10. ^{13}C NMR spectrum of 2-[(2S,3R)-3-Allyloxymethyl-1-trityl-aziridin-2-yl]-5-[(1R) and (1S) , (2R) and (2S)- tert-butyldimethylsilyloxy-1,2-dimethylpropyl]oxazole (40) 81

Figure A11. ^{1}H NMR spectrum of 2-[(2S,3R)-3-Allyloxymethylaziridin-2-yl]-5-[(1R) and (1S) , (2R) and (2S)- tert-butyldimethylsilyloxy-1,2-dimethylpropyl]oxazole (41). 82

Figure A12. ^{13}C NMR spectrum of 2-[(2S,3R)-3-Allyloxymethylaziridin-2-yl]-5-[(1R) and (1S) , (2R) and (2S)- tert-butyldimethylsilyloxy-1,2-dimethylpropyl]oxazole (41). 83

Figure A13. ^{1}H NMR spectrum of 2-[(2S,3R)-3-Allyloxymethyl-1-methyaziridin-2-yl]-5-[(1R) and (1S) , (2R) and (2S)- tert-butyldimethylsilyloxy-1,2-dimethylpropyl]oxazole (42). 84

Figure A14. ^{13}C NMR spectrum of 2-[(2S,3R)-3-Allyloxymethyl-1-methyaziridin-2-yl]-5-[(1R) and (1S) , (2R) and (2S)- tert-butyldimethylsilyloxy-1,2-dimethylpropyl]oxazole (42). 85

Figure A15. ^{1}H NMR spectrum of (2S,3R)-2-(5-[(1R) and (1S), (2R) and (2S)-3-tert-butyldimethylsilyloxy-1,2-dimethylpropyl]oxazol-2-yl)-3-hydroxymethyl-1-methylaziridine (43). 86

Figure A16. ^{13}C NMR spectrum of (2S,3R)-2-(5-[(1R) and (1S), (2R) and (2S)-3-tert-butyldimethylsilyloxy-1,2-dimethylpropyl]oxazol-2-yl)-3-hydroxymethyl-1-methylaziridine (43). 87

Figure A17. ^{1}H NMR spectrum of (2S,3R)-2-(5-[(1R) and (1S), (2R) and (2S) -3-tert-butyldimethylsilyloxy-1,2-dimethylpropyl]oxazol-2-yl)-3-iodomethyl-1-methylaziridine (44). 88

Figure A18. ^{13}C NMR spectrum of (2S,3R)-2-(5-[(1R) and (1S), (2R) and (2S) -3-tert-butyldimethylsilyloxy-1,2-dimethylpropyl]oxazol-2-yl)-3-iodomethyl-1-methylaziridine (44). 89

Figure A19. ^{1}H NMR spectrum of (2S,3R)-2-(5-[(1R) and (1S), (2R) and (2S) -3-hydroxy-1,2-dimethylpropyl]oxazol-2-yl)-3-iodomethyl-1-methylaziridine (45). 90

Figure A20. ^{13}C NMR spectrum of (2S,3R)-2-(5-[(1R) and (1S), (2R) and (2S) -3-hydroxy-1,2-dimethylpropyl]oxazol-2-yl)-3-iodomethyl-1-methylaziridine (45). 91

Figure A21. ^{1}H NMR spectrum of 2S,3R)-3-Iodomethyl-1-methyl-2-(5-[(1R) and (1S), (2R) and (2S) -1,2-dimethyl-3-oxopropyl]oxazol-2-yl)aziridine (46). 92

Figure A22. ^{13}C NMR spectrum of 2S,3R)-3-Iodomethyl-1-methyl-2-(5-[(1R) and (1S), (2R) and (2S) -1,2-dimethyl-3-oxopropyl]oxazol-2-yl)aziridine (46). 93

Figure A23. ^{1}H NMR spectrum of (2S,3R)-2-[5-[(1R,2R,3R), (1R,2R,3S), (1R,2S3R) ,((1S,2R,3R), (1S,2S,3S) (1R,2S,3S), (!R,2R,3S),(1S,2S,3R)-3-hydroxy-1,2-dimethyl-6-tert-butyldimethylsilyloxy-4-hexynyl]oxazol-2-yl]-3-iodomethyl-1-methylaziridine (47) 94

Figure A24. ^{13}C NMR spectrum of (2S,3R)-2-[5-[(1R,2R,3R), (1R,2R,3S), (1R,2S3R) ,((1S,2R,3R), (1S,2S,3S) (1R,2S,3S), (!R,2R,3S),(1S,2S,3R)-3-hydroxy-

1,2-dimethyl-6-tert-butyldimethylsilyloxy-4-hexynyl]oxazol-2-yl]-3-iodomethyl-1-methylaziridine (47). 95

Figure A25. ^{1}H NMR spectrum of 2S,3R)-2-[5-[(1R,2R,3R), (1R,2R,3S), (1R,2S3R), ((1S,2R,3R), (1S,2S,3S) (1R,2S,3S), (1R,2R,3S),(1S,2S,3R)-3-Acetoxy-1,2-dimethyl-6-tert-butyldimethylsilyloxy-4-hexynyl]oxazol-2-yl]-3-iodomethyl-1-methylaziridine (48). 96

Figure A26. ^{13}C NMR spectrum of 2S,3R)-2-[5-[(1R,2R,3R), (1R,2R,3S), (1R,2S3R), ((1S,2R,3R), (1S,2S,3S) (1R,2S,3S), (1R,2R,3S),(1S,2S,3R)-3-Acetoxy-1,2-dimethyl-6-tert-butyldimethylsilyloxy-4-hexynyl]oxazol-2-yl]-3-iodomethyl-1-methylaziridine (48). 97

Figure A27. ^{1}H NMR spectrum of (1S,2S, -[(1R,2R,8R), (1R,2R,8S), (1R,2S,8R) ,((1S,2R,8R), (1S,2S,8S) (1R,2S,8S), (1R,2R,8S),(1S,2S,8R)-8-Acetoxy-9-(tert-butyldimethylsilyloxymethyl)-2,3,5,6,7,8-hexahydro-6,7-dimethyl-1,2-(N-methylaziridino)-5-oxo-1H-pyrrolo[1,2-a]indole (49)..... 98

Figure A28. ^{13}C NMR spectrum of (1S,2S, -[(1R,2R,8R), (1R,2R,8S), (1R,2S,8R) ,((1S,2R,8R), (1S,2S,8S) (1R,2S,8S), (1R,2R,8S),(1S,2S,8R)-8-Acetoxy-9-(tert-butyldimethylsilyloxymethyl)-2,3,5,6,7,8-hexahydro-6,7-dimethyl-1,2-(N-methylaziridino)-5-oxo-1H-pyrrolo[1,2-a]indole (49)..... 99

Figure A29. ^{1}H NMR spectrum of (1S,2S,6S,7S) and (1S,2S,6R,7R) (1S,2S,6S,7R) and (1S,2S,6R,7S)-9-(tert-Butyldimethylsilyloxymethyl)-5,8-dioxo-2,3,5,6,7,8-hexahydro-6,7-dimethyl-1,2-(N-methylaziridino)-1H-pyrrolo[1,2-a]indole (51) 100

Figure A30. ^{3}C NMR spectrum of (1S,2S,6S,7S) and (1S,2S,6R,7R) (1S,2S,6S,7R) and (1S,2S,6R,7S)-9-(tert-Butyldimethylsilyloxymethyl)-5,8-dioxo-2,3,5,6,7,8-hexahydro-6,7-dimethyl-1,2-(N-methylaziridino)-1H-pyrrolo[1,2-a]indole (51) 101

Figure A31. ^{1}H NMR spectrum of (1S,2S)-9-(tert-Butyldimethylsilyloxymethyl)-2,3-dihydro-6,7-dimethyl-1,2-(N-methylaziridino)-1H-pyrrolo[1,2-a]indole-5,8-dione (52). 102

Figure A32. ^{13}C NMR spectrum of (1S,2S)-9-(tert-Butyldimethylsilyloxymethyl)-2,3-dihydro-6,7-dimethyl-1,2-(N-methylaziridino)-1H-pyrrolo[1,2-a]indole-5,8-dione (52). 103

Figure A33. ^{1}H NMR spectrum of (1S,2S)-2,3-Dihydro-9-hydroxymethyl-6,7-dimethyl-1,2-(N-methylaziridino)-1H-pyrrolo[1,2-a]indole-5,8-dione (53). 104

Figure A34. ^{13}C NMR spectrum of (1S,2S)-2,3-Dihydro-9-hydroxymethyl-6,7-dimethyl-1,2-(N-methylaziridino)-1H-pyrrolo[1,2-a]indole-5,8-dione (53). 105

Figure A35. ^{1}H NMR spectrum of (1S,2S)-2,3-Dihydro-9-{9-fluorenylmethoxycarbonylcarbamoyloxymethyl)-6,7-dimethyl-1,2-(N-methylaziridino)-1H-pyrrolo[1,2-a]indole-5,8-dione (54)..... 106

Figure A36. ^{13}C NMR spectrum of (1S,2S)-2,3-Dihydro-9-{9-fluorenylmethoxycarbonylcarbamoyloxymethyl)-6,7-dimethyl-1,2-(N-methylaziridino)-1H-pyrrolo[1,2-a]indole-5,8-dione (54)..... 107

Figure A37. ^{1}H NMR spectrum of (1S,2S)-9-Carbamoyloxymethyl-2,3-dihydro-6-methyl-1,2-(N methylaziridino)-1H-pyrrolo[1,2-a]indole-5,8-dione (3).108

Figure A38. ^{13}C NMR spectrum of (1S,2S)-9-Carbamoyloxymethyl-2,3-dihydro-6-methyl-1,2-(N methylaziridino)-1H-pyrrolo[1,2-a]indole-5,8-dione (3).109

Figure B1. UV-Vis spectrum of Methanolysis of AZM 3 at pH 6.0 over 4500 Minutes 112

Figure B2. UV-Vis spectrum of methanolysis of AZM 3 at pH 7.0 over 4500 Minutes 113

Figure B3. UV-Vis absorbance at 480 nm over 4500 minutes (methanolysis of AZM 3 at pH 7.0) 114

Figure B4. UV-Vis spectrum of methanolysis of AZM 3 at pH 8.7 over 300 Minutes 115

LIST OF ABBREVIATIONS

AZM	Aziridinomitosene
Ac_2O	Acetic anhydride
Ac	Acetate
AgOTf	Silver trifluoromethanesulfonate
BH_3·THF	Borane tetrahydrofuran complex solution
CaH_2	Calcium hydride
Cp_2ZrCl_2	Bis(cyclopentadienyl)zirconium(IV) dichloride
$Co(salen)_2$	N,N′-Bis(salicylidene)ethylenediaminocobalt(II) hydrate
DMAP	Dimethylaminopyridine
d	Doublet
dd	Doublet of doublets
DCM	Dichloromethane
DM	Dess-Martin
DNA	Deoxyribonucleic acid
DPC	AZM-DNA-protein adduct
DIBAL	Diisobutylaluminum hydride
DMF	Dimethylformamide
DEAD	Diethyl azodicarboxylate
DABCO	1,4-Diazabicyclo[2.2.2]octane

Et_3N	Triethylamine
Et_3SiH	Triethylsilane
FDA	Food and Drug Administration
Fmoc-NCO	N-(9-Fluorenylmethoxycarbonyl)isocyanate
HCN	Hydrogen cyanide
Hz	Hertz
IR	Infrared radiation
ICL	Interstrand crosslinks
LD_{50}	Lethal dose for 50% of the animal test population
μM	Micromole
μg	Microgram
μL	Microliter
MC	Mitomycin C
MeCN	Acetonitrile
MHz	Megahertz
MeI	Methyl iodide
MeOH	Methanol
min	Minutes
mL	Milliliters
mmol	Millimole
MnO_2	Manganese(IV) oxide
MsCl	Methanesulfonyl chloride
m/z	Mass to charge ratio

NDA	New drug application
$NaBH_4$	Sodium borohydride
NaH	Sodium hydride
NaN_3	Sodium azide
NH_3	Ammonia
NaOEt	Sodium ethoxide
n-BuLi	n-Butyllithium
NaOH	Sodium hydroxide
NMR	Nuclear magnetic resonance
NMO	4-methylmorpholine N-oxide
PCC	Pyridinium chlorochromate
P_2O_5	Phosphorus pentoxide
Ph_3P	Triphenylphosphine
q	Quartet
RT	Room temperature
s	Singlet
t	Triplet
THF	Tetrahydrofuran
Tr	Triphenylmethyl group
TFA	trifluoroacetic acid
TPAP	Tetrapropylammonium perruthenate
TMEDA	Tetramethylethylenediamine
UV-Vis	Ultraviolet–visible spectroscopy

CHAPTER ONE: MITOMYCIN C: ISOLATION AND ANTICANCER PROPERTIES

Mitomycins are a family of natural antibiotic, anticancer agents that were discovered in the 1950s by Hata and coworkers from fermentation cultures of the soil bacterium *Streptomyces caespitosus*.[1] An important member of this family is mitomycin C (Figure 1.1), which was isolated from the fermentation broth of the same bacteria in 1958 by Wakaki and coworkers.[2] The original structure, assigned in 1963 by chemical degradation and spectrophotometric analysis, was shown to contain a unique tetracyclic core with an aziridine ring fused to a pyrrolo[1,2-a] indole system, as well as an aminobenzoquinone.[3] The absolute configuration was revised in 1983 to that shown in Figure 1-1, following studies using X-ray dispersion techniques.[4] The methylated analog of MC was isolated from *Streptomyces verticillatus,* and named poriformycin (**2**, Figure 1.1).[3,5]

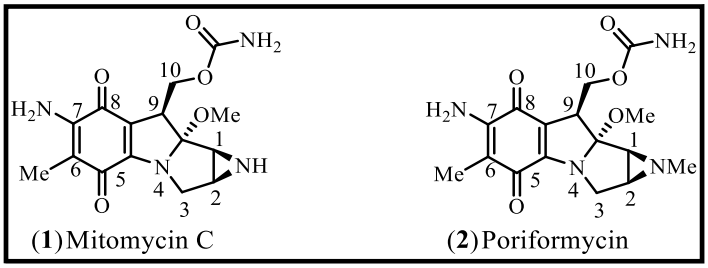

Figure 1.1 Structures of Mitomycin C and Poriformycin.

An early in vivo bioactivity study found that MC has good antitumor activity with an effective dose range between 8-1000 μg/kg, and the LD_{50} values were found to be 5000 μg /kg in mice.[1,2] Also, it was found that hypoxic cancer cells are sensitive to MC at

low doses,[6] while non-hypoxic cancer cells and non-cancerous cells are sensitive at higher doses.[7]

Clinical Use of Mitomycin C

In 1960, MC was introduced into clinical trials in Japan after a case study of 351 patients treated demonstrated a tumor response rate of 37%.[8] In the U.S.A., the drug was approved by the Food and Drug Administration (FDA) in 1974, and the new drug application (NDA) included "usefulness in the treatment of many kind of cancers".[9] MC is effective against hypoxic solid tumors that respond poorly to radiotherapy,[6] and is effective against colorectal, gastric and lung tumors when used in monotherapy.

Historically, MC has a role in the treatment of bladder, head and neck, and non-small-cell lung cancers.[8,10] MC has been shown to covalently bond to complementary DNA strands to form interstrand crosslinks (ICLs), and other adducts, which prevent DNA replication and cause cancer cell death.[11] However, MC requires intracellular enzymatic reduction to activate it in order to covalently bond to DNA.[12]

Bioreduction of MC produces reactive oxygen species that lead to adverse side effects, such as myelosuppression and hemolytic uremic syndrome.[13,14] While these side effects have minimized its clinical use, MC is still active as a single agent in localized treatment of bladder cancer. MC has also found applications in other medicinal fields. It has been used as an antimetabolite therapy in eye surgery to prevent scarring during wound healing, and to promote continuous open filtration to decrease intraocular pressure. In pterygium excision (eliminating the abnormal tissue from the cornea and sclera), MC works as an inhibitor of fibrovascular activity reducing its vascularity, thereby decreasing the risk of recurrent pterygium.[15]

Mitomycin C and DNA Adducts

MC is a very active anticancer and antibacterial agent because of its ability to form MC-DNA adducts, but in order to modify the DNA, reduction steps are required. For example, MC does not react with purified DNA in the absence of reducing enzymes or added one or two electron chemical reductants.[12,13] Evidence indicates that damage to DNA in the tumor cell is generated by mono and bi-functional alkylation of guanine residues by MC, leading to MC-guanine monoadducts **3** and MC-guanine bisadducts; the latter include the DNA interstrand and intrastrand crosslinks **4** and **5** (Figure 1.2).[16]

DNA monoalkylation and crosslinking by MC is very selective for particular DNA sequences. Monoalkylation occurs at 5'-CG-3' sequences approximately five times over other 5'-NG-3' sequences (C= cytosine, G= guanine, N= any base). The covalent bond is formed between MC and the 2-exocyclic amine group on guanine bases, indicating that the DNA adduct is formed in the minor groove of the DNA duplex. While monoalkylation of DNA exhibits a preference for 5'-CG-3' sequences, crosslinking occurs exclusively at this sequence, as demonstrated by the fully characterized crosslinked DNA adduct **4** that was isolated after enzymatic digestion.[17,18] The solution structures of intact DNA duplexes, either monoalkylated or crosslinked by MC, have been solved by the NMR-molecular mechanics method that-include NOE intensity-based refinement. In the case of a crosslinked DNA duplex, the MC residue fits inside the minor groove causing little perturbation of the DNA backbone.[19]

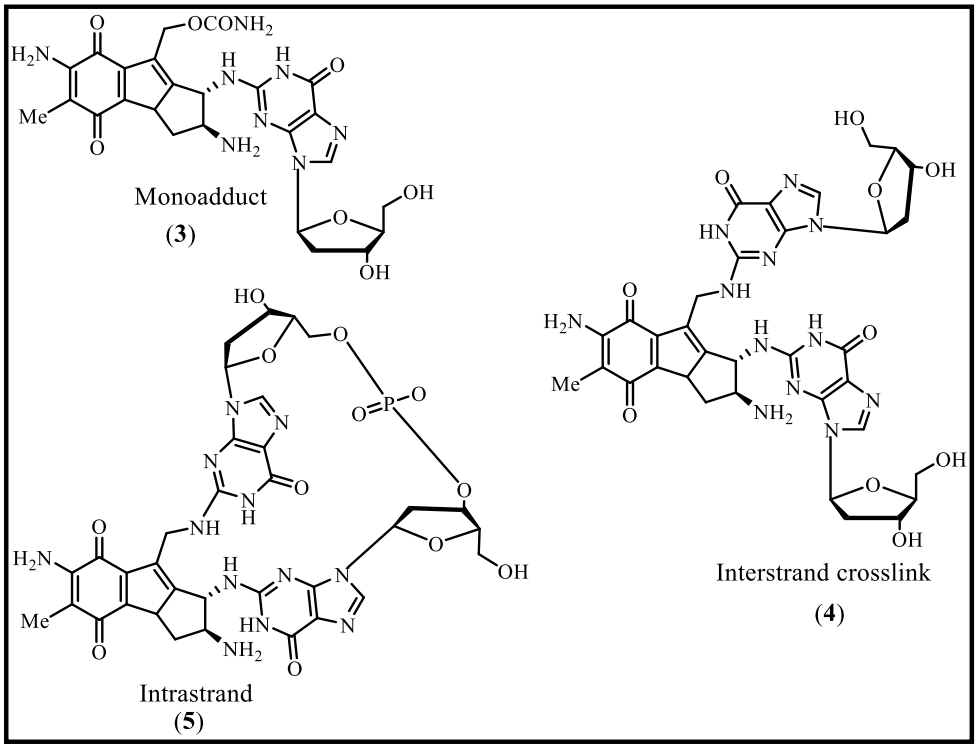

Figure 1.2 Structures of DNA adducts resulting from MC treatment.

The solution structure of the monoadduct indicates a specific alignment of the MC residue in the minor groove of the DNA duplex.[20] The conformation is supported by a hydrogen bond between the oxygen atom at the C-10 of MC and the exocyclic amino group of a guanine base on the strand complementary to the alkylated DNA strand (Figure 1.3). Formation of an analogous hydrogen-bonded pre-covalent complex of an activated form of MC has been suggested to explain the remarkable sequence recognition in the alkylation process.[21]

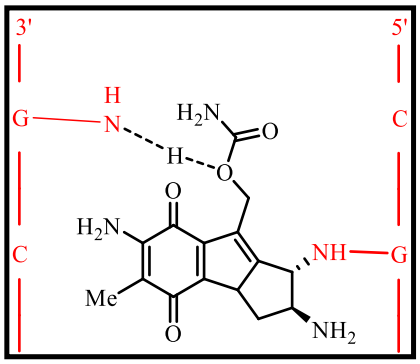

Figure 1.3 Monoalkylated MC-DNA adduct with proposed hydrogen bonding. The monoalkylated [MC] dG adduct involves a covalent bond between C-1 and an amino group on guanine and an intermolecular hydrogen bond between the ester oxygen attached to C-10 and the amino group of another guanine base (G= guanine, C= cytosine).

Proposed Mechanism of DNA Alkylation: Path 1 to ICLs

MC has many reactive groups, including the aziridine ring, the redox active quinone, the carbamate at C-10, and the tertiary methoxy group at C-9a. Typically, aziridine rings are very reactive due to the intrinsic ring strain. However, the aziridine ring in MC, in its natural oxidized form and in moderately alkaline conditions, was found to be unreactive.[22] In contrast, under mildly acidic conditions, aziridine ring-opening is accompanied by subsequent loss of the methoxy group at C-9a.[3,23] The lack of reactivity at neutral pH may be related to the stability of the tertiary methoxy group at C-9a, due to the partial withdrawal of electrons from N-4 into the quinone ring, as represented by the resonance forms shown in Figure 1.4.

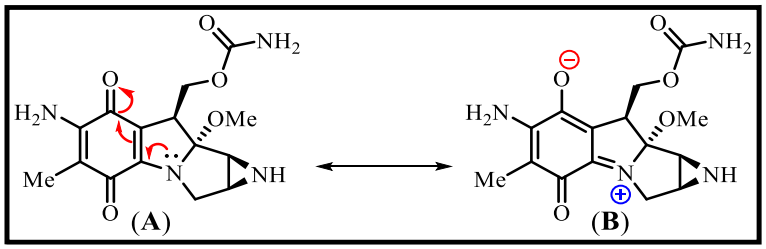

Figure 1.4 Resonance forms of MC in the natural oxidation state. Resonance from **B** depicts partial withdrawal of electrons from N-4 into the quinone ring.

Because of the previously described lack of reactivity, MC does not react with purified DNA unless the reaction mixture is supplemented with some source of chemical or enzymatic reductant.[24] At least five different enzymes have been shown to catalyze the bioreduction of MC in vitro. These enzymes may also be present in solid tumors, including a series of novel mitochondrial reductases such as cytochrome P450 reductase.[23]

The first step in the proposed reductive activation mechanism involves the enzymatic conversion of the quinone moiety in MC to the hydroquinone **6**, as shown in Figure 1.5. The reduced quinone ring loses the capacity to withdraw electrons from N-4, which localizes them on this center. The regaining of electrons and increase in basicity of N-4 starts the remaining chain of events illustrated in Figure 1.5.[9] The lone electron pair on N-4 is able to facilitate the departure of the angular methoxy group. This event affords, after loss of a proton, the intermediate **8**, which is termed a leuco-aziridinomitosene. Compound **8**, with the reactive indolic tetracyclic ring system, acts as the central branch point for two different pathways, monofunctional activation that leads to DNA monoadducts and bifunctional activation that produces the more cytotoxic DNA crosslinks.

The leuco-aziridinomitosene **8** has two “benzylic" electrophile sites, the C-N bond at C-1 and the C-O bond at C-10. Due to the strained aziridine ring, the C-1 site is more reactive. Upon acid catalyzed ring-opening, the resulting carbocation at C-1 is stabilized as a result of conjugation with the aromatic system on **9**. The previously described hydrogen bonding, depicted above in Figure 1.3, situates the cation such that it is readily able to react with DNA to form the monoadduct. Slower expulsion of the carbamate

leaving group at C-10 generates a conjugated iminium ion **9b** that will react with DNA to give the crosslink **10**. Upon exposure to air, the reduced hydroquinone is oxidized to the more stable quinone **11**.[17,18]

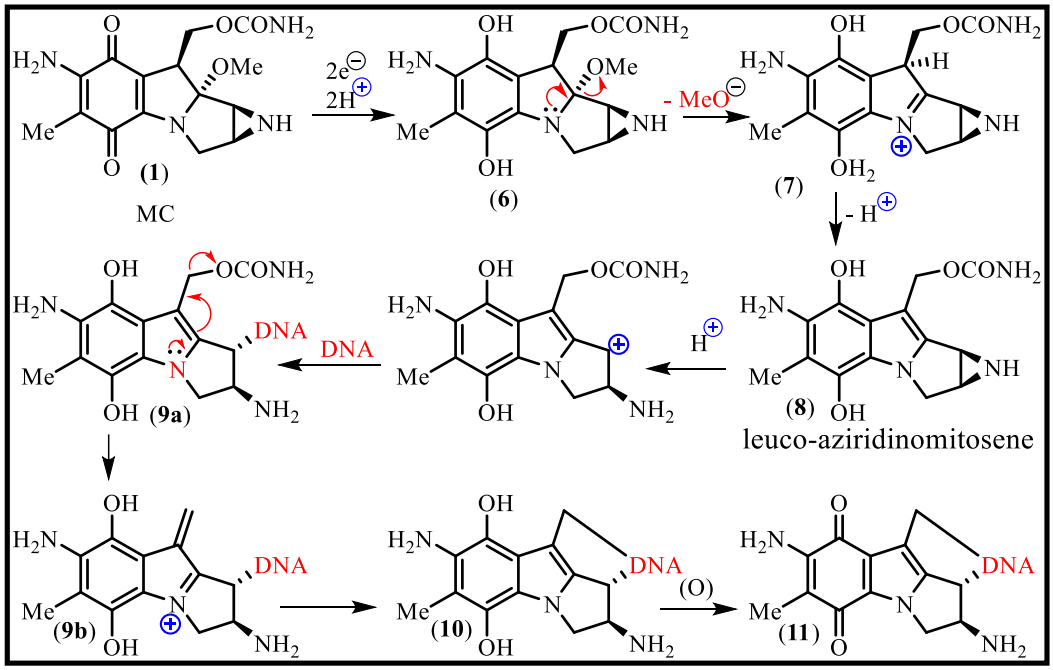

Figure 1.5 Proposed Mechanism of DNA Alkylation: Path 1 to ICLs. Reduction of MC and loss of methanol generates a leuco-aziridinomitosene that bis-alkylates DNA.[17,18]

Proposed Mechanism: Path 2 to Form DNA Monoadducts

The crosslinking of DNA by MC is the most effective way to kill cancer cells. However, forming an ICL is only one example of how MC can bind to DNA. In fact, monoalkylation of DNA is actually 10-20 times more predominant than the lethal DNA crosslink.[25] Furthermore, monoalkylated adducts block DNA polymerases from synthesizing DNA producing moderate cytotoxicity.[26]

In vitro, reaction conditions have been shown to control the extent of alkylation. At higher pH (>7.4), slow reduction or high concentration of MC forms DNA monoadducts preferentially over DNA crosslinks.[17,18,27] Under these conditions, path 2

dominates, and the leuco-aziridinomitosene **8** is rapidly converted to AZM **12 (**Figure 1.6). Structurally, **12** is similar to MC, but has eliminated methanol such that the aziridine ring and the carbamate remain activated. As before, strain associated with the three-membered aziridine ring allows for acid-catalyzed ring opening and subsequent DNA monoalkylation at C-1. Although AZM **12** retains the carbamate at C-10, which is the functional group responsible for the second alkylation step leading to ICL formation with MC, the electron deficient quinone ring prevents its departure due to the resonance effects described earlier and shown in Figure 1.4. Further, enzymatic reduction of the quinone ring, analogous to that required for MC activation, is disfavored due to congestion once bound to DNA in the minor groove.[19,21] Consequently, DNA binding does not proceed beyond the monoalkylation step.

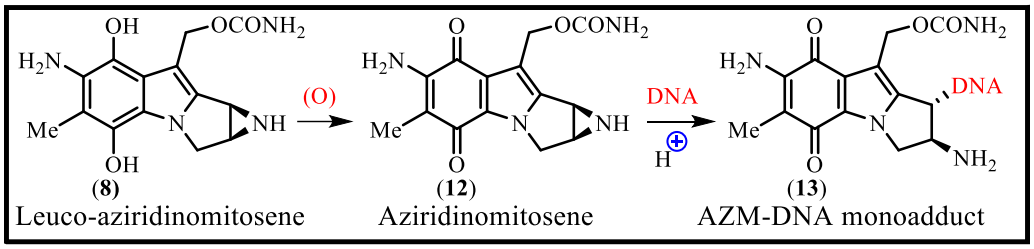

Figure 1.6 Proposed Mechanism of DNA Alkylation: Path 2 to DNA Monoadducts. Oxidation of the leuco-aziridinomitosene generates an AZM that monoalkylates DNA.

Patrick and coworkers were able to isolate degradation products of the parent mitomycins, such as **12**, and reported that they had similar reactivity to the parent mitomycins under reductive conditions.[28] However, they were more sensitive to acid-catalyzed degradation compared to the parent mitomycins, as demonstrated by a half-life of 3 minutes in solution at pH 7.0.[28] Additionally, purified **12** was shown to bind to DNA in vitro and to form the monoadduct **13** without reductive activation, lending support to

the role of path 2 that results in formation of only monoadducts.[29] For crosslinking to occur, carbamate departure via an S_N1 mechanism is required. This reaction is only favorable at the reduced hydroquinone oxidation state, since the electron rich ring system stabilizes the iminium ion intermediate **9b** (from Figure 1.5).[23] For the AZM **12**, an analogous iminium ion is destabilized due to the presence of the strong electron-withdrawing quinone. To restate the proposed mechanistic details, the ring strain associated with the aziridine ring render it susceptible to opening at either the hydroquinone (i.e., **8**) or indoloquinone (AZM **12**) oxidation states. On the other hand, only the reduced form affords a viable pathway for carbamate departure and ensuing DNA crosslinking, which explains why AZMs typically only monoalkyate DNA under non-reductive conditions.

Introduction to Aziridinomitosenes

The reaction mechanism of path 2 involves formation of the intermediate AZM **12**, followed by monoalkylation of with DNA.[17,18,27] Studies with radioactively labeled MC showed that formation of monoadducts occurs 10-20 times more than formation of the crosslink.[25] The monoalkylation of DNA prevent DNA polymerases from synthesizing DNA and has moderate cytotoxicity.[26] Crosslinking is still more potent than the monoadducts. It was found, for example, that an estimated one ICL per 20,000 nucleotide base pairs was sufficient to stop further cell replication.[27]

In 1964, Patrick and coworkers investigated the structure of the mitomycins and found that during hydrogenation of *N*-methylmitomycin A (**14**) over a platinum catalyst at atmospheric pressure in *N*,*N*-dimethylformamide (DMF) solution, one molar equivalent of hydrogen was absorbed.[28] When the resulting colorless solution was

reoxidized with air, a new compound was obtained in up to 40% yield (Figure 1.7). This new compound, named 7-methoxy-1,2-(*N*-methylaziridino)mitosene (**15**), was the first AZM to be isolated. The name "mitosene" was used to reflect the formal elimination of methanol from the "mitosane" of the mytomycin core. A bioassay of the new compound in vitro showed that it was an active antibiotic with a broad spectrum of antibacterial activity similar to the parent mitomycin. In mice, the compound was found to be active by both oral and subcutaneous routes against infections.[28]

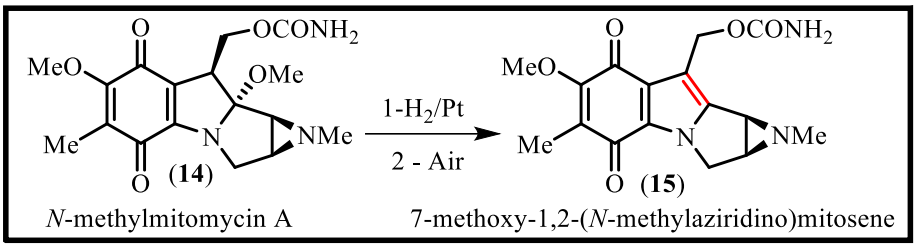

Figure 1.7 Formation of an AZM from an mitomycin. Hydrogenation of a mitomycin over platinum catalyst at and reoxidation results in an aziridinomitosene.[28]

In 1987, Danishefsky and coworkers generated and characterized aziridinomitosene **15** in 90% yield by reacting *N*-methylmitomycin A (**14**) with 0.1 equivalent of ascorbic acid in pyridine. Ascorbic acid acted as a one-electron reducing agent to form the active intermediate (semiquinone radical or radical anion) **16** and **17** (Figure 1.8).[30] With **15** in hand, they were able to prepare the highly reactive leuco-aziridinomitosene **18** by hydrogenation over Pd/C.[31,32]

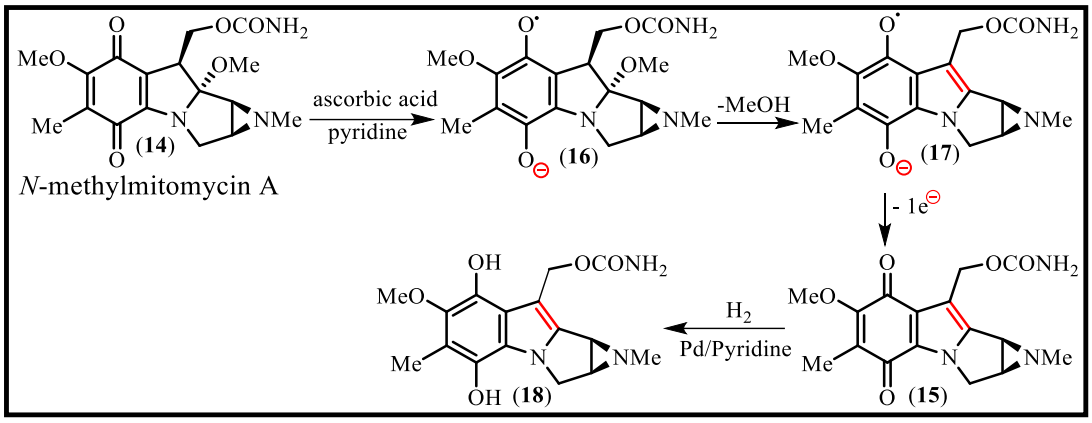

Figure 1.8 Danishefsky's synthesis of an AZM and leuco-aziridinomitosene.

Total Synthesis of Mitomycins and Aziridinomitosenes

There have been a variety of synthetic approaches to the mitomycin and aziridinomitosene skeleton. The majority of the published routes are concerned with the formation of the tricyclic pyrrolo[l,2-a]indole ring system. A few research groups have successfully introduced the carbamate at C-9 and achieved the correct quinone substitution pattern.[33] However, the mitomycins themselves were not synthesized until Kishi and coworkers reported their syntheses of mitomycins A, C, and porfiromycin in 1977. [34] The lack of reported syntheses may be due to difficulties encountered during the introduction of the angular C-9a methoxy group, since this is arguably the most labile functionality present in the mitomycins.[34,35]

A number of aziridinomitosenes have been prepared by reduction of natural mitomycins, followed by reoxidation of the intermediate hydroquinone.[28,30] However, no total synthesis of an aziridinomitosene at the correct oxidation state was reported until 1999, when Jimenez and Dong published their racemic synthesis.[36] The preparation of the fully functionalized aziridinomitosene was accomplished in 16 steps (3.4% overall yield) from 2,5-dimethylanisole. Although the Jimenez/Dong sequence will be discussed in detail in the next chapter, it is worth noting that their route is not amenable to the

formation of single enantiomeric product since the aziridine ring was formed at late stage from an achiral intermediate.

Vedejs and coworkers developed an enantiocontrolled route towards AZM **19** from nonaromatic precursors (Figure 1.19).[37] The Vedejs approach was designed to allow greater potential for variation of substituents at C-6 and C7 than is possible from the natural products. However, the Vedejs aziridinomtiosene **19** lacks substituents at C-6 and C-7, and therefore has additional electrophilic sites compared to the parent mitomycin. The aziridinomitosene **19** and the C-6 methyl analog **20** relied on an azomethine ylide cycloaddition sequence to construct the tetracyclic core. Overall, the two compounds were prepared in 2.9% overall yield, in a longest linear sequence of 20 steps starting from L-serine methyl ester hydrochloride.[38] The Vedejs work is directly relevant to the synthesis of the aziridinomitosene described in the next chapter.

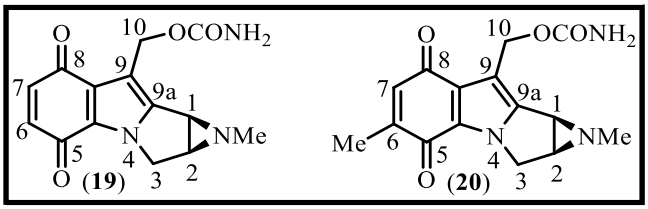

Figure 1.9 Structures of AZMs synthesized and studied by Vedejs.

The Solvolytic Stability of Synthetic Aziridinomitosenes

The solvolytic stability of AZM **19** and other analogues were evaluated in methanolic solutions buffered with the Tris and Bis-Tris amine hydrochlorides (Figure 1.10).[38] The process was monitored by UV spectroscopy and compared with results obtained by Kohn and Han for the methanolysis of AZM **21** under similar conditions.[39] At pH 7.0, the results showed that methanolysis of AZM **19** is 160 times slower than **21**. Electron donation from the amino group on C-7 of **21** into the quinone π-system may

explain the increased reactivity. The C-7 amine presumably provides additional stabilization of the carbocation **25** that is formed upon S_N1 aziridine ring-opening. Carbocation **24** lacks a comparable electron-donating group, which affords aziridinomitosene **19** increased stability under acidic conditions, compared to **21**.

Under basic conditions, **21** was more stable than **19**. In fact, **19** rapidly decomposes to unidentifiable products in methanolic solutions buffered at pH 8.5. It appears that the lack of functionalization at C-6 and C-7 enables nucleophilic attack at one or both of these sites, initiating a process that leads to decomposition. AZM **21** has a methyl at C-6 and an amine at C-7, rendering these sites unreactive to nucleophiles. The methanolysis of **19** was also conducted under acidic conditions, at pH 5.8, and the ring-opened **26** was obtained in 41% yield as a 1:1.2 mixture of the cis/trans isomers.

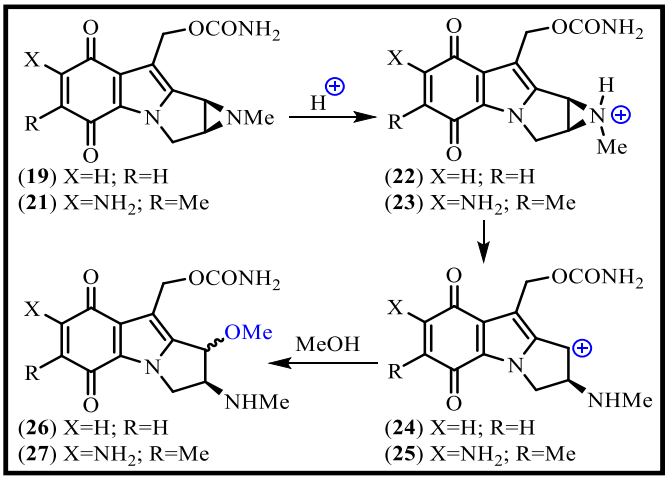

Figure 1.10 Methanolysis of the aziridinomitosenes 19 and 21.

Reactivity and Cytotoxicity of Synthetic Aziridinomitosenes

ICLs are the primary adducts formation that stop cancer cells from further replication.[40,41] AZM-DNA crosslinking experiments have been evaluated in vitro, and the adducts characterized. The results showed that under hypoxic conditions in the

presence of reducing agents, DNA crosslinking of the AZM and the parent mitomycin are consistent and both are selective to 5'-d(CG) sequences.[42,43]

The ability of the synthetic AZM **19** to modify DNA was evaluated under nonreductive conditions using the BstNI-EcoRI 129-bp fragment from pBR322 plasmid that was 3' end-labeled with ^{32}P.[38] The site of DNA modification was determined using the UvrABC nuclease assay, and it was found that AZM **19** modified DNA at guanine residues. Also, increased incubation times gave a greater percentage of DNA adducts.[38]

The ability of AZM **19** to crosslink specific DNA sequences under aerobic, nonreductive reaction conditions was tested and reported by using self-complimentary 14-base pair sequences.[44] The results confirmed that AZM **19** produced AZM-DNA interstrand crosslinks only in duplex DNA having the sequence 5'-d(CG). Also, no ICL formation was observed with the inverted 5'-d(GC) dinucleotide sequence. The reaction between DNA and AZM **19** was found to be pH-dependent, with the highest yield of ICL observed at pH∼6.1, which indicates that moderate acid catalysis enhances DNA modification. This data was the first evidence of sequence-specific DNA interstrand crosslinking by an aziridinomitosene without prior activation by a reducing agent.

Warner and coworkers reported that the synthetic AZMs **19** and **20** were able to form DNA crosslinks and DNA-protein adducts (DPCs) in Jurkat and HeLa cancer cells after one hour of treatment in an aerobic environment.[45] Cytotoxicity assays showed that **20** was up to 72 and 520 times more potent than MC and **19**, respectively, against a variety of adherent and non-adherent cancer cell lines. The IC_{50} values for MC and **19** were typically in the low micromolar range, and in the sub-micromolar range for **20**.

The greater potency of **20** over MC may be due to a variety of chemical features. First, the presence of the methyl group at C-6 will render **20** less susceptible than **19** to Michael addition to the quinone ring, which should result in prolonged half-life within the cell. Second, lack of a hydrophilic amine group at C-7 should allow for more facile diffusion into cell. Third, the presence of the methyl group on the aziridine ring adds additional stability in slightly acidic and neutral environments. All three of these factors may improve the electrophilic integrity of the Me-AZM **20** and stabilize the molecule for productive reactions with cellular nucleophiles. Finally, AZM **19** is more reactive under basic/nucleophilic conditions and this may account for its decreased potency. This is because the two electrophiles on C-6 and C-7 are very reactive to nucleophilic addition that will give **19** a shorter half-life comparing with **20**.[45]

While the mechanism of ICL and DPC formation by **19** and **20** is not completely understood, Warner and coworkers have proposed two potential mechanisms involving either acidic (Path A) or nucleophilic (Path B) activation that result in the formation of crosslinks and/or DNA-protein adducts in tumor cells and in purified DNA. As shown in Figure 1.11, Path A involves acidic ring-opening of the aziridine ring to produce a relatively stable benzylic carbocation that is captured by nucleophilic DNA in the minor groove to form monoadduct **29**. Next, a slow, acid catalyzed carbamate cleavage sequence forms an iminium intermediate that undergoes a second nucleophilic addition that forms the ICL **31**. Path A is consistent with the observation that **19** or **20** gives an optimum yield of DNA ICLs in moderately acidic conditions (pH 6).[44] Also, the methyl group at the C-6 carbon on **20** is a mild electron donor that provides additional stabilization to the cations formed upon aziridine ring-opening and carbamate departure.

This enhanced stability may account for the increased activity of **20**, compared to **19**, against the cancer cell lines tested.

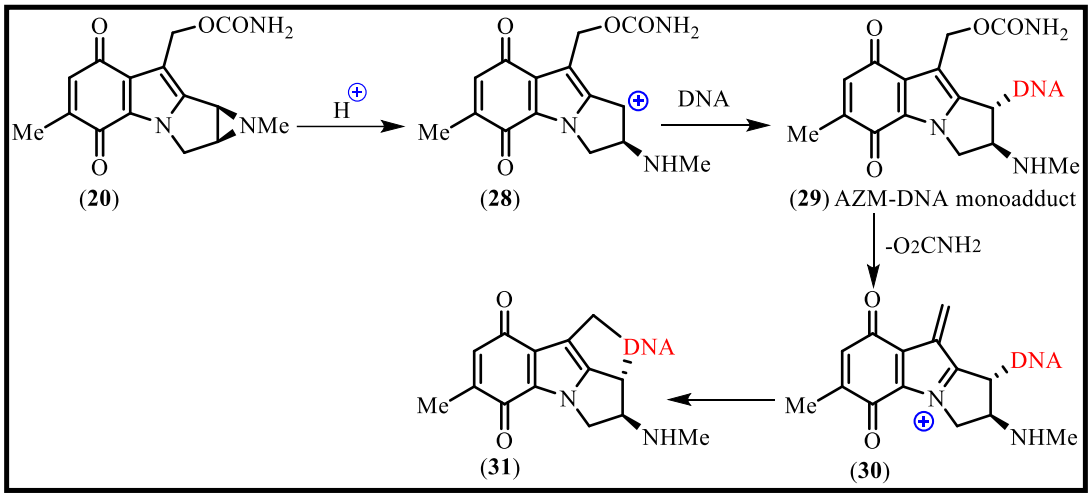

Figure 1.11 Proposed mechanism of AZM ICL formation: Path A. Acidic activation of **20** results in aziridine ring-opening and carbamate departure to form an ICL.

The proposed mechanism that invokes a nucleophilic activation sequence (Path B, Figure 1.12) also relies upon acid catalyzed aziridine ring-opening to form the DNA-monoadduct **29** as the first step. Next, nucleophilic addition to C-7 by a DNA-associated protein or other cellular nucleophile will result in an intermediate **32** that can tautomerize to the hydroquinone species **33**. This intermediate is analogous to the previously described leuco-aziridinomitosene, from Figure 1.5, that has sufficient electron density to allow carbamate departure and crosslink formation. Compared to the acidic activation sequence, the nucleophilic mechanism has the advantage of explaining the formation of DNA-protein adducts. Additionally, this mechanism offers an explanation as to why **19** isn't as active against cancer cells as **20**. On aziridinomitosene **19**, there are two sites for nucleophilic addition (C-6 and C-7), whereas **20** has only one site (C-6). Consequently, **19** is more accessible to nucleophilic attack that occurs prior to DNA alkylation, which results in aziridinomitosene decomposition before cell-killing events. The methyl group

at C-6 on **20** prevents nucleophilic attack at that carbon and offers moderate steric hindrance that slows attack at C-7. Together, these things are proposed to allow **20** to alkylate DNA with minimal prior decomposition.[45]

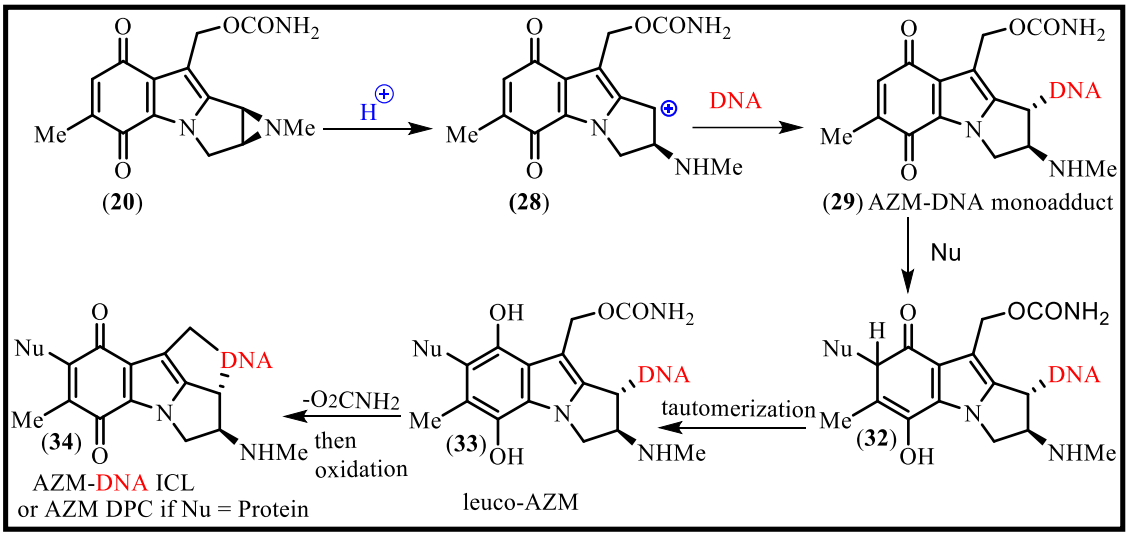

Figure 1.12 Proposed mechanism of AZM ICL formation: Path B. Nucleophilic addition, by a protein or cellular nucleophile, activates the quinone ring for carbamate departure and ICL or DPC formation.

To test the validity of the two proposed mechanisms, a new AZM, compound **35**, that has methyl groups at both C-6 and C-7 needs to be constructed. If the acidic activation sequence predominates, then the new aziridinomitosene **35** is expected to form DNA crosslinks to a greater extent than both compounds **19** and **20**. If the nucleophilic mechanism is most important, then the new compound would not exhibit crosslinking to any extent since both C-6 and C-7 would no longer be available to cellular and other nucleophiles. Also, we expect that in acidic conditions the aziridine ring on **35** should open faster than **19** and **20** since the methyl groups on C-6 and C-7 will stabilize the carbocation on C-1. In basic/nucleophilic conditions, we expect that **35** will be more stable than **19** and **20** because the methyl groups at C-6 and C-7 will prevent nucleophilic attack, which will prevent formation of **33**. Thus, the focus of this thesis project is to

complete the synthesis of aziridinomitosene **35** and to conduct preliminary experiments to explore its reactivity. Results of these efforts are described in the next chapter.

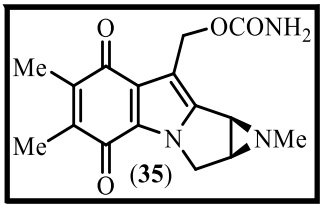

Figure 1.13 The C-6/C-7 dimethyl AZM 35, designed to test the nucleophilic addition mechanism.

References

1-Hata, T., Sano, Y., Sugawara, R., Matsumate, A., Kanamori, K., Shima, T., and Hoshi, T. (1956). Mitomycin, a new antibiotic from Streptomyces. I. The Journal of Antibiotics, 9(4), 141-146.

2-Wakaki, S., Marumo, H., Tomioka, K., Shimizu, G., Kato, E., Kamada, H., and Fujimoto, Y. (1958). Isolation of new fractions of antitumor mitomycins. Antibiotics and Chemotherapy, 8(5), 228-240.

3-Webb, J. S., Cosulich, D. B., Mowat, J. H., Patrick, J. B., Broschard, R. W., Meyer, W. E., and Lancaster, J. E. (1962). The Structures of Mitomycins A, B and C and Porfiromycin--Part I. Journal of the American Chemical Society, 84(16), 3185-3187. Webb, J. S., Cosulich, D. B., Mowat, J. H., Patrick, J. B., Lancaster, J. E., Broschard, R. W., and Pidackas, C. (1962). The Structures of Mitomycins A, B, and C and Porfiromycin--Part II. Journal of the American Chemical Society, 84(16), 3187-3188.

4-Shirahata, K. and Hirayama, N. (1983). Revised absolute configuration of mitomycin C. X-ray analysis of 1-N-(p-bromobenzoyl) mitomycin C. Journal of the American Chemical Society, 105(24), 7199-7200.

5-Lefemine, D. V., Dann, M., Barbatschi, F., Hausmann, W. K., Zbinovsky, V., Monnikendam, P., and Bohonos, N. (1962). Isolation and characterization mitiromycin and other antibiotics. Journal of the American Chemical Society, 84(16), 3184-3185.

6-Kennedy, K. A., Teicher, B. A., Rockwell, S., and Sartorelli, A. C. (1980). The hypoxic tumor cell: a target for selective cancer chemotherapy. Biochemical Pharmacology, 29(1), 1-8.

7-Kennedy, K. A., Rockwell, S., and Sartorelli, A. C. (1980). Preferential activation of mitomycin C to cytotoxic metabolites by hypoxic tumor cells. Cancer Research, 40(7), 2356-2360.

8-Frank, W. and Osterberg, A. E. (1960). Mitomycin C (NSC-26980)--an evaluation of the Japanese reports. Cancer Chemotherapy Reports, 9, 114.

9-Bradner, W. T. (2001). Mitomycin C: a clinical update. Cancer Treatment Reviews, 27(1), 35-50.

10-Ross, D., Beall, H., Traver, R. D., Siegel, D., Phillips, R. M., and Gibson, N. W. (1994). Bioactivation of quinones by DT-diaphorase, molecular, biochemical, and chemical studies. Oncology Research Featuring Preclinical and Clinical Cancer Therapeutics, 6(10-11), 493-500.

11-Tomasz, M. (1995). Mitomycin C: small, fast and deadly (but very selective). Chemistry and Biology, 2(9), 575-579.

12-Szybalski, W. and Iyer, V. N. (1964). Crosslinking of DNA by enzymatically or chemically activated mitomycins and porfiromycins, bifunctionally "alkylating" antibiotics. Federation Proceedings (23), 946-957.

13-Verweij, J. and Stoter, G. (1987). Severe side effects of the cytotoxic drug mitomycin-C. The Netherlands Journal of Medicine, 30(1-2), 43-50.

14-El-Ghazal, R., Podoltsev, N., Marks, P., Chu, E., and Saif, M. W. (2011). Mitomycin-C-induced thrombotic thrombocytopenic purpura/hemolytic uremic syndrome: cumulative toxicity of an old drug in a new era. Clinical Colorectal Cancer, 10(2), 142-145.

15-Radke, P. M., Bitrian, E., Kaufman, S. C., and Grajewski, A. L. (2016). A Review of mitomycin use in ophthalmic surgery: Clarification of safety standards for patients and hospital personnel. Current Ophthalmology Reports, 4(4), 187-197.

16-Paz, M. M., Das, A., and Tomasz, M. (1999). Mitomycin C linked to DNA minor groove binding agents: synthesis, reductive activation, DNA binding and cross-linking properties and in vitro antitumor activity. Bioorganic and Medicinal Chemistry, 7(12), 2713-2726.

17-Tomasz, M., Lipman, R., Chowdary, D., Pawlak, J., Verdine, G. L., and Nakanishi, K. (1987). Isolation and structure of a covalent cross-link adduct between mitomycin C and DNA. Science, 235(4793), 1204-1208.

18-Tomasz, M. and Palom, Y. (1997). The mitomycin bioreductive antitumor agents: cross-linking and alkylation of DNA as the molecular basis of their activity. Pharmacology and Therapeutics, 76(1-3), 73-87.

19-Norman, D., Live, D., Sastry, M., Lipman, R., Hingerty, B. E., Tomasz, M., and Patel, D. J. (1990). NMR and computational characterization of mitomycin cross-linked to adjacent deoxyguanosines in the minor groove of the d(T-A-C-G-T-A).cntdot.d(T-A-C-G-T-A) duplex. Biochemistry, 29(11), 2861-2875.

20-Sastry, M., Fiala, R., Lipman, R., Tomasz, M., and Patel, D. J. (1995). Solution structure of the monoalkylated mitomycin C-DNA complex. Journal of Molecular Biology, 247(2), 338-359.

21-Li, V. S., Choi, D., Wang, Z., Jimenez, L. S., Tang, M. S., and Kohn, H. (1996). Role of the C-10 substituent in mitomycin C-1-DNA bonding. Journal of the American Chemical Society, 118(10), 2326-2331.

22-Schwartz, H. S., Sodergren, J. E., and Philips, F. S. (1963). Mitomycin C: chemical and biological studies on alkylation. Science, 142(3596), 1181-1183.

23-Cummings, J., Spanswick, V. J., Tomasz, M., and Smyth, J. F. (1998). Enzymology of mitomycin C metabolic activation in tumour tissue: implications for enzyme-directed bioreductive drug development. Biochemical Pharmacology, 56(4), 405-414.`

24-Iyer, V. N. and Szybalski, W. (1964). Mitomycins and porfiromycin: chemical mechanism of activation and cross-linking of DNA. Science, 145(3627), 55-58.

25-Weissbach, A. and Lisio, A. (1965). Alkylation of nucleic acids by mitomycin C and porfiromycin. Biochemistry, 4(2), 196-200.

26-Basu, A. K., Hanrahan, C. J., Malia, S. A., Kumar, S., Bizanek, R., and Tomasz, M. (1993). Effect of site specifically located mitomycin C-DNA monoadducts on in vitro DNA synthesis by DNA polymerases. Biochemistry, 32(18), 4708-4718.

27-Iyer, V. N. and Szybalski, W. (1963). A molecular mechanism of mitomycin action: linking of complementary DNA strands. Proceedings of the National Academy of Sciences, 50(2), 355-362.

28-Patrick, J. B., Williams, R. P., Meyer, W. E., Fulmor, W., Cosulich, D. B., Broschard, R. W., and Webb, J. S. (1964). Aziridinomitosenes: A new class of antibiotics related to the mitomycins. Journal of the American Chemical Society, 86(9), 1889-1890.

29-Li, V. S., Choi, D., Tang, M. S., and Kohn, H. (1996). Concerning in vitro mitomycin-DNA alkylation. Journal of the American Chemical Society, 118(15), 3765-3766.

30-Danishefsky, S. J. and Egbertson, M. (1986). The characterization of intermediates in the mitomycin activation cascade: a practical synthesis of an aziridinomitosene. Journal of the American Chemical Society, 108(15), 4648-4650.

31-Egbertson, M. and Danishefsky, S. J. (1987). Modeling of the electrophilic activation of mitomycins: chemical evidence for the intermediacy of a mitosene semiquinone as the active electrophile. Journal of the American Chemical Society, 109(7), 2204-2205.

32-Cera, C., Egbertson, M., Teng, S. P., Crothers, D. M., and Danishefsky, S. J. (1989). DNA cross-linking by intermediates in the mitomycin activation cascade. Biochemistry, 28(13), 5665-5669.

33-Siuta, G. P., Franck, R. W., and Kempton, R. P. (1974). Mitomycin synthesis. The Journal of Organic Chemistry, 39(25), 3739-3744.

34-Nakatsubo, F., Cocuzza, A. J., Keeley, D. E., and Kishi, Y. (1977). Synthetic studies toward mitomycins. 1. Total synthesis of deiminomitomycin A. Journal of the American Chemical Society, 99(14), 4835-4836.

35- Fukuyama, T., Nakatsubo, F., Cocuzza, A. J., and Kishi, Y. (1977). Synthetiic studies toward mitomycins. III. Total syntheses of mitomycins A and C. Tetrahedron Letters, 18(49), 4295-4298.

36-Dong, W. and Jimenez, L. S. (1999). Synthesis of a Fully Functionalized 7-Methoxyaziridinomitosene. The Journal of Organic Chemistry, 64(7), 2520-2523.

37-Vedejs, E., Klapars, A., Naidu, B. N., Piotrowski, D. W., and Tucci, F. C. (2000). Enantiocontrolled synthesis of (1 S, 2 S)-6-desmethyl-(methylaziridino) mitosene. Journal of the American Chemical Society, 122(22), 5401-5402.

38-Vedejs, E., Naidu, B. N., Klapars, A., Warner, D. L., Li, V. S., Na, Y., and Kohn, H. (2003). Synthetic enantiopure aziridinomitosenes: preparation, reactivity, and DNA alkylation studies. Journal of the American Chemical Society, 125(51), 15796-15806.

39-Han, I. and Kohn, H. (1991). 7-Aminoaziridinomitosenes: synthesis, structure, and chemistry. The Journal of Organic Chemistry, 56(15), 4648-4653.

40-Palom, Y., Suresh Kumar, G., Tang, L. Q., Paz, M. M., Musser, S. M., Rockwell, S., and Tomasz, M. (2002). Relative toxicities of DNA cross-links and monoadducts: new insights from studies of decarbamoyl mitomycin C and mitomycin C. Chemical Research in Toxicology, 15(11), 1398-1406.

41-Suresh Kumar, G., Lipman, R., Cummings, J., and Tomasz, M. (1997). Mitomycin C− DNA adducts generated by DT-diaphorase. Revised mechanism of the enzymatic reductive activation of mitomycin C. Biochemistry, 36(46), 14128-14136.

42-Teng, S. P., Woodson, S. A., and Crothers, D. M. (1989). DNA sequence specificity of mitomycin cross-linking. Biochemistry, 28(9), 3901-3907.

43- Kohn, H., Li, V. S., and Tang, M. S. (1992). Recognition of mitomycin C-DNA monoadducts by UVRABC nuclease. Journal of the American Chemical Society, 114(14), 5501-5509.

44-Rink, S. M., Warner, D. L., Klapars, A., and Vedejs, E. (2005). Sequence-specific DNA interstrand cross-linking by an aziridinomitosene in the absence of exogenous reductant. Biochemistry, 44(42), 13981-13986.

45-Mallory, C. M., Carfi, R. P., Moon, S., Cornell, K. A., and Warner, D. L. (2015). Modification of cellular DNA by synthetic aziridinomitosenes. Bioorganic and Medicinal Chemistry, 23(23), 7378-7385.

CHAPTER TWO: TOTAL SYNTHESIS OF A 6,7-DIMETHYL-N-METHYL AZIRIDINOMITOSENE

Introduction

Recent efforts in the Warner laboratory have focused on the biological evaluation of synthetic aziridinomitosenes (AZMs) that are structurally related to MC. Two of these, AZMs **1** and **2** (Figure 2-1) were evaluated for their cytotoxic activity against cancer cells, and tested for their DNA-modifying abilities in Jurkat cells.[1] The study showed that **2** is at least 2.75 and 5.5 fold more potent than MC and **1**, respectively; and is up to 72 and 520 times more potent, against a variety of cancer cell lines. Also, evidence for the formation of interstrand crosslinks (ICLs) and DNA-protein crosslinks (DPCs) in cellular systems was obtained using a modified alkaline single cell gel electrophoresis (COMET) assay and a K-SDS DNA-protein crosslinking assay. These results support that modification of DNA by AZMs **1** and **2** is a potential mechanism of their cytotoxicity.

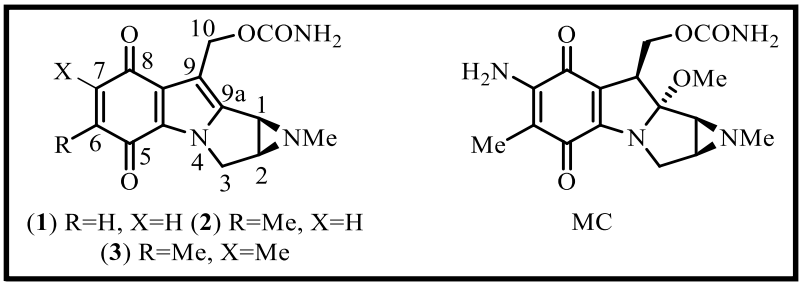

Figure 2.1 Structures of Synthetic AZMs and MC. AZM **1** is unsubstituted at C-6 and C-7, while **2** has a methyl group at C-6. AZM **3** is the focus of this thesis project.

Two potential mechanisms were proposed to explain the formation of ICLs and DPCs in reactions with DNA, one involving acidic activation and the other nucleophilic

activation. The nucleophilic mechanism, which is most consistent with the observed data, invokes addition of a nucleophile at the unsubstituted C-6 or C-7 sites as the key step leading to ICLs and DPCs. To test the validity of this hypothesis, the focus of the research described herein involves the synthesis of the new AZM **3** (Figure 2.1) where both sites are blocked to prevent nucleophilic attack. AZM **3** retains the reactive aziridine ring at C-1 and carbamate at C-10, as well as the indoloquinone group present in other AZMs. The new AZM is hypothesized to either reduce the extent of ICL and DPC formation, or prevent them from forming in the first place, under non-reductive conditions. This chapter first presents prior syntheses of AZMs in order to place this work in context, and then describes the synthesis of AZM **3**, along with preliminary results investigating the new compound's activity in methanolic buffered solutions at different pH values.

Previous Syntheses of Aziridinomitosenes

Since the isolation of mitomycins and AZMs over 60 years ago,[2,3] much attention has been devoted to the study and synthesis of these compounds, primarily due to their unique tetracyclic structure and high cytotoxicity. The total syntheses of mitomycin A, C, and porfiromycin was achieved in 1977 by Fukuyama and Kishi.[4] While there have been many attempts at the total synthesis of AZMs, very few researchers have succeeded. In 1985, Rapoport and coworkers reported an asymmetric synthesis of the AZM-type compound **4** (Figure 2.2).[5] Notably, the reduction of the carbonyl at C-10 was problematic, which prohibited installation of the essential carbamate group. Also, removal of the benzyl protecting group from the nitrogen of the strained aziridine ring could not be accomplished.

To understand the mode of action for MC and related agents, Edstrom and co-workers reported their synthesis of analog **6** (Figure 2.2).[6] The synthesis involved the conversion of tricyclic compound **5** to the final tetracyclic product **6**. The compound contains the indoloquinone, an N-H aziridine ring, a methyl group at C-6, and the appropriate amine functionalization at C-7. However, Edstrom's final product contained an ester moiety at C-10, the same group that was problematic in Rapoport's synthesis. As before, the carboxyl could not be reduced and Edstrom's final compound lacked the reactive carbamate required for DNA ICL formation.

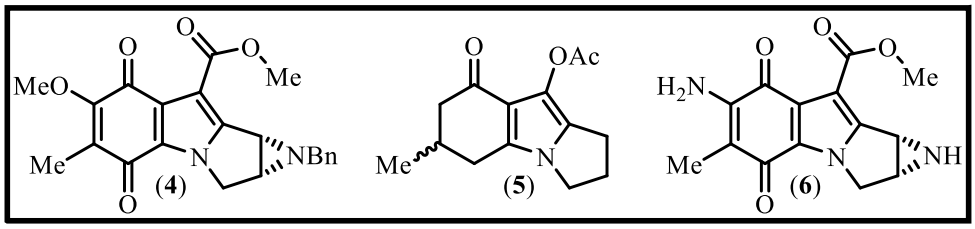

Figure 2.2 AZMs prepared by Rapoport and Edstrom. In both methods, the reduction of the carbonyl at C-10 was problematic.

The total synthesis of a fully functionalized aziridinomitosene, at the correct oxidation state at all carbons, continued to be unsuccessful until 1999 when Jimenez and Dong report their racemic synthesis of AZM **20** (Figure 2.3).[7] The Jimenez AZM is fully functionalized, including the N-H aziridine ring and the carbamate functional group at C-10. Starting from 2,5-dimethyl anisole, the synthesis required 16 steps and produced the final product in 3.4% overall yield.

In the first step, 2,5-dimethylanisole was nitrated on a 50 g scale with sodium nitrite in trifluoroacetic acid to prepare **7** (Figure 2.3). The α-keto ester **8** was prepared in a 63% yield from **7**, using dimethyl oxalate and potassium tert-butoxide. Reaction of **8** with 3 equivalents of stannous chloride in methanol resulted in a 60% yield of the

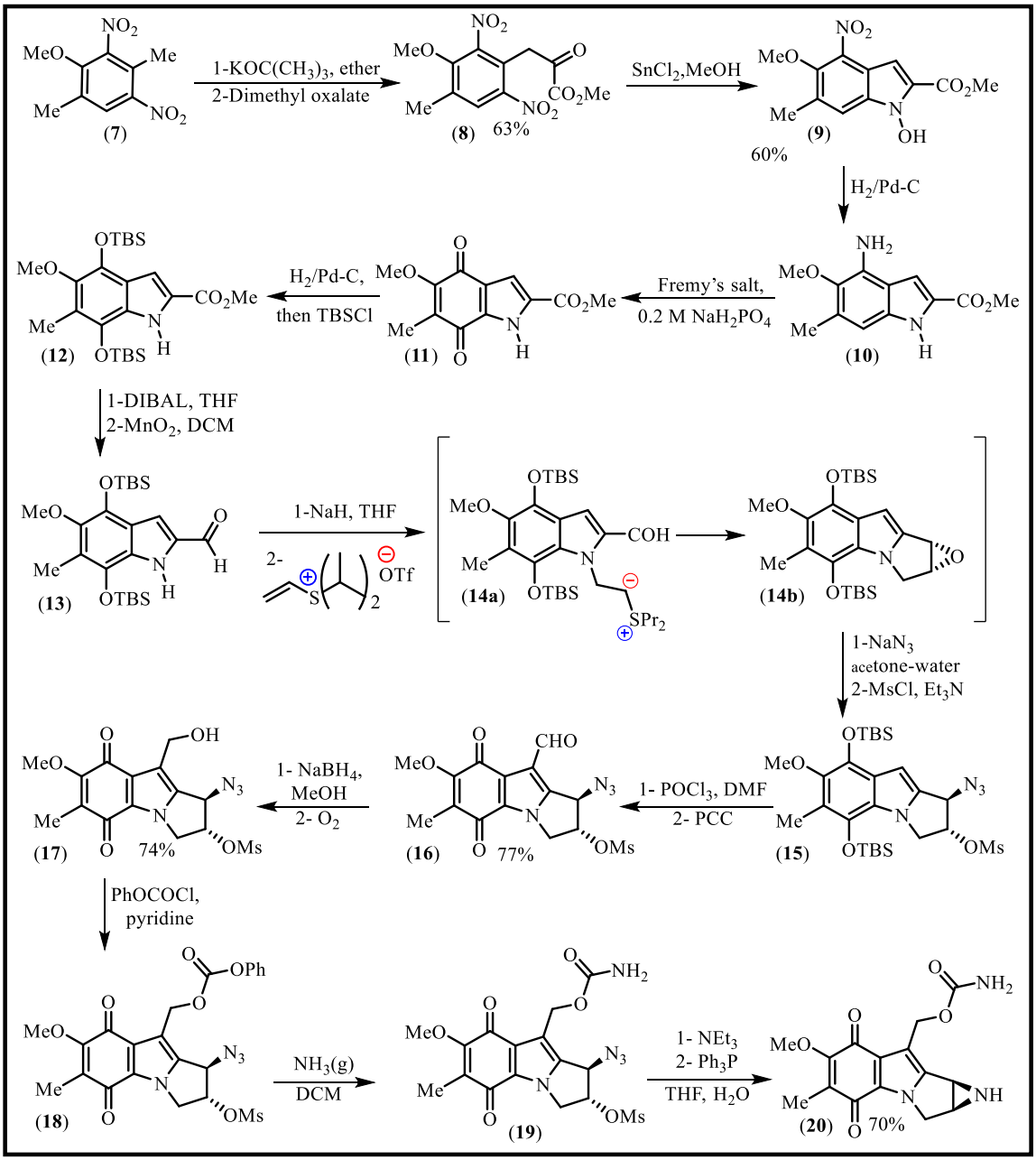

Figure 2.3 The Jimenez and Dong racemic synthesis of an AZM. The first synthesis of an AZM (**20**) required 16 steps from 2,5-dimethylanisole and gave the final product in 3.4% overall yield.

hydroxyindole **9**, and subsequent hydrogenation over Pd/C in methanol gave a quantitative yield of **10**. Potassium nitrosodisulfonate (Fremy's salt) was used to oxidize indole **10** to the corresponding quinone **11**. This compound was used in the next reaction without further purification to give the protected hydroquinone **12**, which was formed by

catalytic hydrogenation of **11**, followed by treatment with 4 equivalents of *tert*-butyldimethylsilyl chloride and imidazole. Reduction of **12** with DIBAL gave a primary alcohol that was converted to the corresponding aldehyde **13** with MnO_2 in 85% yield.

In the key step that forms the third ring and sets the stage for aziridine formation, indole **13** is treated with diisopropylvinylsulfonium triflate in the presence of sodium hydride to give the intermediate **14b**. The resulting tetracyclic epoxide was treated with sodium azide to form a racemic azido alcohol that is then mesylated to give compound **15**. The aldehyde **16** was obtained from **15** by Vilsmeier-Haack formylation in 96% yield, followed by formation of the quinone ring by oxidative cleavage of the TBS groups with PCC in 81% yield over the two steps. Alcohol **17** was obtained in 74% yield after the aldehyde was reduced with $NaBH_4$ in methanol. The quinone ring, which had been reduced in the $NaBH_4$ step, was reoxidized with molecular oxygen. The carbamate **19** was obtained in 77% by treating alcohol **17** with phenyl chloroformate and then ammonia. Lastly, the aziridine ring was formed by reduction of the azide with triphenylphosphine and ensuing ring-closure and mesylate departure to give AZM **20** in 70% yield. The synthesis is noteworthy in that it was the first to accomplish the synthesis of a fully functionalized AZM. However, the key step that allows for installation of the aziridine ring was racemic. Thus, an enantiocontrolled route to a functionalized AZM still remains elusive.

Enantiocontrolled Synthesis of Aziridinomitosenes

Relevant to the thesis work described herein, Vedejs and coworkers developed an enantiocontrolled route towards aziridinomitosenes that uses an azomethine ylide cycloaddition approach to construct the tetracyclic core (Figure 2-4).[8,9] The synthesis

began by preparation of oxazole **22**, which was formed via treatment of methyl ester **21a** or lactone **21b** with lithiated methyl isocyanide using the Schöllkopf oxazole synthesis. Oxazole **22** was treated with borane, then n-butyllithium to give the lithiated borane complex **23**. The resulting intermediate was coupled with a serine-derived aldehyde, to give amino alcohol **24** as an inseparable 6:1 diastereomeric mixture, in 93% yield.

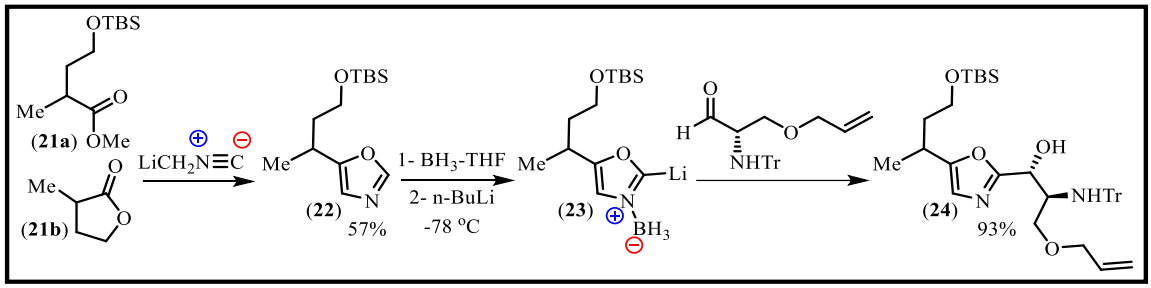

Figure 2.4. Vedejs synthesis of oxazole 22 and amino alcohol 24.

Treatment of **24** with diethyl azodicarboxylate and triphenylphosphine under Mitsunobu conditions closed the aziridine ring and allowed separation of the diastereomeric mixture (Figure 2.5). The desired cis-fused ring **25** was obtained in 71% yield and 98.1% enantiomeric excess. Intermediate **25** was converted to cycloaddition precursor **26** over 7 steps and in 26% yield.

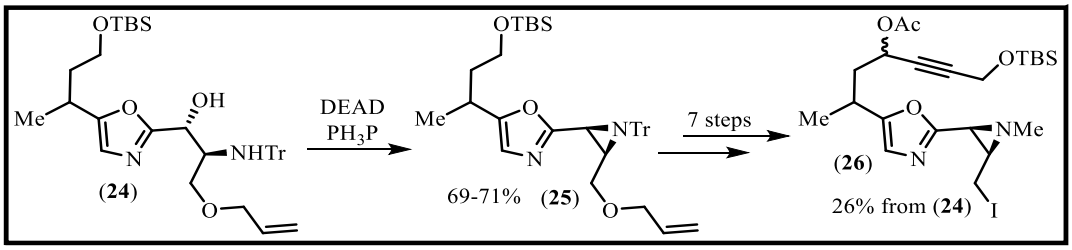

Figure 2.5 Vedejs synthesis of tetracyclic precursor.

The tetracyclic compound **27** was prepared in 37% yield by the internal azomethine ylide cycloaddition sequence shown in Figure 2.6. First, the oxazolium salt **28a** was formed by intramolecular N-alkylation upon treatment of precursor **27** with

AgOTf. Addition of **28a** to a solution of $BnMe_3N^+CN^-$ afforded 4-oxazoline **28b**, which spontaneously ring opens to the azomethine ylide **28c**. The reactive azomethine ylide undergoes a [3+2] cycloaddition to give **28d**, which, upon HCN elimination, aromatizes to form tetracycle **29**.

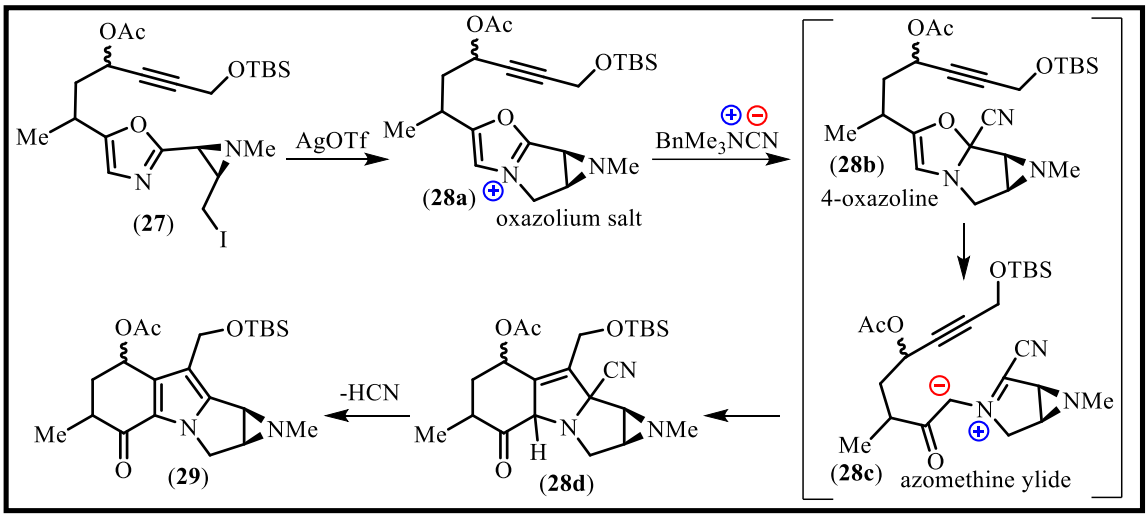

Figure 2.6 Mechanism of the oxazolium salt/azomethine ylide cycloaddition.

The desired aziridinomitosene **2** was formed after 6 steps that included removing the acetate group, oxidation to the quinone, and, finally, attaching the carbamate group (Figure 2.7). The C-6 methyl **AZM 2** was isolated in an overall yield of 0.03% from L-serine methyl ester hydrochloride. An analogous route was used to prepare the corresponding C6/C7 unsubstituted AZM **1**, which was obtained in 2.9% overall yield.

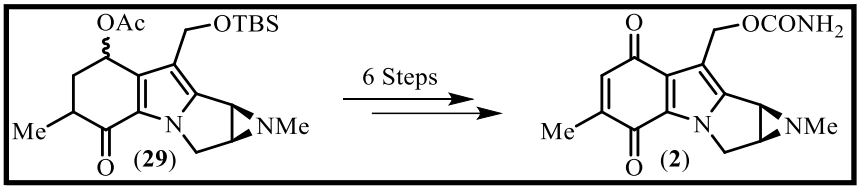

Figure 2.7 Formation of aziridinomitosene 2.

Results and Discussion

The Vedejs route previously used to prepare the C-6/C-7 unsubstituted and C-6 methyl substituted aziridinomitosenes was envisioned to provide access to the C-6/C-7 dimethyl substituted analog that is the target of this work (i.e., compound **3**). As a result, the first problem that needed to be solved was the synthesis of either an ester or lactone that would serve as an entry into the complete synthesis. The simplest protocol involved a four-step sequence that converted 1,2-propanediol to the ester **34**, subsequent oxazole formation, and then formation of the oxazolium salt cycloaddition precursor (Figure 2.8). The only drawback to this approach stems from the lack of stereocontrol, since several reactions would require purification of mixtures that contained up to 8 different stereoisomers. However, this potential problem was deemed acceptable given that all of the epimeric centers are erased during the synthesis and the final product would be produced as a single enantiomer.

To begin, the primary alcohol of commercially available 1,2-propanediol (**30**) was selectively protected using *tert*-butyldimethylsilyl chloride and catalytic dimethylaminopyridine (DMAP).[10,11] Presumably, the increased steric hindrance of the secondary alcohol directs the silane to the primary alcohol and the desired product **31** was generated in sufficient purity to be used in the next step without any purification. The resulting secondary alcohol was oxidized via PCC to give ketone **32**.[12,13] The overall yield for the two step sequence was 41.4%, with most of the material lost due to difficulties extracting the product from the chromium waste generated during the PCC reaction. As a result, a Dess-Martin periodinane oxidation was also attempted, but it did

not result in any improvements, possibly due to the adjacent sterically hindered silyl ether slowing the reaction rate.[14]

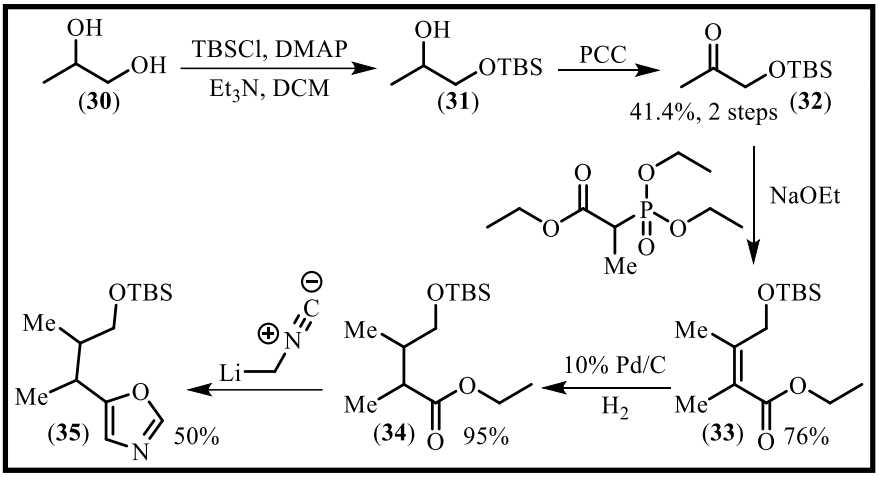

Figure 2.8 Synthesis of oxazole intermediate 35. The compound **35** was prepared in 15% yield over 5 steps from the starting diol.

Next, a Horner-Wadsworth-Emmons reaction with commercially available triethyl 2-phosphonopropionate was used to convert the ketone into the unsaturated ester **33**.[15] Owing to the product being a somewhat sterically hindered tetra-substituted olefin, the reaction required stirring for 24 hours to consume all starting material. However, the product could be obtained in good yield (76%), as an inseparable mixture of *E* and *Z* isomers in approximately a 1:1 ratio. Conjugate reduction of the enoate **33** was accomplished using H_2 and Pd/C to give the saturated ester **34** in 95% yield.[16] On paper, this reduction seems quite trivial. In practice, however, it proved a bit troublesome. For example, if the precursor **31** was oxidized using a Swern oxidation, the reduction failed. This was the outcome even if the product was purified via distillation or via silica gel chromatography, and even though the alcohol to ketone oxidation step was conducted several steps prior to reduction of **33**. It is surmised that residual dimethyl sulfide, a by-product of Swern oxidation, poisoned the palladium catalyst and prevented reduction.

When the oxidation of alcohol **31** was conducted with PCC, alkene reduction occurred without any difficulty.

To prepare oxazole **35**, ester **34** was treated with lithiated methyl isocyanide, in what is termed a Schöllkopf oxazole synthesis.[17] To conduct this reaction, methyl isocyanide (MeNC) is first prepared by dehydrating *N*-methyl formamide with toluenesulfonyl chloride (TsCl),[18] distilling the foul-smelling isocyanide, deprotonating with nBuLi at -78 °C, and then adding **34** dropwise. The most notable aspect of this reaction is that care must be taken to minimize exposure to the noxious odors that result from the MeNC, complicating the purification steps. Ultimately, oxazole **35** is formed in 50% yield after purification by column chromatography and then vacuum distillation. A total of 6.83 g of the oxazole was formed, which corresponds to an overall yield of 14.9% for the 5 steps from the diol.

Alkylation of oxazole **35** to yield amino alcohol **39** was accomplished over several steps by treating the lithiated oxazole with a serine-derived aldehyde (Figure 2.9). First, the oxazole-borane complex **36** was formed to prevent electrocyclic ring-opening after adding n-BuLi,[19] and this allowed alkylation at C-2 specifically without competing alkylation at C-4. Second, adding n-BuLi to the prepared complex gave **37**, which then underwent nucleophilic addition reaction to the aldehyde **38**. The amino alcohol **39** was obtained in 80% yield as a mixture of six inseparable diastereomers, in a 6:6:6:1:1:1 ratio.

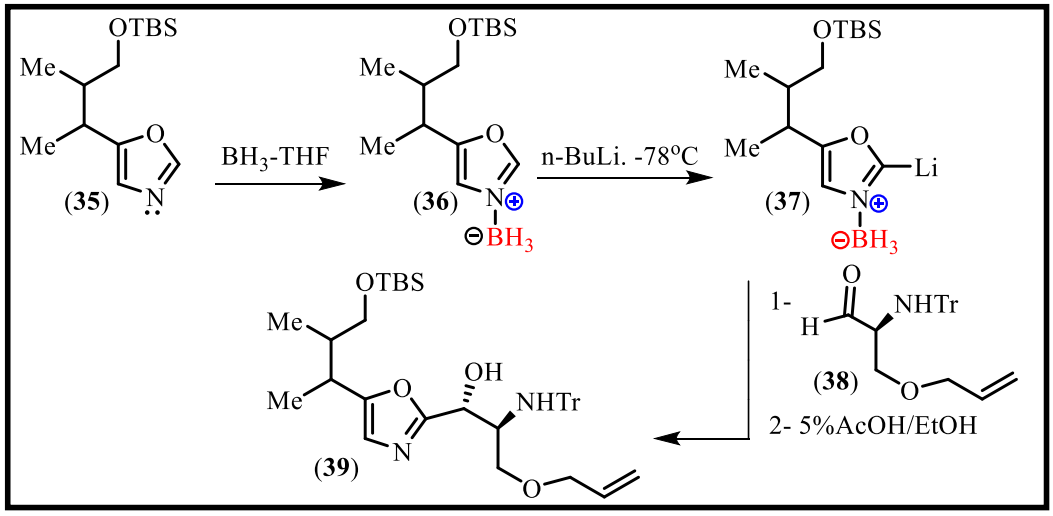

Figure 2.9 Nucleophile addition to aldehyde 38. The amino alcohol **39** is formed in 80% yield as a mixture of six diastereomers in a 6:6:6:1:1:1 ratio.

Although the reaction sequence shown in Figure 2.9 was eventually successful, the nucleophilic addition of the oxazole to the aldehyde reaction required significant optimization in order to provide **39** in an acceptable yield. In order to identify problems with the reaction, the ability to form intermediate **37** was tested by duplicating the reaction under similar conditions, but instead of adding the aldehyde **38** to form the amino alcohol **39,** the intermediate was quenched by deuterated methanol to yield **35b** (Figure 2.10). According to NMR assay, 80% of **35** was converted to **35b**.This result confirmed that while **36** and **37** were formed, the intermediate **37** was not reacting with the more hindered aldehyde at the reaction temperature (-78 °C) or during the allotted time (originally 1 hour at -78 °C). To remedy this problem, the stirring time was increased as was the reaction temperature. Eventually, after conducting the reaction 12 different times, it was found that the optimum conditions involved first stirring **37** with the aldehyde **38** for 2 hours at -78 °C, slowly warming the reaction to 0 °C over 2 hours, and then stopping the reaction. This protocol reliably provided the desired product in at least 80% yield.

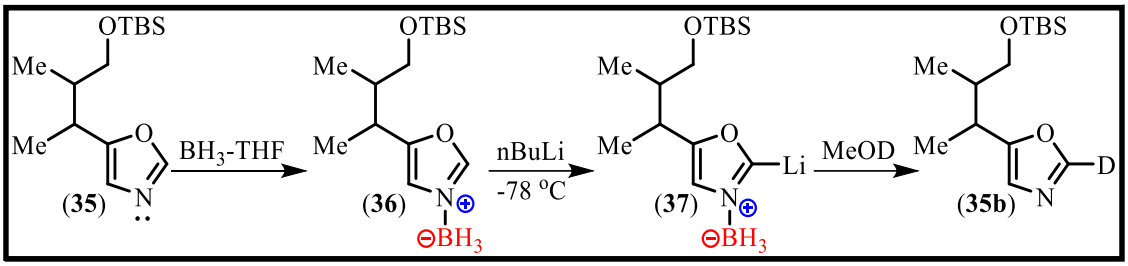

Figure 2.10 Formation of the deutoro-oxazole to confirm the formation of the intermediate 37.

The stereochemistry of the amino alcohol and, ultimately, the absolute configuration of the final aziridinomitosene product relies upon the aldehyde **38**, which was prepared from the commercially available *N*-trityl-L-serine methyl ester (Figure 2.11). To produce the aldehyde, the primary alcohol was protected as an allyl ether and then the ester was reduced to the corresponding aldehyde in high yield using DIBAL at -78 °C following a published protocol.[9]

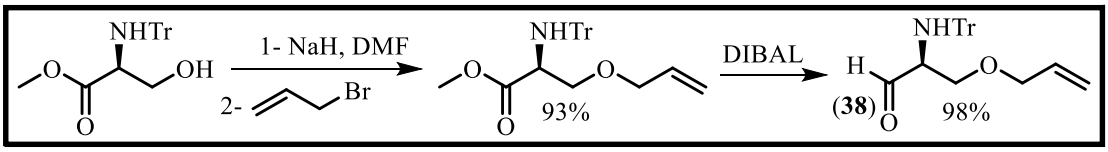

Figure 2.11 Synthesis of aldehyde 38 from N-Trityl-L-serine methyl ester.

With the amino alcohol **39** now available, the aziridine ring was closed using Mitsunobu conditions, affording the aziridine **40** in 86% yield as a single epimer at the aziridine ring after purification, indicating that the trans aziridine by-product could be removed via silica gel chromatography (Figure 2.12).[20] Next, removal of the trityl protecting group was achieved using ionic reduction conditions. Specifically, **40** was treated with triethylsilane and trifluoroacetic to provide **41** in 84% yield.[8] The N-methyl aziridine was generated by deprotonation of the N-H aziridine at -78 °C using n-BuLi, and the resulting anion was treated with methyl iodide to provide the desired product **42**

in 83% yield. Removal of the allyl protecting group from **42**, achieved using an in situ generated zirconium (II) reagent, provided the desired alcohol **43** in 83% yield.[21]

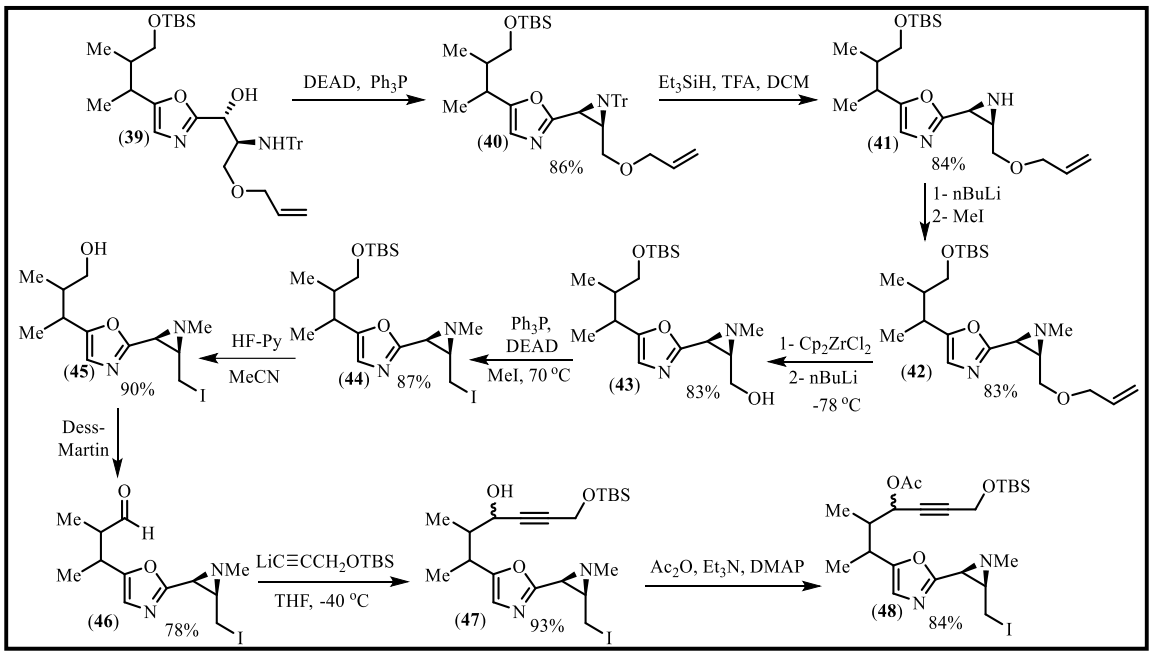

Figure 2.12 Synthesis of the cycloaddition precursor 48 in 2.8% overall yield. The sequence required 15 steps from 1,3-propanediol and 10 steps from oxazole **39** (and 19% overall yield).

The next step in the synthesis involved converting the just produced alcohol to a corresponding primary iodide in order to achieve the intramolecular oxazolium salt formation. To accomplish this, Mitsunobu conditions were applied to form iodide **44** in 87% yield.[22] Remarkably, even though the primary iodide is situated between two neighboring nucleophiles, the aziridine and oxazole nitrogen atoms, it displays remarkable stability over the remaining reaction steps, most likely due to steric protection from the cis-fused aziridine ring.

The remaining steps required to synthesize the cycloaddition precursor involved removing the tert-butyldimethylsilyl protecting group from **44** to yield the alcohol **45** in 90% yield by using the HF-pyridine reagent.[23] The Dess-Martin reagent was used to

oxidize alcohol **45** to generate the aldehyde **46** in 78% yield.[14] Of the potential mild oxidizing agents that could afford the same product, the Dess-Martin reagent was chosen since the product could be obtained in pure form after a simple extraction step and without silica gel chromatography. Addition of aldehyde **46** to lithiated tert-butyldimethylsilyl propargyl ether at -40 °C generated the alcohol **47** in 93% yield, which was subsequently treated with acetic anhydride to afford the fully protected cycloaddition precursor **48** in 84% yield as an inseparable 1:1:1:1 mixture of four diastereomers (Figure 2-12). The sequence to prepare the cycloaddition precursor **48** from the oxazole **39** required 10 steps and produced the compound in 19% yield. Overall, the synthesis of **48** was accomplished in 2.8% overall yield in 15 steps from commercially available 1,2-propanediol.

The next step in the synthesis relies on the Vedejs oxazolium salt/azomethine ylide cycloaddition sequence to form the tetracycle present in the final product.[9] The reaction proceeds following the mechanism shown in Figure 2.13. First, silver triflate (AgOTf) is added to the primary iodide **48**, and the strong affinity for silver towards halides assists in formation of the oxazolium salt via an intramolecular S_N2 reaction, although the reaction still requires heating at 70 °C in acetonitrile for 3 hours for complete consumption of the starting iodide. Next, the dark brown solution is transferred dropwise via cannula to a flask containing a solution of $BnMe_3N^+CN^-$ in acetonitrile to initiate the cycloaddition sequence. Specifically, cyanide adds to C-2 of the oxazolium salt to give the 4-oxazoline **48b**. This intermediate spontaneously ring opens to form the azomethine ylide **48c**, which undergoes an intermolecular [3+2]-cycloaddition to give the 3-pyrroline **48d**. Lastly, elimination of proton and cyanide group aromatizes the five-

membered ring and gives the product **49**.[8,9] Interestingly, a bright yellow color appears and quickly dissipates after each drop. This yellow color is tentatively attributed to the transient azomethine ylide intermediate and offers tentative evidence that the reaction is generating the desired product.

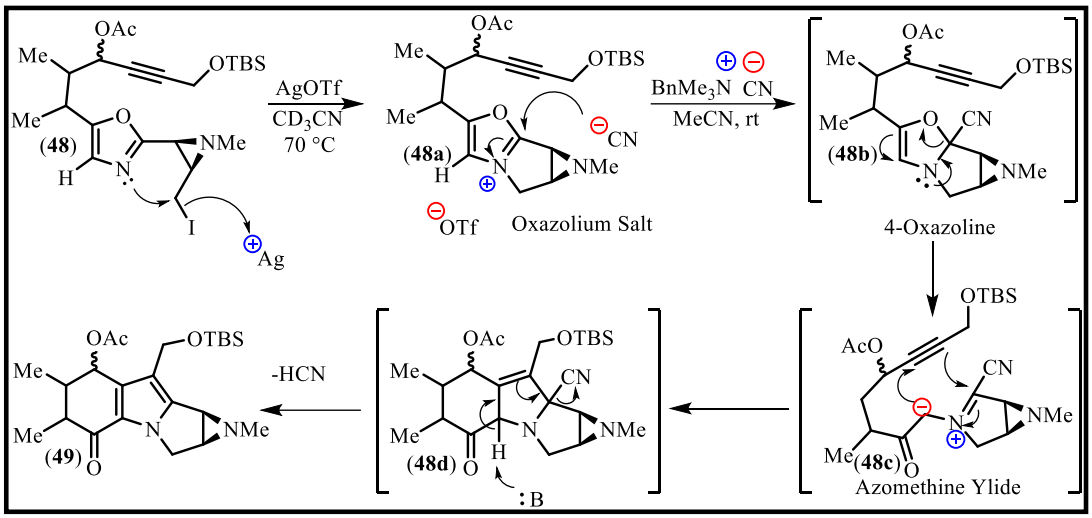

Figure 2.13 Oxazolium salt/azomethine ylide cycloaddition mechanism.

Unfortunately, the cycloaddition reaction typically gave product in about a 30% yield. While this low yield is not too disappointing considering the complexity of the reaction to form the tetracyclic core, generating enough material to complete the synthesis became somewhat problematic. As a result, the reaction was subjected to additional investigation in order to increase the yield. To choose better conditions, we decided to monitor the formation of the oxazolium salt by ^{1}H NMR. The reaction began by heating a solution of iodide **48** in CD_3CN with silver triflate at 70 °C in an NMR tube. Over several hours, the color of the yellow solution began to change to light brown and a yellow solid, corresponding to AgI, began to form. Progress of the reaction was checked every hour, and the results showed increasing formation of **48a** each hour, where the peak corresponding to the aromatic proton on C-4 (δ=6.89 ppm) started to disappear, and a

new, downfield peak (δ=7.46 ppm) began to appear. The new peak is attributed to the aromatic proton at C-4 on the oxazolium salt that has been shifted downfield due to the deshielding effects of the positively charged oxazolium salt (figure 5-14). After seven hours, the decision was made to stop the reaction as new peaks started to appear, which indicated that decomposition may have occurred. The highest yield obtained from the cycloaddition reaction was 44%, after modifying the conditions of the oxazolium salt forming step to stir while heating for 6 hours instead of 3 hours. After silica gel purification, the product was more than 90% pure, since achieving 100% purity was difficult because tetracycle **49** is moderately unstable and decomposes during the purification process.

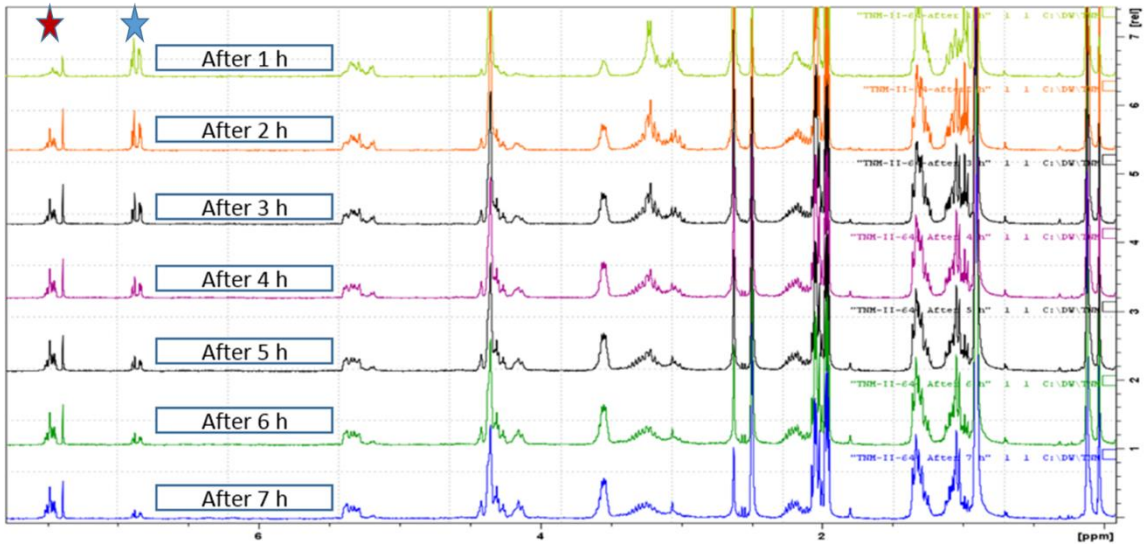

Figure 2.14 Oxazolium salt formation process monitored by ^{1}H NMR. The peaks under the blue star, corresponding to the aromatic proton on C-4 (δ=6.89 ppm), started to disappear over the time. The peaks under the red star, corresponding to a new peak at δ=7.46 ppm, began to appear and increase over the reaction time.

After the cycloaddition sequence, the remaining steps involve formation of the quinone ring and installation of the carbamate leaving group. The first step in the process to form the quinone ring involves removal of the acetate protecting group from **49** to

provide the corresponding secondary alcohol **50** (Figure 2-15), which was very sensitive to decomposition on silica gel. Since even a fast filtration of the reaction mixture resulted in loss of product, it was decided that it was better to go to the next step without purification. Next, a non-acidic oxidation was needed to convert **50** to diketone **51**, and this was accomplished using the mildly basic tetrapropylammonium perruthenate/*N*-methyl morpholine *N*-oxide (TPAP/NMO) in the presence of molecular sieves. The diketone **51** was produced in 48% yield over two steps from the acetate **49**.[24]

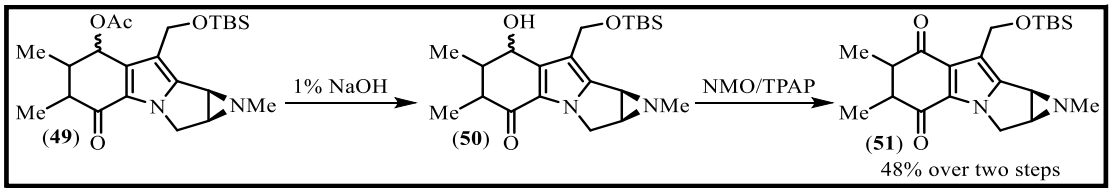

Figure 2.15 Formation of diketone 51 in two steps and 48% yield.

Quinone **52** was formed by treating diketone **51** with diazabicyclo[2.2.2]octane (DABCO) as a base in acetonitrile under an oxygen atmosphere with a catalytic additive of *N*,*N*′-bis(salicylidene)ethylenediaminocobalt(II) complex (Figure 2.16).[25] The purification of the quinone by silica gel column chromatography was difficult since the starting diketone and the quinone product have similar polarities and tend to co-elute. A better method involved preparative thin layer silica gel chromatography, but this method caused some of the product to decompose since the products are in contact with the mildly acidic silica gel for a greater amount of time. Ultimately, the quinone was obtained in 35% yield, which allowed for the next deprotection step to be conducted. The highly sensitive quinone, carefully treated with HF-pyridine buffered with trimethylamine, generated alcohol **53** in 60% yield and with 28% recovery of the starting quinone.

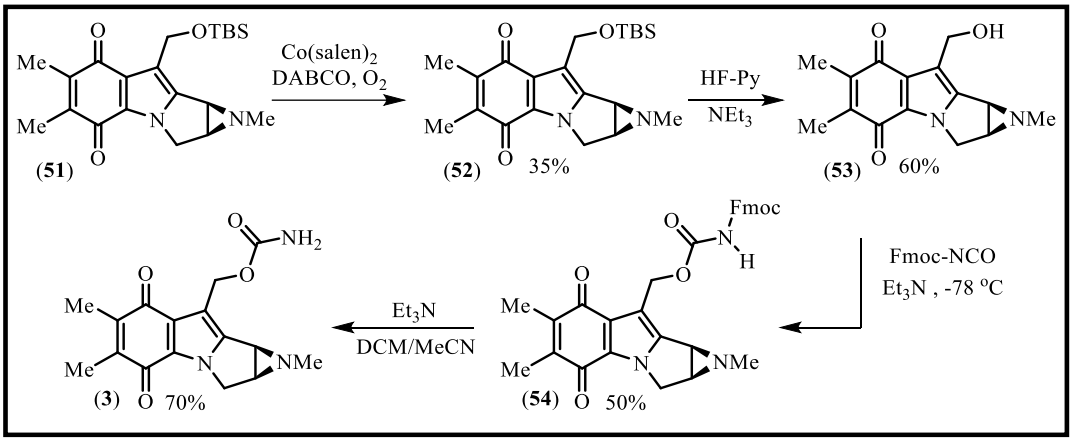

Figure 2.16 Final four steps to produce C-6/C-7 dimethyl AZM 3.

The last step in the synthesis required attaching the carbamate group. Previous experience with other AZMs relied on a one-pot procedure that involved first installing an Fmoc-protected carbamate and then subsequent removal of the protecting group to give the final product. However, in this instance, the one-pot reaction did not achieve the desired product. As a result, the final product was prepared using a 2-step sequence where the Fmoc-protected AZM **54** was isolated and purified in 50% yield, and then a second deprotection step gave the final product **3** in 70% yield.[8,9,26] The AZM was characterized by ^{1}H NMR, ^{13}C NMR, and high resolution mass spectrometry. In summary, the oxazole **35** was produced in 15% yield over 5 steps, the cycloaddition precursor in 2.8% yield over 15 steps, and the final product in 0.04% yield from the starting diol. In general, the synthesis of all intermediates up to the cycloaddition precursor **48** proceeded without too much difficulty. However, all of the reactions post-cycloaddition were more troublesome than has been observed for other aziridinomitosenes. It appears that compounds **49** to **54** and the final product **3** are all more sensitive than the comparable intermediates in other systems. As is discussed

below, AZM **3** appears to be more susceptible to acid-catalyzed decomposition pathways and this may be the cause of the reduced yields.

The Solvolytic Stability of a 6,7-Dimethyl Aziridinomitosene

The solvolytic stability of **3** was evaluated in methanolic solution buffered with the Tris and Bis-Tris amine hydrochlorides and the results were compared to those obtained for previously studied aziridinomitosenes (Figure 2.17).[27,28] UV spectroscopy was used to monitor the solvolysis process in acidic, neutral, and basic buffer solution (pH 6, pH 7, pH 8.7), respectively. The rate of solvolysis was measured by monitoring the decrease in UV absorption at 480 nm over time. The results were fitted to the first order rate equation to generate first order rate constants and half-lifes. Each solvolysis experiment was repeated 2 times, and the mean values are reported in Table 2-1, as are literature values for the previously known AZMs **1** and **55**.

Table 2.1. Methanolysis of Aziridinomitosene 1, 3, and 55, at 20 °C.

pH	**1**		**3**		**55**	
	k (s^{-1})	$t_{1/2}$ (min)	k (s^{-1})	$t_{1/2}$ (min)	k (s^{-1})	$t_{1/2}$ (min)
6.0	$3x10^{-5}$	400	$15x10^{-5}$	74	-	-
7.0	$5x10^{-6}$	2000	$21x10^{-6}$	537	$8x10^{-4}$	14
8.5	Decomp	Decomp	0	0	$3.6x10^{-5}$	324

At pH 6, the new AZM **3** underwent methanolysis about five times faster than **1**. Under acidic pH, the AZMs undergo solvolysis by the sequence of events depicted in Figure 2.17.[9] Following protonation of the aziridine nitrogen, rapid ring-opening generates a carbocation on C-1. Comparing the carbocations **1b** and **3b**, the electron-donating methyl groups at C-6 and C-7 on **3b** provide additional stabilization, which

results in faster S_N1 ring-opening of the aziridine ring. A similar trend is observed at pH 7, where methanolysis of **3** was about 4 times faster than AZM **1**. A comparison of **3** to **55** was permissible at pH 7, since the experimental results have been reported at this pH.[9,27,28] The synthetic AZM **3** underwent methanolysis about 38 times slower than **55**. It is reasonable to presume that the C-7 amino group present in **55** is a much better electron donating group than the methyl group in **3**. This will provide much greater stabilization of the carbocation **55b**, compared to **3b**.

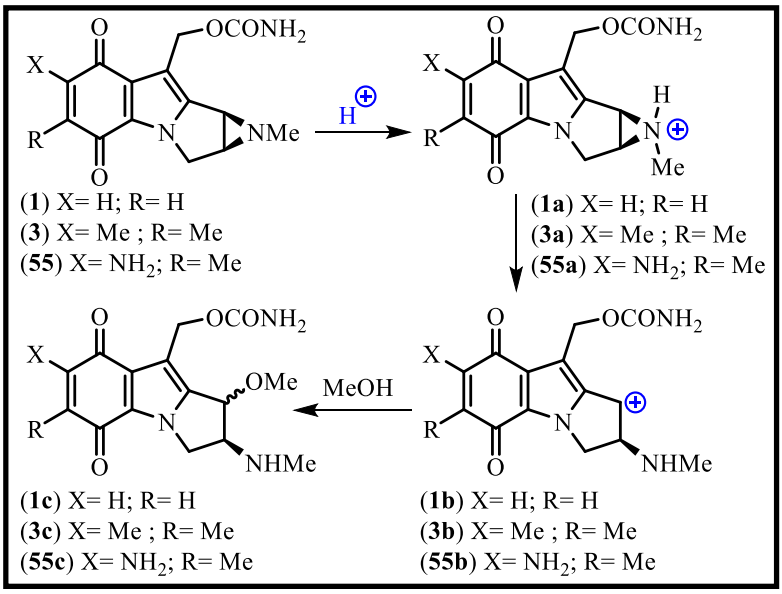

Figure 2.17 Methanolysis and azridine ring opening of AZMs 1, 3, and 55 in buffered methanol solutions.

Under basic conditions, at pH 8.5, AZM **3** displays remarkable stability that is in stark contrast to both AZM **1** and **55**. Indeed, synthetic **3** did not undergo any detectible change over 3000 minutes in methanolic solutions at pH 8.5. AZM **1** completely decomposed after 10 hours, while **55** underwent aziridine ring-opening with a half-life of 228 minutes at this pH 8.5.[28] The base catalyzed decomposition of **1** is postulated to involve nucleophilic attack at the C-6 and C-7 positions on the quinone ring. Since

aziridinomitosene **3** is substituted with methyl groups at both of these positions, this decomposition pathway is no longer available and offers an explanation for the remarkable stability in basic solutions.

Conclusions

The total synthesis of AZM **3** started from commercially available reagents to form the oxazole **35** in 5 steps (overall yield of 14.9%), followed by the addition of a protected aldehyde that is converted to the required aziridine ring via a Mitsunobu reaction. Once the aziridine ring is formed, all of the reaction conditions were performed in mild conditions in order to prevent aziridine ring-opening. In an additional eight steps, the cycladdition precursor **48** was formed in 19% yield from the prepared oxazole **35,** and in 2.8% overall yield from the starting diol. The completion of the synthesis and formation of the tetracyclic core **49** was achieved by performing an oxazolium salt/azomethine ylide, [3+2] cycloaddition sequence. This sequence was conducted multiple times, and the highest yield obtained was 44%. The final steps were most challenging, requiring several transformations to accomplish a deprotection and an oxidation to give a diketone that was then further oxidized to a quinone. Finally, the carbamate was attached in two steps using FmocNCO to yield the desired AZM **3** product in an overall yield of 0.04% from the starting diol over the 22 step reaction sequence.

The solvolytic stability of **3** was evaluated in a methanolic solution buffered with Tris and Bis-Tris amine hydrochlorides and compared to other AZM's analogs. The results of the study showed that under acidic conditions, at pH 6, AZM **3** was about five times reactive than **1**. The electron-donating methyl groups at C-6 and C-7 on AZM **3** provide additional stabilization to the carbocation that formed on the C-1, which results

in faster S_N1 ring-opening of the aziridine ring. A similar trend is observed at pH 7. Under basic conditions (pH 8.5), AZM **3** is more stable than **1** and **55**, and no aziridine ring opening was observed over 50 hours. AZM **1** completely decomposed after 10 hours, while **55** underwent aziridine ring-opening with a half-life of 5.4 Hours at this pH. The presence of the methyl group on C-6 and C-7 in **3** was able to prevent any nucleophile attack on the quinone moiety and did not undergo any change over 50 hours in methanolic solutions at pH 8.5.

The results support that the nucleophile activation mechanism offers a viable path for **1** and **2** to form ICLs or DPCs. To explain the results, the aziridine ring in synthetic AZM **3** opens rapidly at pH 6 and pH 7, which is essential for the formation of DNA monoadducts. AZM **3** was stable in more basic solutions, which suggests that nucleophile attack on the quinone moiety is prevented due to the methyl groups at C-6 and C-7. Nucleophilic addition to C-6 or C-7 in AZM **1** and to C-7 in AZM **2** by a DNA-associated protein or other cellular nucleophile will result in an intermediate that can tautomerize to the hydroquinone species. This intermediate is analogous to the previously described leuco-aziridinomitosene, from Figure 1.5, that has sufficient electron density to allow carbamate departure and then crosslink formation. Future work will be directed to determining the DNA crosslinking ability of AZM **3** and to improve the overall yield of the final aziridinomitosenes.

Experimental

General Methods. Solvents and reagents were purified as follows: diethyl ether and tetrahydrofuran (THF) were distilled from sodium/benzophenone; dichloromethane (CH_2Cl_2) was distilled from P_2O_5; CH_3CN was distilled from P_2O_5; DMF was stored over

activated molecular sieves (3 Å, 4-8 mesh beads) for three days prior to distilling from P_2O_5; benzene, toluene, triethylamine, NEt*i*Pr_2, and TMEDA were distilled from CaH_2; methanol was distilled from magnesium, the purified reagents and solvents were used immediately or stored under nitrogen. NMR solvents ($CDCl_3$, CD_3CN) were stored over activated molecular sieves (3 Å, 4-8 mesh beads). Molecular sieves (Aldrich, 3 Å, 4-8 mesh beads, or 4 Å, <5 micron powder) were activated at 200 °C and 0.5 mm Hg vacuum for 24 h and stored under argon. Unless otherwise noted, all chemicals were used as obtained from commercial sources and all reactions were performed under nitrogen atmosphere in glassware dried in an oven (140 °C) and cooled with a stream of nitrogen. All reaction mixtures were stirred magnetically and liquid reagents were dispensed with all PP/PE plastic syringes or Hamilton Gastight microsyringes. Preparatory layer chromatography (PLC) was performed using MN-Silica gel P/UV_{254} or Whatman PK6F Silica gel 60 and analytical TLC was performed on EM glass plates coated with a 250 μm layer of silica gel 60 F_{254}. Flash chromatography was performed with 230-400 mesh silica gel 60.

4-(tert-Butyldimethylsilyloxy)-2,3-dimethyl-2-butenoic acid ethyl ester (33). Sodium metal (2.560 g, 111.500 mmol) was added portion wise to 84 mL dry ethanol and allowed to fully dissolve. (23.92 mL, 111.500 mmol) triethyl 2-phosphonopropionate was then added dropwise and stirred for 20 minutes. (14.0 g, 74.333 mmol) ketone **32** was dissolved in (30+20) mL ethanol and cannulated to the reaction mixture dropwise .The resulting yellow solution was then stirred for 24 hours at room temperature . By the time the color of the solution start to be orange. After 24 hour the consumption of the starting ketone was checked by TLC eluted by (hexane 8:1 acetone), no starting materials was

present. (84 mL) of saturated NH_4Cl was added and then transferred to separation funnel (150 mL) H_2O was added and extracted with 3x200 mL DCM. The combined extracts were dried ($MgSO_4$), filtered and concentrated by rotary evaporation and the residue was purified by flash chromatography on silica gel (25x18.5 cm, 20:1 hexane/ethyl acetate eluent, 25 mL fractions). Fractions 18-50 gave 15.7g (76%) of the unsaturated ester **33** as a colorless oil, analytical TLC on silica gel 60 F254, 20:1 hexane/ ethyl acetate, Rf= 0.2. Molecular ion ($M+H^+$) calcd for $C_{14}H_{29}O_3Si$: 273.1880; found m/z= 273.1908, error= 10.249 ppm; IR (neat, cm^-1) 1710.55, C=O, 1635.91, C=C; 600 MHz NMR ($CDCl_3$, ppm) δ 4.50 (1 H, s) 4.24 (1 H, s) 4.1 (2 H, dq, J=7.2, 5.9) 2.01 (1 H, s) 1.89 (2 H, s) 1.87-1.85 (3 H, s) 1.33-1.30 (3 H, m) 0.93 (3 H, s) 0.92 (6 H, s) 0.09 (2 H, s)0.08 (4 H, s). ^{13}C NMR (150 MHz, CDCl3, ppm) δ 175.03, 175.29, 151.70, 149.46, 128.38, 128.24, 69.50, 68.99, 65.46, 31.11, 23.59, 23.57, 22.60, 21.46, 21.01, 20.06, 19.54, 19.53, -0.12, -0.13.

4-(tert-Butyldimethylsilyloxy)-2,3-dimethyl-butyric acid ethyl ester (34). To a solution of (15.4g, 56.513 mmol) unsaturated ester **33** in 110 mL dry ethyl acetate was added (1.52g) of Pd/C 10% followed by attaching hydrogen balloon to bubble through the solution. The reaction process was checked by TLC (Hexane 8:1 ethyl acetate), ^1H NMR, and IR to confirm the reduction process. After 4 hours 100% of the double bond was reduced .The crude was filtered and concentrated by rotary evaporation to give 15.322g as colorless oil without purification.

5-[3-(tert-Butyldimethylsilyloxy)-1,2-dimethylpropyl]-oxazole (35). To a stirring solution of methyl isocyanide (3.69 mL, 67.566 mmol) in 100 mL of anhydrous THF at -78 °C was added n-BuLi (1.6 M solution in hexanes, 47.27 mL, 75.6339 mmol)

dropwise under argon. The pale yellow creamy suspension was stirred at -78 °C for 1h, at which time ester **34** (13.84 g, 50.4226 mmol) in anhydrous THF (20 + 20 mL, including cannula and flask washings) was added dropwise via cannula. After stirring for 2 hours at -78 °C, the cooling bath was removed and the solution was stirred for an additional 2 hours. The resulting brown solution was poured into 200 mL of a 1:1 water/ brine solution and extracted with 3x200 mL ether. The combined extracts were dried (Na_2SO_4), concentrated by rotary evaporation, and the residue was purified by distillation at reduced pressure (0.5mm Hg) and short path distillation. The first drip of the colorless oil start at 73 °C to continue dripping at 80 °C .The combined fractions give 6.8399 g as a colorless oil. Analytical TLC on silica gel 60 F254, 3:1 hexane/ ethyl Et_2O, Rf= 0.29. Molecular ion ($M+H^+$) calcd for $C_{14}H_{28}NO_2Si$: 270.1884; found m/z= 270.1909, error= 9.25 ppm; IR (neat, cm-1) 1509; 600 MHz NMR ($CDCl_3$, ppm) δ 7.76 (0.8 H, s) 7.75 (0.2 H, s) 6.75 (1 H, s) δ 3.45 (2H, m) 3.10 (1 H, p, J=6.4 Hz) 2.03 (0.3 H, quin, J=6.6 Hz) 1.85 (0.7 H, quin, J=6.6 Hz) 1.36 (0.3 H, d, J=7.4) 1.34 (0.2 H, d, J=7.4 Hz) 1.27 (1.6 H, d, J=7.4 Hz) 1.18 (0.9 H, d, J=7.4 Hz) 0.92 (1.2 H, d, J=2.3) 0.89 (7.8 H, d, J=3.05 Hz) 0.82 (1 H, d, J=7) 0.79 (1.6 H, d, J=7 Hz) 0.135 (0.9 H, s) 0.039 (5.2 H, d, J=5 Hz). ^{13}C NMR (150 MHz, $CDCl_3$, ppm) δ 156.5, 155.7, 149.9, 135.9, 134.8, 122.2, 121.6, 117.7, 65.6, 40.1, 38.9, 35.0, 32.1, 31.6, 0.28.9, 25.8, 25.6, 18.2, 17.0, 16.4, 15.5, 13.4, 13.0, 12.5, 9.6, -5.3, -5.4.

2-D- 5-[3-(tert-Butyldimethylsilyloxy)-1,2-dimethylpropyl]-oxazole (35b). To a solution of the oxazole **(33)** (63.5 mg, 0.235 mmol) in 1.5 mL of anhydrous THF at 0 °C was added BH_3-THF (1.0 M solution in THF, 0.26 mL, 0.26 mmol). After 5 minutes the ice-bath was then removed and the solution was stirring at rt for 1h, the colorless

solution was cooled to -78 °C, and n-BuLi (1.6 M solution in hexanes, 0.173 mL, 0.26 mmol) was added dropwise over 10 min. The yellow solution was stirred at -78 °C for 1 h, and then a solution MeOD (0.1 mL, 0.26 mmol) in anhydrous THF (0.5 mL, including cannula and flask washings) was added via cannula dropwise. The resulting yellow solution was stirred at -78 °C for 90 minutes. The reaction was quenched with 1 mL of 5% solution of AcOH in EtOH dropwise. The cooling bath was removed, and the reaction mixture was allowed to warm to rt. After stirring at rt overnight, the resulting pale yellow solution was concentrated by rotary evaporation to 1/4 from original volume. 3 mL of aqueous $NaHCO_3$ was added and then poured into 5 mL of ether, the aqueous layer was extracted with 2 x 3 mL of ether, and all organic extracts were combined, dried (Na_2SO_4), and concentrated by rotary evaporation.

2-[(lR,2S) and (lS,2S)-3-Allyloxy-l-hydroxy-2-tritylaminopropyl)-5-[(1R) and (1S) , (2R) and (2S)- tert-butyldimethylsilyloxy-1,2-dimethylpropyl]oxazole (39) To a solution of the oxazole **(35)** (1.55 g , 5.75 mmol) in 20 mL of anhydrous THF at 0 °C was added BH_3-THF (1.0 M solution in THF,6.32 mL, 6.32 mmol). After 5 minutes the ice-bath was then removed and the solution was stirring at rt for 1h, the colorless solution was cooled to -78 °C, and n-BuLi (1.6 M solution in hexanes, 3.95 mL, 6.32 mmol) was added dropwise over 10 min. The yellow solution was stirred at -78 °C for 1 h, and then a solution of the aldehyde **38** (2.136 g, 5.75 mmol) in anhydrous THF (20 mL, including cannula and flask washings) was added via cannula dropwise. The resulting yellow solution was stirred at -78 °C for 2 h, then slowly warmed to reach 0°C within additional 2 h. The reaction cooled back to -78 °C, and then quenched with 20 mL of 5% solution of AcOH in EtOH dropwise. The cooling bath was removed, and the reaction mixture was

allowed to warm to rt. After stirring at rt for 21 h, the resulting pale yellow solution was concentrated by rotary evaporation to 1/3 from original volume, 40 mL of aqueous $NaHCO_3$ was added and then poured into 100 mL of ether + 100 mL of H_2O, The aqueous layer was extracted with 2 x 50 mL of ether, all organic extracts were combined, washed with 100 mL of brine, dried (Na_2SO_4), and concentrated by rotary evaporation. The residue was purified by flash chromatography on silica gel (25x14 cm, 10:1 hexane/acetone eluent, followed by 5:1 hexane/acetone eluent 20 mL fractions). Fractions 26-38 were concentrated to give the amino alcohol **39** Fractions 7-10 were concentrated and repurified by flash chromatography on silica gel (25x8 cm, 10:1 hexane/acetone eluent, followed by 5:1 hexane/acetone eluent 10 mL fractions). Fractions 15-20 were concentrated to give the amino alcohol **39**.The combined purified **39** give 3.001 g as a pale yellow very sticky oil. Analytical TLC on silica gel 60 F254, 5:1 hexane/ether, Rf= 0.30. Molecular ion ($M+H^+$) calcd for $C_{39}H_{53}N_2O_4Si$: 641.3769; found m/z= 641.3679, error= 14 ppm; IR (neat, cm-1) 1563; 600 MHz NMR (CDCl3, ppm) δ 7.58-7.48 (6 H, m) 7.22 (6 H, m) 7.15 (3 H, m) 6.64-6.55 (1 H, s) 5.75-5.58 (1 H, m) 5.71-4.98 (2 H, m) 4.53-4.44 (1 H, m) 3.51 (2 H, d, J=5.3 Hz) 3.46-3.35 (2 H, m) 3.283.21 (1 H, br) 3.09-3.96 (1 H, m) 2.90-2.79 (1 H, m) 2.69-2.47 (1 H, br) 2.44-2.33 (1 H, m) 2.10-1.96 (0.4 H, m) 1.86-1.73 (0.6 H, m) 1.24-1.20 (1 H, dd, J=7.3,3.3 Hz) 1.16 (1 H, d, J=6.10 Hz)1.13-1.10 (1 H, dd, J=4.4,2.7 Hz) 0.86 (6 H, s) 0.83 (3 H, s) 0.79 0.71 (3 H, m) 0.043 (0.5 H,s) 0.05-0.01 (5.5 H, s). ^{13}C NMR (150 MHz, CDCl3, ppm) δ 162.98, 162.94, 162.86, 162.83, 156.88, 156.82, 155.80, 155.78, 146.61, 146.50, 134.25, 128.76, 128.71, 127.99, 127.91, 126.57, 122.35, 121.84, 116.93, 116.89, 71.89, 70.92, 70.90, 69.37, 69.35, 69.24, 69.15, 69.01, 68.93, 65.79, 65.68, 65.65, 64.33, 54.98, 54.95, 54.92, 40.17, 40.10, 38.70,

38.69, 32.50, 32.48, 31.74, 31.71, 25.94, 25.39, 18.28, 16.51, 16.44, 13.96, 13.93, 12.73, 12.65, 12.41, 12.36, 1.06, -5.35, -5.38, -5.4135.

2-[(2*S*,3*R*)-3-Allyloxymethyl-1-trityl-aziridin-2-yl]-5-[(1R) and (1S) , (2R) and (2S)- tert-butyldimethylsilyloxy-1,2-dimethylpropyl]oxazole (40)

To a solution of amino alcohol **39** (2.922 g, 4.56 mmol) in 42 mL anhydrous THF at 0 °C was added Ph_3P (2.45 g, 9.34 mmol), followed by diethyl azodicarboxylate (1.436 mL, 9.12 mmol) dropwise. The cooling bath was removed, and the reaction mixture was allowed to warm to rt. After stirring at rt for 30 h, the yellow solution was concentrated by rotary evaporation. The residual oil was dissolved in 1 mL of CH_2Cl_2 and purified by flash chromatography on silica gel (25x14, 3:1 hexane/EtOAc eluent, 15 mL fractions). Fractions 6-15 were concentrated to yield poor purified product, and the residue was purified by another flash chromatography on silica gel (25x14, 5:1 hexane/EtOAc eluent, 15 mL fractions). Fractions 28-48 were concentrated to give 2.457 g (86%) as a pale yellow to colorless oil, analytical TLC on silica gel 60 F254, 3:1 hexane/EtOAc, Rf= 0.36. Molecular ion ($M+H^+$) calcd for $C_{39}H_{51}N_2O_3Si$: 623.3663; found (electrospray) *m/z*= 623.3682, error= 3 ppm; IR (neat, cm^{-1}) 1570; 600 MHz NMR ($CDCl_3$, ppm) δ 7.58 (6 H, m) 7.30 (6 H, m) 7.26 (3 H, m) 6.78 (1 H, s) 5.84-5.73 (1 H, dddd, J= 17.3,10.4, 5.5,5.5 Hz)5.20 (1 H, dddd, J= 17.3,10.4, 5.5,5.5 Hz) 5.10 (1 H, dddd, J= 10.3,10.4, 5.5,5.5 Hz) 4.07 (1 H, m) 3.88-3.73 (3 H, m) 3.63-3.48 (2 H, m) 3.19-3.11 (1 H, m) 2.54 (1 H, dd, J=2.64 Hz) 2.22-2.09 (0.3 H, m) 2.02-1.90 (1.7 H, m) 1.36 (2 H , dd, J=2.46 Hz) 1.25 (1 H, dd, J=2.64 Hz) 0.98 (9 H, s) 0.93-0.87 (3 H, m) 0.15 (3 H, s) 0.13 (1.7 H, s) 0.08 (1.8 H, s). ^{13}C NMR (150 MHz, CDCl3, ppm) δ 160.35, 156.72, 155.79, 155.57, 143.78, 134.67, 129.58, 129.33, 128.94, 127.97, 127.76, 127.37, 127.01, 123.22, 122.60,

116.99, 116.95, 75.08, 71.95, 71.90, 68.60, 68.57, 65.98, 65.87, 40.53, 40.29, 39.13, 38.94, 38.54, 26.05, 18.41, 16.86, 16.78, 13.87, 13.71, 13.22, 12.74, 12.41, -5.22, -5.2479.

2-[(2S,3R)-3-Allyloxymethylaziridin-2-yl]-5-[(1R) and (1S) , (2R) and (2S)-tert-butyldimethylsilyloxy-1,2-dimethylpropyl]oxazole (41). To a solution of the Tr-aziridine **40** (7.5 g, 12.040 mmol) in 100 mL dry DCM at 0°C was added triethylhydrosilane (7.953 mL, 49.245 mmol) followed by adding trifluoroacetic acid (3.932 mL, 51.049 mmol). After stirring at 0 °C for 80 minutes, triethylamine (7.887 mL, 56.588 mmol) was added dropwise, the ice bath was then removed to let the solution to stir additional 20 minutes. Poured into 320 mL of DCM, and washed with 2x250 mL of saturated aqueous NaCl, dried over (Na_2SO_4), and concentrated by rotary evaporation. The residue was purified by flash chromatography on silica gel (25x18.5 cm, 3:1 hexane/ acetone eluent, 25 mL fractions). Fractions 18-47 were concentrated to give 3.879 g (84%) as a clear colorless oil, analytical TLC on silica gel 60 F254, 3:1 hexane/acetone, Rf= 0.29. Molecular ion ($M+H^+$) calcd for $C_{20}H_{37}N_2O_3Si$: 381.2568; found (electrospray) *m/z*= 381.2589, error= 7 ppm; IR (neat, cm^{-1}) 3242, N-H; 1572; 300 MHz NMR ($CDCl_3$, ppm) 6.65 (1 H, s) 5.81 (1 H, m) 5.16 (1 H, dddd, J=7.45, 1.4,1.4,1.4 Hz) 5.08 (1 H, dddd, J=10.3, 1.4,1.4,1.4 Hz) 3.90 (2 H, br) 3.64-3.51 (2 H, m) 3.49-3.37 (2 H, m) 3.14-2.96 (1 H, m)2.80-2.44 (1 H, d, J=43.82 Hz) 2.02 (0.5 H, br) 1.82 (0.5 H, br)1.5-1.29 (2 H, m) 1.25-1.12 (3 H, dd, J=15.3, 6.95 Hz) 0.97 (6 H,s) 0.85 (3 H,s) 0.81-0.76 (2.6 H, m) 0.60-0.52 (0.4 H, m)) 0.12-0.02 (6 H, s) .^{13}C NMR (75 MHz, CDCl3, ppm) δ 159.51, 159.44, 156.91, 156.00, 134.45, 122.68, 117.12, 71.90, 69.23, 68.14, 65.67, 65.57, 40.01,

38.66, 37.69, 36.06, 35.07, 32.32, 31.67, 30.89, 29.64, 25.87, 25.62, 18.23, 16.51, 13.80, 12.79, 12.36, 6.77, 4.35, -5.42, -5.45, -5.4999.

2-[(2S,3R)-3-Allyloxymethyl-1-methyaziridin-2-yl]-5-[(1R) and (1S) , (2R) and (2S)- tert-butyldimethylsilyloxy-1,2-dimethylpropyl]oxazole (42). To a solution of H-Aziridine **41** (1.1 g, 2.89 mmol) in 23.5 mL dry THF at -78 °C under argon was added n-BuLi (1.60 M solution in hexanes, 2.02 mL, 3.237 mmol) was added dropwise. The yellow solution was stirred at -78 °C for 30 minutes .to the resulting brown solution MeI (0.216 mL, 3.468 mmol) was added dropwise, then the cold bath was removed and the reaction mixture was allowed to warm to rt. After 1h at rt, the resulting solution poured into 100 mL of Et_2O, and washed with 2 x 100 mL brine dried over (Na_2SO_4), and concentrated by rotary evaporation. The residue was purified by flash chromatography on silica gel (25x8 cm, 5:1 hexane/ acetone eluent, 15 mL fractions). Fractions 11-20 were concentrated to give 0.956 g of product as yellow oil. Analytical TLC on silica gel 60 F254, 5:1 hexane/acetone, Rf= 0.31. Molecular ion ($M+H^+$) calcd for $C_{21}H_{39}N_2O_3Si$: 395.2724; found (electrospray) *m/z*= 395.2742, error= 5 ppm; IR (neat, cm^{-1}) 1572; 600 MHz NMR ($CDCl_3$, ppm) δ 6.65 (1 H, S) 5.85 (1 H, m) 5.2 (1 H, dddd, J=17.25,1.4, 1.4,1.4 Hz) 5.14 (1 H, dddd, J=10.4,1.4, 1.4,1.4 Hz) 3.98-3.88 (2 H, m) 3.66 (1 H, m) 3.57 (1 H, m) 3.50-3.38 (2 H, m) 3.11-2.97 (1 H, m) 2.62-2.58 (1 H, m) 2.54 (3 H, s) 2.08-1.98 (1.5 H, m) 1.82 (0.7 H, ddd, J=6.24, 6.0, 6.0 Hz) 1.23 (2 H, dd,, J=3.35 Hz) 1.13 (1 H, dd, J=2,88,4.24 Hz) 0.97 (6 H, s) (.91 (2 H, s) 0.88 (1 H, s) 0.79 (3 H, m) 0.58 (0.5 H, ddd, J=4.9,3.2, 3.2 Hz) 0.34 (3, H, s) 0.34 (3H, s). ^{13}C NMR (150 MHz, CDCl3, ppm) δ 164.81, 162.26, 161.40, 161.22, 140.04, 128.27, 128.24, 127.89, 122.48, 122.45, 77.33, 74.10, 74.83, 70.99, 52.87, 51.82, 51.7, 45.34, 44.78, 44.73, 44.71, 44.04, 44.00,

37.97, 37.13, 31.3, 23.68,21.96, 21.70, 19.45, 19.33, 18.35, 17.98, 17.84, 17.69, 12.25, 12.24, 9.81, 0.00

(2S,3R)-2-(5-[(1R) and (1S), (2R) and (2S)-3-tert-butyldimethylsilyloxy-1,2-dimethylpropyl]oxazol-2-yl)-3-hydroxymethyl-1-methylaziridine (43). A solution of zirconocene dichloride (Aldrich, 341 mg, 1.167 mmol) in 9 mL of anhydrous THF was cooled to -78 °C, and n-BuLi (1.6 M solution in hexanes, 1.556 mL, 2.499 mmol) was added dropwise. After the resulting yellow solution was stirred at -78 °C for 1 h, a solution of the allyl ether **42** (307 mg, 0.778 mmol) in anhydrous THF (9 mL, including cannula and flask washings) was added dropwise via cannula. The yellow solution was stirred at -78 °C for 5 min, the cooling bath was removed, and the reaction mixture was allowed to warm to rt. After 1 h, the resulting dark brown solution was cooled to 0 °C, and 9 mL of saturated aqueous NH_4Cl was added. The resulting suspension was stirred at rt for 2 h and then filtered through Celite (3x5 cm) eluting with 80 mL of ether. The filtrate was washed with 2x40 mL of brine, dried (Na_2SO_4), and concentrated by rotary evaporation. The residue was purified by flash chromatography on silica gel (25x8cm, 2:1 hexane/acetone eluent, 15 mL fractions). Fractions 14-30 furnished 228 mg (83%) of the product as a pale yellow oil, analytical TLC on silica gel 60 F254, 2:1 hexane/acetone, Rf= 0.3. Molecular ion ($M+H^+$) calcd for $C_{18}H_{35}N_2O_3Si$: 355.2411; found (electrospray) *m/z*= 355.2491, error= 22 ppm; IR (neat, cm^{-1}) 3339, O-H; 1571; 600 MHz NMR ($CDCl_3$, ppm) δ 6.63 (1 H, S) 3.39 (1 H, ddd, J=12.5 6.3, 5.9 Hz) 3.8 (1 H, dd, J=6.6, 6.5 Hz) 3.64 (1 H, dd, J=10.5 Hz) 3.51-3.41(2 H, m) 3.05 (1 H, m) 2.55 (3 H, s) 2.52 (1 H, d, J=6.4 Hz) 2.11 (1 H, ddd, J=6.0, 6.0, 6.0 Hz) 2.03 (0.4 H, m) 1.86 (0.8 H, m) 1.25 (2 H, d, J=7.17 Hz) 1.15 (0.8 H,d, J=7.17 Hz) 0.90 (9 H, s) 0.80 (3 H, dd,

J=2.9,4.10) 0.04 (3 H, s) 0.0358 (3 H, s). ^{13}C NMR (150 MHz, CDCl3, ppm) δ 165.10, 162.98, 161.95, 127.7, 127.25, 71.16, 71.02, 66.68, 66.59, 52.97, 52.7, 45.41, 44.61, 44.11, 37.82, 37.16, 31.33, 23.70, 21.71, 19.12, 18.23, 18.19, 17.84, 17.81, 12.23, 9.79, 0.00

(2S,3R)-2-(5-[(1R) and (1S), (2R) and (2S) -3-tert-butyldimethylsilyloxy-1,2-dimethylpropyl]oxazol-2-yl)-3-iodomethyl-1-methylaziridine (44). A solution of Ph_3P (260 mg, 0.99 mmol) in 6 mL of anhydrous toluene was cooled to 0 °C, and diethyl azodicarboxylate (0.156 mL, 0.99 mmol) was added, followed by a solution of the alcohol **43** (228 mg, 0.640 mmol) in anhydrous toluene (3 mL, including cannula and flask washings), followed by MeI (0.06 mL, 0.99 mmol). After stirring the resulting white suspension at 0 °C for 5 min, the cooling bath was removed, and the reaction mixture was heated at 70°C for 2 h. The precipitate dissolved forming a yellow solution, which was concentrated to approximately 1 mL by rotary evaporation. The residual liquid was purified by flash chromatography on silica gel (25x8 cm, 3:1 hexane/acetone eluent, 15 x 15 mL fractions). Fractions 8-12 were concentrated to give 260 mg (87) of pure (**37)** as a clear colorless oil, analytical TLC on silica gel 60 F254, 3:1 hexane/acetone, Rf= 0.45. Molecular ion ($M+H^+$) calcd for $C_{18}H_{34}IN_2O_2Si$: 465.1429; found (electrospray) *m/z*= 465.1533, error= 22 ppm; IR (neat, cm^{-1}) 1571; 600 MHz NMR ($CDCl_3$, ppm) δ 6.68 (0.7 H, s) 6.66 (0.3 H, s) 3.52-3.38 (3 H, m) 3.30-3.19 (1 H, m) 3.12-2.96 (1 H, m) 2.78 (1 H, td, J=2.55, 1.0 Hz) 2.54 (3 H, s) 2.30-2.20 (1 H, m) 2.03 (0.3 H, m) 1.91-1.77 (0.7 H, m) 1.25 (2 H, d, J=7.23 Hz) 1.15 (1 H, d, J=7.1 Hz) 0.89 (9 H, s) 0.84-0.77 (3 H, m) 0.08-0.009 (6 H, s). ^{13}C NMR (150 MHz, $CDCl^3$, ppm) δ 158.57, 157.20, 156.26, 156.17, 123.04, 123.02, 122.61, 122.48, 77.45, 77.03, 76.60, 65.75, 65.63, 65.60, 49.05,

48.97, 47.30, 44.14, 44.11, 44.06, 40.05, 39.96, 38.68, 32.50, 32.40, 31.74, 25.91, 18.27, 16.50, 16.31, 13.91, 13.79, 13.00, 12.74, 12.52, 12.43, 6.83, 4.40, 3.61, 3.55, 3.47, -5.37, -5.403.

(2S,3R)-2-(5-[(1R) and (1S), (2R) and (2S) -3-hydroxy-1,2-dimethylpropyl]oxazol-2-yl)-3-iodomethyl-1-methylaziridine (45). To a solution of the silyl ether **44** (250 mg, 0.538 mmol) in 4 mL of anhydrous CH_3CN at rt was added HF-pyridine (ca.70% HF, 0.18 mL, 7 mmol). After stirring at rt for 45 minutes, then quenched with 4 mL of saturated aqueous $NaHCO_3$. The resulting solution was poured into 25 mL of saturated aqueous $NaHCO_3$ and extracted with 2x25 mL of CH_2Cl_2. The combined organic extract was dried (Na_2SO_4),Filtered then concentrated by rotary evaporation, and the residue was purified by flash chromatography on silica gel (28x8 cm, 3:2 hexane/acetone eluent, 15 mL fractions). Fractions 12-20 gave 170 mg (90%) of the desired product as a yellow oil, analytical TLC on silica gel 60 F254, 3:2 hexane/acetone, Rf= 0.2. Molecular ion ($M+H^+$) calcd for $C_{12}H_{20}IN_2O_2$: 465.1429; found (electrospray) *m/z*= 465.1533, error= 3 ppm; IR (neat, cm^{-1}) 3360, O-H; 1569; 600 MHz NMR ($CDCl_3$, ppm) δ 6.671 (1 H, S) 3.57 (2 H, m)3.41 (1 H, m) 3.27-3.20 (1 H, m) 3.11-3.01 (1 H, m) 2.7 (1 H, t, J=6.9) 2.55 (3 H, s) 2.27 (1 H, m) 2.06-1.89 (1 H, m) 1.27 (2 H, dd, J=4.5,2.75) 1.20 (1 H, dd, J=5.7,1.3) 0.87 (3 H, ddd, J=6.25). ^{13}C NMR (150 MHz, CDCl3, ppm) δ 158.64, 158.61, 156.80, 155.85, 155.77, 123.18, 123.17, 122.70, 122.56, 65.73, 65.62, 49.04, 48.99, 47.26, 47.21, 44.09, 44.04, 39.92, 39.86, 32.47, 32.20, 16.13, 13.45, 12.89, 3.56.

(2S,3R)-3-Iodomethyl-1-methyl-2-(5-[(1R) and (1S), (2R) and (2S) -1,2-dimethyl-3-oxopropyl]oxazol-2-yl)aziridine (46). To a solution of the alcohol **45** (147

mg, 0.420 mmol) in 3 mL of CH_2Cl_2 at °C was added Dess-Martin periodinane (285 mg, 0.670 mmol) followed by adding drop of H_2O and the resulting milky suspension was stirred at rt for 2 h. 8 mL of aqueous $NaHCO_3$-$Na_2S_2O_3$ (5% $NaHCO_3$, 15% $Na_2S_2O_3$) was added and the resulting solution was stirred for an additional 20 minutes. The reaction mixture was poured into 25 mL of aqueous NaHCO3-Na2S2O3 (5% $NaHCO_3$, 15% $Na_2S_2O_3$) and extracted with 2x50 mL of CH_2Cl_2. The combined organic extract was dried (Na_2SO_4) and concentrated by rotary evaporation and the residue was purified by flash chromatography on silica gel (28x8 cm, 3:1 hexane/acetone eluent, 20 mL fractions). Fractions 13-23 gave 114 mg (78%) of product as a pale yellow oil, analytical TLC on silica gel 60 F254, 3:1 hexane/acetone, Rf= 0.11. Molecular ion ($M+H^+$) calcd for $C_{12}H_{18}IN_2O_2$: 349.0408; found (electrospray) *m/z*= 349.0417, error= 3 ppm; IR (neat, cm^{-1}1723, C=O; 1570; 600 MHz NMR ($CDCl_3$, ppm) δ 9.73 (0.23 H, d, J=1.3 Hz) δ 9.71 (0.35 H, d, J=1.3 Hz) δ 9.73 (0.3 H, d, J=0 Hz)) 6.76 (0.6 H, s) 6.7 (0.4 H, s) 3.48-3.31 (2 H, m) 3.22 (1 H, ddd, J=2.95 Hz) 2.82-2.61 (2 H, m) 2.56 (3 h, d, J=4.9 Hz) 2.28 (1 H, quin, J=6.2 Hz) 1.33 (2 H, dd, J=3.3 Hz) 1.23 (1 H, dd, J=2.75 Hz) 1.08 (1 H, t, J=7.5 Hz) 1.03 (2 H, dd, J=7.00 Hz). ^{13}C NMR (150 MHz, CDCl3, ppm) δ 203.38, 203.27, 203.17, 203.13, 159.34, 159.27, 159.16, 154.76, 154.14, 154.76, 123.72,123.62, 123.46, 123.38, 50.42, 50.24, 49.33, 49.25, 49.16, 48.99, 47.27, 47.24, 43.93, 43.92, 43.75, 31.97, 31.77, 30.97, 30.89, 16.27, 16.18, 13.91, 13.65, 10.88, 10.59, 9.37, 9.28, 3.41, 3.40, 3.30.

(2*S*,3*R*)-2-[5-[(1*R*,2R,3*R*), (1*R*,2R,3*S*), (1R,2S3R) ,((1*S*,2R,3*R*), (1*S*,2S,3*S*) (1R,2S,3S), (!R,2R,3S),(1S,2S,3R)-3-hydroxy-1,2-dimethyl-6-*tert*-butyldimethylsilyloxy-4-hexynyl]oxazol-2-yl]-3-iodomethyl-1-methylaziridine (47). A solution of tert-butyldimethylsilyl propargyl ether[29] (838 mg, 4.92 mmol) in 38 mL of

anhydrous THF was cooled to -40 °C (Dry Ice-CH_3CN bath), and n-BuLi (1.6 M solution in hexanes, 3.07 mL, 4.92 mmol) was added dropwise. The yellowish solution was stirred at -40 °C for 1 h. The aldehyde **46** obtained as above (952 mg, 2.734 mmol) was dissolved in anhydrous THF (50 mL, including cannula and flask washings) and added dropwise via cannula. After stirring at -40 °C for 2 h, 20 mL of saturated aqueous $NaHCO_3$ was added, the cooling bath was removed and the reaction was stirred an additional 5 minutes. Poured into 200 mL $NaHCO_3$, extracted with 3x350 mL CH_2Cl_2. The combined organic extracts were dried (Na_2SO_4), concentrated by rotary evaporation, and the residue was purified by flash chromatography on silica gel (28x8 cm, 2:1 hexane/acetone eluent, 20 mL fractions). Fractions 9-17 gave 1.33 g (93%) of the desired alcohol as a pale yellow oil, analytical TLC on silica gel 60 F254, 2:1 hexane/acetone, Rf= 0.31. Molecular ion ($M+H^+$) calcd for $C_{21}H_{36}IN_2O_3Si$: 519.1534; found (electrospray) *m/z*= 519.1562, error= 5 ppm; IR (neat, $cm^{-1)}$ 3291, C=H; 1571; 600 MHz NMR ($CDCl_3$, ppm) δ 6.73 (1 H, s) 4.36 (2 H, m) 3.51-3.42 (1 H, m) 3.30-3.13 (2 H, m) 2.83 2.77 (1 H, m) 2.56 (3 H, s) 2.33 1.85 (3 H, m) 1.33-1.21 (3 H, m) 1.06-0.93 (3 H m) 0.922 (7 H, s) 0.91 (2 H, s) 0.14 (3.5 h, s) 0.12 (2.5 H, s). ^{13}C NMR (150 MHz, CDCl3, ppm) δ 158.83, 158.76, 155.65, 155.59, 123.31, 123.29, 122.94, 122.81, 84.90, 84.86, 84.72, 84.67, 84.65, 83.98, 64.88, 64.83, 64.79, 64.61, 64.47, 51.73, 51.70, 49.09, 49.01, 48.97, 47.29, 47.26, 44.02, 43.98, 43.89, 43.85, 43.81, 33.15, 25.80, 17.12, 17.01, 14.28, 13.52, 11.94, 11.90, 11.17,3.58,3.49,3.40, -5.10.

(2*S*,3*R*)-2-[5-[(1*R*,2R,3*R*), (1*R*,2R,3*S*), (1R,2S3R), ((1*S*,2R,3*R*), (1*S*,2S,3*S*) (1R,2S,3S), (1R,2R,3S),(1S,2S,3R)-3-Acetoxy-1,2-dimethyl-6-*tert*-butyldimethylsilyloxy-4-hexynyl]oxazol-2-yl]-3-iodomethyl-1-methylaziridine (48).

To a solution of alcohol **47** (1.331 g, 2.567 mmol) in 36 mL dry CH_2Cl_2 was added at rt Et_3N (1.789 mL, 12.837 mmol) dropwise, followed by Ac_2O (0.482 mL, 5.135 mmol), followed by DMAP (125 mg, 1.020 mmol). The resulting solution was stir at rt for 1h. 9 mL MeOH was added, the resulting brown solution was stirred at rt for additional 10 minutes. Poured into 300 mL Et_2O, washed with 2x300 mL brine. The organic layer were dried (Na_2SO_4), concentrated by rotary evaporation, and the residue was purified by flash chromatography on silica gel (28x8 cm, 4:1 hexane/acetone eluent, 10 mL fractions). Fractions 7-17 gave 1.213 g (84%) of the desired acetate as a pale yellow oil, analytical TLC on silica gel 60 F254, 4:1 hexane/acetone, Rf= 0.2.6. Molecular ion ($M+H^+$) calcd for $C_{23}H_{38}IN_2O_4Si$: 561.1640; found (electrospray) *m/z*= 561.1721, error= 14 ppm; IR (neat, $cm^{-)}$ 1742, C=O; 1571; 600 MHz NMR ($CDCl_3$, ppm) δ 6.74 (0.2 H, s) 6.72 (0.3 H, s) 6.69 (0.5 H, s) 5.46-5.22 (1 H, m) 4.34 (2 H, s) 3.50-3.38 (1 H, m) 3.30-2.97 (2 H, m) 2.82-2.74 (1 H, m) 2.55 (3 H, s) 2.29-2.05 (5 H, m) 1.311.18 (3 H, m) 1.02-0.92 93 H, m) 0.90 (9 H, s) 0.11 (6 H,s).). ^{13}C NMR (150 MHz, $CDCl_3$, ppm) δ169.79, 169.66, 169.63, 158.96, 158.93, 158.88, 155.94, 155.90, 155.59, 155.04, 155.02, 154.92, 123.47, 123.42, 123.36, 51.65, 51.63, 49.13, 49.08, 49.04,49.03, 49.00, 48.95, 48.93, 47.26, 47.22, 44.20, 44.16, 44.11, 44.01, 43.97, 43.94, 43.90, 42.01, 41.99, 41.11, 41.08, 40.72, 40.67, 40.19, 39.98, 33.16, 33.07, 33.03, 32.98, 32.53, 32.50, 32.33, 32.15, 25.75, 20.98, 20.95, 20.92, 20.86, 18.22, 17.37, 17.13, 16.85, 16.53, 14.05, 13.61, 13.54, 13.42, 12.81, 12.73, 12.60, 11.64, 11.57, 11.47, 11.42, 3.68, 3.60, 3.56, 3.46, 3.42, -0.0002

(1*S*,2*S*, -[(1R,2R,8R), (1R,2R,8S), (1R,2S,8R) ,((1S,2R,8R), (1S,2S,8S) (1R,2S,8S), (1R,2R,8S),(1S,2S,8R)-8-Acetoxy-9-(*tert*-butyldimethylsilyloxymethyl)-2,3,5,6,7,8-hexahydro-6,7-dimethyl-1,2-(*N*-methylaziridino)-5-oxo-1*H*-pyrrolo[1,2-

***a*]indole (49).** A solution of **48** (260 mg, 0.463 mmol) in 4.5 mL of anhydrous CH_3CN was transferred via cannula into a 10 mL round bottom flask, charged with silver triflate (190 mg, 0.742 mmol), and supported with condenser. The resulting solution was heated in an oil bath at 70 °C under N_2 for 6h. A tan solution containing a yellow precipitate of AgI formed as the reaction mixture was heated. The resulting dark brown reaction mixture was cooled to rt, and the supernatant solution was carefully transferred via cannula (2.5 mL CH_3CN used to wash to transfer) dropwise into a stirred suspension of $BnMe_3N^+CN^-$ (327 mg, 1.855 mmol) in 7.5 mL of anhydrous CH_3CN at rt. After stirring at rt for 45 min, the brown solution was poured into 60 mL of brine and extracted with 3x100 mL CH_2Cl_2. The organic extract was dried (Na_2SO_4), concentrated by rotary evaporation, and the residue was purified by flash chromatography on silica gel treated with Et_3N (11x5 cm, 50 mL/50 mL/0.5 mL hexane/EtOAc/Et_3N eluent, 5 mL fractions). Fractions 6-16 gave 44 mg (60%) purity of the **49**, Fractions 14-17 give17 mg of (90%) purity of the **49** as a pale yellow oil. Analytical TLC on silica gel 60 F254 pretreated with NEt_3 (5 min in a chamber saturated with NEt_3 vapor), neat EtOAc eluent, Rf= 0.7. Molecular ion ($M+H^+$) calcd for $C_{23}H_{37}N_2O_4Si$: 561.1640; found (electrospray) *m/z*= 561.1721, error= 9 ppm; 600 MHz NMR ($CDCl_3$, ppm) δ 6.29-5.78 (1 H, m) 4.74-4.59 (2 H, m) 4.42-4.28 (1 H, m) 4.18-4.4.06 (1 H, m) 3.06 -2.95 (1 H, m) 2.64-2.51 (1 H, m) 2.4 7-2.38 (3 H, m) 1.251.04 (3 H, m) 0.95 (9 H, s) 0.943-0.89 (3 H ,m) 0.16 (1.5 H, S) 0.13 (1.5 H, S) 0.1 (1.5 H, S) 0.7 (1.5 H, S). ^{13}C NMR (150 MHz, CDCl3, ppm) δ 190.05, 170.47, 170.30, 141.34, 140.76, 130.82, 129.36, 123.68, 123.00, 117.07, 116.45, 106.42, 71.15, 70.04, 69.85, 57.83, 57.78, 57.65, 57.52, 49.91, 49.85, 47.98, 47.93, 47.84, 47.63, 46.88, 45.59, 45.44, 44.61, 44.59, 42.38, 41.60, 40.99, 40.92, 40.84, 26.01, 25.75, 21.23,

21.05, 21.01, 18.432, 18.40, 17.38, 15.64, 12.96, 11.55, 11.49, -0.0079, -5.2818, -5.2943, -5.3607.

(1*S*,2*S*, -[(1R,2R,8R), (1R,2R,8S), (1R,2S,8R) ,((1S,2R,8R), (1S,2S,8S) (1R,2S,8S), (1R,2R,8S),(1S,2S,8R)-8-Hydroxy-9-(*tert*-butyldimethylsilyloxymethyl)-2,3,5,6,7,8 hexahydro-6,7-dimethyl-1,2-(*N*-methylaziridino)-5-oxo-1*H*-pyrrolo[1,2-*a*]indole (50). A 10 mL pear shaped flask was charged with the acetate **49** (140 mg, 0.3235 mmol), and 1% solution of NaOH in MeOH (3.3 mL) was added. After stirring at rt for 1 h, the pale tan solution was poured into 15 mL of 50% brine and extracted with 3x30 mL of CH_2Cl_2. The combined organic extract was dried (Na_2SO_4), concentrated by rotary evaporation to give a brown oil (124 mg), and the residue was carried on to the next reaction without further purification to prevent decomposition of the compound during chromatography.

(1S,2S,6S,7S) and (1S,2S,6R,7R) (1S,2S,6S,7R) and (1S,2S,6R,7S)-9-(tert-Butyldimethylsilyloxymethyl)-5,8-dioxo-2,3,5,6,7,8-hexahydro-6,7-dimethyl-1,2-(N-methylaziridino)-1H-pyrrolo[1,2-a]indole (51) To a solution of alcohol **50** (124 mg, 0.317 mmol) and *N*-methylmorpholine *N*-oxide (74.45 mg, 0.6355 mmol) in 24.0 mL of anhydrous CH_2Cl_2 was added (0.870 g) of 4Å molecular sieves (<5 micron powder activated at 150 C and 0.5 mm Hg vacuum for 10 h) in one portion. After stirring the white suspension at rt for 5 min, tetrapropylammonium perruthenate (27.91 mg, 0.0790 mmol) was added in one portion. The resulting blackish suspension was stirred at rt for 1 h, and then quickly filtered through silica (0.5x2 cm) eluting with 15 mL of EtOAc. The filtrate was concentrated by rotary evaporation, and the residue was purified by flash chromatography on silica gel (11x5 cm, neat EtOAc eluent, 10 mL fractions). Fractions

3-6 gave 87 mg (48% from the starting acetate) of the diketone as a pale yellow oil. All chromatography operations were carried out as fast as possible. Analytical TLC on silica gel 60 F254, EtOAc, Rf= 0.45 and 0.42. Molecular ion ($M+H^+$) calcd for $C_{21}H_{33}N_2O_3Si$: 389.2255; found (electrospray) *m/z*= 389.2288, error= 8 ppm; 600 MHz NMR ($CDCl_3$, ppm) δ 5.00 (1 H, AB q, J=14.7Hz) 4.95 (1 H AB q, J=14.7 Hz) 4.35 (1 H, d, J=14.00,15.6 Hz) 4.16-4.08 (1 H, m) 3.13 (1 H, d, J=5.1 Hz) 3.02-2.93 (1 H, m) 2.86 (1 h, dd, J=4.15,4.41 Hz) 2.65-2.56 (1 H, m) 2.44 (3 H, s) 1.29-1.26 (4 H, m) 1.14 (2 h, d, J=6.3 Hz) 0.96 (9 H, s) 0.14 (3 H, s) 0.134 (3 H, s). ^{13}C NMR (150 MHz, $CDCl_3$, ppm) δ 197.75, 196.84, 191.49, 190.49, 190.38, 141.36, 141.13, 128.47, 128.40, 126.96, 126.88, 126.79, 119.25, 119.20, 119.15, 59.31, 59.29, 59.20, 50.83, 50.65, 49.78, 49.76, 49.67, 49.61, 49.55, 48.96, 48.16, 47.70, 47.55, 44.58, 41.13, 26.06, 18.41, 16.16, 16.12, 15.98, 15.91, 13.52, 13.35, 0.002, -5.32, -5.4118.

(1*S*,2*S*)-9-(*tert*-Butyldimethylsilyloxymethyl)-2,3-dihydro-6,7-dimethyl-1,2-(*N*-methylaziridino)-1*H*-pyrrolo[1,2-*a*]indole-5,8-dione (52). A 10 mL flask was charged with the diketone **51** (34 mg, 0.0874 mmol) and N,N'-bis(salicylidene)ethylenediaminocobalt (II) (Aldrich, 5.6 mg, 0.01740 mmol), and filled with O_2 (balloon). A solution of 1,4-diazabicyclo[2.2.2]octane (DABCO, 0.112 mg, 1.006 mmol) in anhydrous CH_3CN (3.5 mL, including cannula and flask washings) was added via cannula under a stream of O_2. The resulting dark brown, blackish suspension was stirred under O_2 (balloon) at rt. After 2.5 h, the reaction mixture was concentrated by rotary evaporation, and the residue was purified by flash chromatography on silica gel (11x5 cm, neat EtOAc eluent, 10 mL fractions). Fractions 3-8 gave 31 mg as a mixture of the product and the starting diketone. The combined fractions was purified again by

preparative TLC on silica gel (20x20x0.025 cm, 1:1 hexane/ethyl acetate eluent) to give 12 mg (35%) of the product as an orange crystal. Analytical TLC on silica gel 60 F254, EtOAc, Rf= 0.6. Molecular ion ($M+H^+$) calcd for $C_{21}H_{31}N_2O_3Si$: 387.2098; found (electrospray) *m/z*= 387.2134, error= 9 ppm; 600 MHz NMR ($CDCl_3$, ppm) δ 5.01 (1 H, AB q, J=15 Hz) 4.99 (1 H,AB q, J=15Hz) 4.32 (1 H, d, J=13.82 Hz) 4.12-4.08 (1 H, dd, J=9.84,3.97 Hz) 3.10 (1 H, d, J=5 Hz) 2.84 (1 H, d, J=4.4, 3.8 Hz) 2.43 (3 H, s) 1.98 (3 H, s) 1.94(3 H, s) 0.96 (9 H, s) 0.15 (3 H, s) 0.875 (3 H,s). 13C NMR (150 MHz, $CDCl_3$, ppm) δ 183.92, 177.53, 141.22, 140.02, 139.46, 126.52, 123.89, 120.26, 59.41, 49.61, 47.70, 44.59, 41.17, 26.06, 18.43, 12.36, 11.89, 1.02, -0.0008, -5.33, -5.4263.

(1S,2S)-2,3-Dihydro-9-hydroxymethyl-6,7-dimethyl-1,2-(N-methylaziridino)-1H-pyrrolo[1,2-a]indole-5,8-dione (53). The HF-NEt_3 reagent was prepared by dropwise addition of HF-pyridine (ca. 70% HF, 0.10 mL, 3.9 mmol) to a solution of NEt_3 (1.4 mL, 10.0 mmol) in 3.0 mL of anhydrous CH_3CN (mildly exothermic process). 0.28 of the resulting HF-NEt_3 reagent (0.242 mmol of HF, 0.622 mmol of NEt_3) was added to a solution of the silyl ether **52** (28 mg, 0.0724 mmol) in 2 mL of anhydrous CH_3CN at rt. After stirring at rt for 11 h, the solution had turned brown and an intractable solid had formed. The brown solution was poured into 20 mL of brine and extracted with 4x15 mL of CH_2Cl_2. The combined organic extract was dried (Na_2SO_4), concentrated by rotary evaporation, and the residue was purified by flash chromatography on silica gel (11x5 cm, neat EtOAc eluent, then 10:1 CH_2Cl_2/MeOH eluent 10 mL fractions). Fractions 10-12 gave 12 mg (60%) of the product as a red crystals. Fractions 3-5 give 8 mg as a starting silyl ether **52** (28%). Analytical TLC on silica gel 60 F254, 10:1 CH_2Cl_2/MeOH, Rf= 0.56. Molecular ion ($M+H^+$) calcd for $C_{15}H_{17}N_2O_3$: 273.1233; found (electrospray)

m/z= 273.1283, error= 18 ppm; 600 MHz NMR ($CDCl_3$, ppm) δ 4.80 (1 H, dd, J=13.48, 5.2 Hz) 4.66 (1 H, dd, J=13.48, 7.1 Hz) 4.36 (1 H, d, J=13.38 Hz) 4.28-4.17 (1 H, br) 4.16 (1 H, dd, J=4.6, 3.86 Hz) 2.94 (1 H, dd, J=4.7, 3.97 Hz) 2.90 (1 H, d, J=5.03) 2.47 (3 H, s) 2.05 (3 H, s) 2.03 (3 H, s). ^{13}C NMR (150 MHz, $CDCl_3$, ppm) δ 184.98, 177.43, 141.38, 140.07, 139.51, 127.47, 126.03, 119.17, 56.66, 49.90, 47.98, 44.62, 39.37, 12.50, 11.9493, -0.0095.

(1S,2S)-2,3-Dihydro-9-{9-fluorenylmethoxycarbonylcarbamoyloxymethyl)-6,7-dimethyl-1,2-(N-methylaziridino)-1H-pyrrolo[1,2-a]indole-5,8-dione (54). To a solution of alcohol **53** (2.6 mg, 0.00954 mmol) in 0.9 mL dry DCM at - 78 °C was added Et_3N (1 M solution in DCM, 26.61 μL, 26.7μmol), followed by FmocNCO (0.33 M solution in CH_2Cl_2, 65 μL, 21.44 μmol). After stirring the red solution at -78 °C for 30 min, the cooling bath was removed, and the reaction mixture was allowed to warm to 0 °C for 1 h. 0.9 mL dry CH_3CN was added and the reaction mixture was allowed to warm to rt. After 6 h, the resulting orange solution was concentrated by rotary evaporation, and the residue was purified by flash chromatography on silica gel (11x5 cm, neat EtOAc eluent, and then 10:1 CH_2Cl_2/MeOH eluent 10 mL fractions). Fractions 3-10 gave 2.6 mg of the product as an orange to red crystals. Analytical TLC on silica gel 60 F254, 10:1 CH_2Cl_2/MeOH, Rf= 0.45. Molecular ion (M^+H^+) calcd for $C_{31}H_{28}N_3O_6$: 538.1973; found (electrospray) m/z= 538.1970, error= 1 ppm; 600 MHz NMR ($CDCl_3$, ppm) δ 7.78 (2H, d, J=7.46 Hz) 7.59 (2 H, d, J=7.46 Hz) 7.42 (2 H, t, J=7.46 Hz) 7.32 (2 H, t, J=7.46 Hz) 7.27 (1 H, s) 5.49 (1 H, d, J=12.08 Hz) 5.38 9 1 H, d, J=12.08 Hz) 4.49 (2 H, d, J=7.10 Hz) 4.36 (1 H, d, J=13.85 Hz) 4.24 (1 H, t, J=6.75 Hz) 4.15 (1 H, dd, J=13.9, 3.9 Hz) 3.31 (1 H, d, J=4.97 Hz) 2.92 (1 H, dd, J=4.9, 4.4 Hz) 2.4 (3 H, s) 2.039 (3 H, s) 2.095 (3

H, s) ^{13}C NMR (150 MHz, $CDCl_3$, ppm) δ 183.85, 177.64, 150.71, 150.54, 143.62, 143.27, 143.22, 141.66, 141.32, 139.51, 127.93, 127.19, 125.40, 124.95, 120.10, 111.13, 67.80, 58.56, 50.20, 47.92, 46.64, 44.50, 39.793, 12.35, 11.87, -0.0076.

(1S,2S)-9-Carbamoyloxymethyl-2,3-dihydro-6-methyl-1,2-(N methylaziridino)-1H-pyrrolo[1,2-a]indole-5,8-dione (3). To a solution of **54** (2.4 mg, 4.464, μL) in 0.27 mL of anhydrous CH_3CN and 0.184 mL of anhydrous CH_2Cl_2 at rt was added Et_3N (9.2 μL, 66.00 μmol). After stirring at rt for 7 h, the tan solution was concentrated by rotary evaporation, and the brown residue was purified by preparative TLC on silica gel (20x20x0.025 cm, 10:1 CH_2Cl_2/MeOH eluent) to give 1 mg (71%) of the product as an orange solid; analytical TLC on silica gel 60 F254, 10:1 CH_2Cl_2/CH_3OH, Molecular ion ($M+H^+$) calcd for $C_{16}H_{18}N_3O_4$: 316.1292; found (electrospray) *m/z*= 316.1293, error= 0 ppm; 600 MHz NMR ($CDCl_3$, ppm) δ 5.37 (1 H, AB q, J=12.4 Hz) 5.33 (1 H, AB q, J=12.4 Hz) 4.80-4.55 (2 H, br) 4.37 (1 H, d, J=13.65 Hz) 4.17 (0.55 H, dd, J=13.6, 3.66 Hz) 3.15 (1 H, d, J=4.83 Hz) 2.92 (1 H, dd, J=4.55,4.09 Hz) 2.48 3 H, s) 2.04 (3 H, s) 2.02 (3 H ,s) . ^{13}C NMR (150 MHz, CDCl3, ppm) δ 183.77, 177.70, 156.81. 142.77, 141.71, 139.36, 127.08, 125.38, 112.82, 57.77, 50.09, 47.85, 44.55, 39.88, 31.93, 29.70, 29.36, 22.69, 14.11, 12.38, 11.84, 1.02, -0.0088.

Solvolysis of the aziridinomitosene 3 in buffered methanolic solutions. General procedures. The effective "pH" of the methanolic solutions was measured using a Coming pH Meter 240 equipped with a Coming Ragged Bulb Combo electrode standardized against aqueous buffer solutions. The solvolysis reactions were carried out in a 1 mL quartz cuvette (10 mm light path) thermostatted at 20.0±0.5 °C, and were monitored using a Varian Cary 50 Bio UV-visible spectrophotometer. A 6.34 mM stock

solution of the AZM **3** (1 mg, 3.171 μmol) was prepared in 500 μL of DMSO-d_6 and was stored at -1 5 °C in the freezer. The buffer solutions were prepared using Fisher Scientific spectrophotometric grade methanol. The first order rate constants were calculated from the time-dependent decrease of the UV absorption at 480 nm using the Kinetics Application of Cary WinUV software employing the Marquardt non-linear regression analysis. Duplicate kinetic runs were performed and the results were averaged.

Methanolysis of the aziridinomitosene 3 at pH 6.0. A kinetic study. A solution of 0.060 M bis(2-hydroxyethyl)iminotris(hydroxymethyl)methane hydrochloride (Bis-Tris·HCl, 354 mg, 1.44 mmol) and 0.037 M bis(2-hydroxyethyl) iminotris (hydroxymethyl)methane (Bis-Tris, 184 mg, 0.879 mmol) was prepared in 24 mL of methanol. The pH of the resulting buffer solution was 6.0±0.1 at 20 °C. The AZM **3** (6.3 mM solution in DMSO- DMSO-d_6, 50 μL, 0.317 μmol) was dissolved in 0.95 mL of the buffer solution prepared above. The resulting yellow solution was immediately transferred into a thermostatted (20.0±0.5 °C) cuvette. The UV absorption at 480 nm was measured every 30 min for a total time of 4500 min yielding the first order rate constant of 21×10^{-6} (s^{-1})A clear yellow solution was formed at the end of the reaction.

Methanolysis of the aziridinomitosene 3 at pH 7.0. A kinetic study. A solution of 0.055 M bis(2-hydroxyethyl)iminotris(hydroxymethyl)methane hydrochloride (Bis-Tris ·HCl, 338 mg, 1.38 mmol) and 0.046 M tris(hydroxymethyl)aminomethane (TRIS, 139 mg, 1.15 mmol) was prepared in 25 mL of methanol. The pH of the resulting buffer solution was 7.0±0.1 at 20 °C. The AZM **3** (6.3 mM solution in DMSO-d_6, 50 μL, 0.317 μmol) was dissolved in 0.95 mL of the buffer solution prepared above. The resulting yellow solution was immediately transferred into a thermostatted (20.0±0.5 °C) cuvette.

The UV absorption at 480 nm was measured every 30 min for a total time of 4500 min yielding the first order rate constant of $15x10^{-5}$ (s^{-1}) A clear yellow solution was formed at the end of the reaction.

Methanolysis of the aziridinomitosene 3 at pH 8.5. A solution of 0.100 M tris-(hydroxymethyl)aminomethane (TRIS, 304 mg, 2.50 mmol) and 0.040 M tris(hydroxymethyl) aminomethane hydrochloride (TRIS HC1, 160.0 mg, 10.15 mmol) was prepared in 25 mL of methanol. The pH of the resulting buffer solution was 8.7±0.1 at 20 °C. The AZM **3** (6.3 mM solution in DMSO-d_6, 50 μL, 0.317 μmol) was dissolved in 0.95 mL of the buffer solution prepared above. The resulting pale yellow solution was immediately transferred into a thermostatted (20.0±0.5 °C) UV cuvette. No care was taken to deoxygenate the solution. The UV spectrum was scanned every 30 min for a total time of 3000 min. A clear, pale yellow solution was formed at the end of the reaction.

References

1-Mallory, C. M., Carfi, R. P., Moon, S., Cornell, K. A., and Warner, D. L. (2015). Modification of cellular DNA by synthetic aziridinomitosenes. Bioorganic and Medicinal Chemistry, 23(23), 7378-7385.

2-Hata, T., Sano, Y., Sugawara, R., Matsumate, A., Kanamori, K., Shima, T., and Hoshi, T. (1956). Mitomycin, a new antibiotic from Streptomyces. I.The Journal of Antibiotics, 9(4), 141-146.

3-Patrick, J. B., Williams, R. P., Meyer, W. E., Fulmor, W., Cosulich, D. B., Broschard, R. W., and Webb, J. S. (1964). Aziridinomitosenes: A new class of antibiotics related to the mitomycins. Journal of the American Chemical Society, 86(9), 1889-1890.

4-Fukuyama, T., Nakatsubo, F., Cocuzza, A. J., and Kishi, Y. (1977). Synthetiic studies toward mitomycins. III. Total syntheses of mitomycins A and C. Tetrahedron Letters, 18(49), 4295-4298.

5-Shaw, K. J., Luly, J. R., and Rapoport, H. (1985). Routes to mitomycins. Chirospecific synthesis of aziridinomitosenes. The Journal of Organic Chemistry, 50(23), 4515-4523.

6-Edstrom, E. D. and Tao, Y. (1997). An efficient synthesis of a fully functionalized 7-aminoaziridinomitosene. Tetrahedron, 53(13), 4549-4560.

7-Dong, W. and Jimenez, L. S. (1999). Synthesis of a fully functionalized 7-methoxyaziridinomitosene. The Journal of Organic Chemistry, 64(7), 2520-2523.

8-Vedejs, E., Klapars, A., Naidu, B. N., Piotrowski, D. W., and Tucci, F. C. (2000). Enantiocontrolled synthesis of (1 S, 2 S)-6-desmethyl-(methylaziridino) mitosene. Journal of the American Chemical Society, 122(22), 5401-5402.

9-Vedejs, E., Naidu, B. N., Klapars, A., Warner, D. L., Li, V. S., Na, Y., and Kohn, H. (2003). Synthetic enantiopure aziridinomitosenes: preparation, reactivity, and DNA alkylation studies. Journal of the American Chemical Society, 125(51), 15796-15806.

10-Chaudhary, S. K. and Hernandez, O. (1979). 4-Dimethylaminopyridine: an efficient and selective catalyst for the silylation of alcohols. Tetrahedron Letters, 20(2), 99-102.

11-Perali, R. S., Mandava, S., and Chunduri, V. R. (2011). An unexpected migration of O-silyl group under Mitsunobu reaction conditions. Tetrahedron letters, 52(23), 3045-3047.

12-Corey, E. J. and Suggs, J. W. (1975). Pyridinium chlorochromate. An efficient reagent for oxidation of primary and secondary alcohols to carbonyl compounds. Tetrahedron Letters, 16(31), 2647-2650.

13-Gregg, B. T., Golden, K. C., and Quinn, J. F. (2007). Indium (III) trifluoromethanesulfonate as an efficient catalyst for the deprotection of acetals and ketals. The Journal of Organic Chemistry, 72(15), 5890-5893.

14-Dess, D. B. and Martin, J. C. (1991). A useful 12-I-5 triacetoxyperiodinane (the Dess-Martin periodinane) for the selective oxidation of primary or secondary alcohols and a variety of related 12-I-5 species. Journal of the American Chemical Society, 113(19), 7277-7287.

15-Wadsworth, W. S. and Emmons, W. D. (1961). The utility of phosphonate carbanions in olefin synthesis. Journal of the American Chemical Society, 83(7), 1733-1738.

16-Rylander, P. N. (1990). Hydrogenation methods. Academic Pr.

17-Schöllkopf, U. and Schröder, R. (1971). 2-Unsubstituted oxazoles from α-metalated isocyanides and acylating agents. Angewandte Chemie International Edition, 10(5), 333-333.

18-Schuster, R. E., Scott, J. E., and Casanova, J. (1966). Methyl isocyanide. Organic Syntheses, 75-75.

19-Vedejs, E. and Monahan, S. D. (1996). Metalation of oxazole-Borane complexes: A practical solution to the problem of electrocyclic ring opening of 2-Lithiooxazoles. The Journal of Organic Chemistry, 61(16), 5192-5193.

20-Pfister, J. R. (1984). A one-pot synthesis of aziridines from 2-aminoethanols. Synthesis, 1984(11), 969-970.

21-Ito, H., Taguchi, T., and Hanzawa, Y. (1993). Practical zirconium-mediated deprotective method of allyl groups. The Journal of Organic Chemistry, 58(3), 774-775.

22-Kunz, H. and Schmidt, P. (1982). Synthese und reaktionen der 3-O-phosphoniogluco-und-allofuranosen. European Journal of Organic Chemistry, 1982(7), 1245-1260.

23-Holton, R. A., Kim, H. B., Somoza, C., Liang, F., Biediger, R. J., Boatman, P. D., and Kim, S. (1994). First total synthesis of taxol. 2. Completion of the C and D rings. Journal of the American Chemical society, 116(4), 1599-1600.

24- Ley, S. V., Norman, J., Griffith, W. P., and Marsden, S. P. (1994). Tetrapropylammonium perruthenate, Pr4N+ RuO4-, TPAP: a catalytic oxidant for organic synthesis. Synthesis, 1994(07), 639-666.

25- Moore, H. W. and Shelden, H. R. (1968). Rearrangement of azidoquinones. Reaction of thymoquinone and 2,5-dimethyl-1, 4-benzoquinone with sodium azide in trichloroacetic acid. The Journal of Organic Chemistry, 33(11), 4019-4024.

26- Kim, M. and Vedejs, E. (2004). A synthetic approach toward the proposed tetracyclic aziridinomitosene derived from FK317. The Journal of Organic Chemistry, 69(21), 7262-7265.

27- Vedejs, E., Naidu, B. N., Klapars, A., Warner, D. L., Li, V. S., Na, Y., and Kohn, H. (2003). Synthetic enantiopure aziridinomitosenes: preparation, reactivity, and DNA alkylation studies. Journal of the American Chemical Society, 125(51), 15796-15806.

28-Han, I. and Kohn, H. (1991). 7-Aminoaziridinomitosenes: synthesis, structure, and chemistry. The Journal of Organic Chemistry, 56(15), 4648-4653.

29- Araki, Y. and Konoike, T. (1997). Enantioselective Total Synthesis of (+)-6-epi-mevinolin and its analogs. Efficient construction of the hexahydronaphthalene moiety by high pressure-romoted intramolecular Diels- Alder reaction of (R, 2 Z, 8 E, 10 E)-1-[(tert-Butyldimethylsilyl) oxy]-6-methyl-2, 8, 10-dodecatrien-4-one. The Journal of Organic Chemistry, 62(16), 5299-5309.

APPENDIX A

^{1}H, ^{13}C NMR Spectra

Figure Number	Compound Name	NMR	Page Number
A1	4-(tert-Butyldimethylsilyloxy)-2, 3-dimethyl-2-butenoic acid ethyl ester (**33**).	^{1}H NMR	74
A 2	4-(tert-Butyldimethylsilyloxy)-2, 3-dimethyl-2-butenoic acid ethyl ester (**33**).	^{13}C NMR	75
A 3	4-(tert-Butyldimethylsilyloxy)-2, 3-dimethyl-butyric acid ethyl ester (**34**).	^{1}H NMR	76
A 4	4-(tert-Butyldimethylsilyloxy)-2, 3-dimethyl-butyric acid ethyl ester (**34**).	^{13}C NMR	77
A 5	5-[3-(tert-Butyldimethylsilyloxy)-1,2-dimethylpropyl]-oxazole (**35**).	^{1}H NMR	78
A 6	5-[3-(tert-Butyldimethylsilyloxy)-1,2-dimethylpropyl]-oxazole (**35**).	^{13}C NMR	79
A 7	2-[(lR,2S) and (lS,2S)-3-Allyloxy-l-hydroxy-2-tritylaminopropyl)-5-[(1R) and (1S) , (2R) and (2S)-tert-butyldimethylsilyloxy-1,2-dimethylpropyl]oxazole (**39**)	^{1}H NMR	80
A 8	2-[(lR,2S) and (lS,2S)-3-Allyloxy-l-hydroxy-2-tritylaminopropyl)-5-[(1R) and (1S) , (2R) and (2S)-tert-butyldimethylsilyloxy-1,2-dimethylpropyl]oxazole (**39**)	^{13}C NMR	81
A 9	2-[(2*S*,3*R*)-3-Allyloxymethyl-1-trityl-aziridin-2-yl]-5-[(1R) and (1S) , (2R) and (2S)- tert-butyldimethylsilyloxy-1,2-dimethylpropyl]oxazole (**40**)	^{1}H NMR	82
A 10	2-[(2*S*,3*R*)-3-Allyloxymethyl-1-trityl-aziridin-2-yl]-5-[(1R) and (1S) , (2R) and (2S)- tert-butyldimethylsilyloxy-1,2-dimethylpropyl]oxazole (**40**)	^{13}C NMR	83
A 11	2-[(2S,3R)-3-Allyloxymethylaziridin-2-yl]-5-[(1R) and (1S) , (2R) and (2S)- tert-butyldimethylsilyloxy-1,2-dimethylpropyl]oxazole (**41**).	^{1}H NMR	84
A 12	2-[(2S,3R)-3-Allyloxymethylaziridin-2-yl]-5-[(1R) and (1S) , (2R) and (2S)- tert-butyldimethylsilyloxy-1,2-dimethylpropyl]oxazole (**41**).	^{13}C NMR	85
A 13	2-[(2S,3R)-3-Allyloxymethyl-1-methyaziridin-2-yl]-5-[(1R) and (1S) , (2R) and (2S)- tert-butyldimethylsilyloxy-1,2-dimethylpropyl]oxazole (**42**).	^{1}H NMR	86
A 14	2-[(2S,3R)-3-Allyloxymethyl-1-methyaziridin-2-yl]-5-[(1R) and (1S) , (2R) and (2S)- tert-	^{13}C NMR	87

	butyldimethylsilyloxy-1,2-dimethylpropyl]oxazole (**42**).		
A 15	(2S,3R)-2-(5-[(1R) and (1S), (2R) and (2S)-3-tert-butyldimethylsilyloxy-1,2-dimethylpropyl]oxazol-2-yl)-3-hydroxymethyl-1-methylaziridine (43).	^{1}H NMR	88
A 16	(2S,3R)-2-(5-[(1R) and (1S), (2R) and (2S)-3-tert-butyldimethylsilyloxy-1,2-dimethylpropyl]oxazol-2-yl)-3-hydroxymethyl-1-methylaziridine (**43**).	^{13}C NMR	89
A 17	(2S,3R)-2-(5-[(1R) and (1S), (2R) and (2S) -3-tert-butyldimethylsilyloxy-1,2-dimethylpropyl]oxazol-2-yl)-3-iodomethyl-1-methylaziridine (**44**).	^{1}H NMR	90
A 18	(2S,3R)-2-(5-[(1R) and (1S), (2R) and (2S) -3-tert-butyldimethylsilyloxy-1,2-dimethylpropyl]oxazol-2-yl)-3-iodomethyl-1-methylaziridine (**44**).	^{13}C NMR	91
A 19	(2S,3R)-2-(5-[(1R) and (1S), (2R) and (2S) -3-hydroxy-1,2-dimethylpropyl]oxazol-2-yl)-3-iodomethyl-1-methylaziridine (**45**).	^{1}H NMR	92
A 20	(2S,3R)-2-(5-[(1R) and (1S), (2R) and (2S) -3-hydroxy-1,2-dimethylpropyl]oxazol-2-yl)-3-iodomethyl-1-methylaziridine (**45**).	^{13}C NMR	93
A 21	2S,3R)-3-Iodomethyl-1-methyl-2-(5-[(1R) and (1S), (2R) and (2S) -1,2-dimethyl-3-oxopropyl]oxazol-2-yl)aziridine (**46**).	^{1}H NMR	94
A 22	2S,3R)-3-Iodomethyl-1-methyl-2-(5-[(1R) and (1S), (2R) and (2S) -1,2-dimethyl-3-oxopropyl]oxazol-2-yl)aziridine (**46**).	^{13}C NMR	95
A 23	(2*S*,3*R*)-2-[5-[(1*R*,2R,3*R*), (1*R*,2R,3*S*), (1R,2S3R) ,((1*S*,2R,3*R*), (1*S*,2S,3*S*) (1R,2S,3S), (!R,2R,3S),(1S,2S,3R)-3-hydroxy-1,2-dimethyl-6-*tert*-butyldimethylsilyloxy-4-hexynyl]oxazol-2-yl]-3-iodomethyl-1-methylaziridine (**47**).	^{1}H NMR	96
A 24	(2*S*,3*R*)-2-[5-[(1*R*,2R,3*R*), (1*R*,2R,3*S*), (1R,2S3R) ,((1*S*,2R,3*R*), (1*S*,2S,3*S*) (1R,2S,3S), (!R,2R,3S),(1S,2S,3R)-3-hydroxy-1,2-dimethyl-6-*tert*-butyldimethylsilyloxy-4-hexynyl]oxazol-2-yl]-3-iodomethyl-1-methylaziridine (**47**).	^{13}C NMR	97
A 25	2*S*,3*R*)-2-[5-[(1*R*,2R,3*R*), (1*R*,2R,3*S*), (1R,2S3R), ((1*S*,2R,3*R*), (1*S*,2S,3*S*) (1R,2S,3S), (1R,2R,3S),(1S,2S,3R)-3-Acetoxy-1,2-dimethyl-6-*tert*-butyldimethylsilyloxy-4-hexynyl]oxazol-2-yl]-1023-iodomethyl-1-methylaziridine (**48**).	^{1}H NMR	98
A 26	2*S*,3*R*)-2-[5-[(1*R*,2R,3*R*), (1*R*,2R,3*S*), (1R,2S3R), ((1*S*,2R,3*R*), (1*S*,2S,3*S*) (1R,2S,3S), (1R,2R,3S),(1S,2S,3R)-3-Acetoxy-1,2-dimethyl-6-*tert*-butyldimethylsilyloxy-4-hexynyl]oxazol-2-yl]-3-iodomethyl-1-methylaziridine (**48**).	^{13}C NMR	99

A 27	(1*S*,2*S*, -[(1R,2R,8R), (1R,2R,8S), (1R,2S,8R) ,((1S,2R,8R), (1S,2S,8S) (1R,2S,8S), (1R,2R,8S),(1S,2S,8R)-8-Acetoxy-9-(*tert*-butyldimethylsilyloxymethyl)-2,3,5,6,7,8-hexahydro-6,7-dimethyl-1,2-(*N*-methylaziridino)-5-oxo-1*H*-pyrrolo[1,2-*a*]indole (**49**).	^{1}H NMR	100
A 28	(1*S*,2*S*, -[(1R,2R,8R), (1R,2R,8S), (1R,2S,8R) ,((1S,2R,8R), (1S,2S,8S) (1R,2S,8S), (1R,2R,8S),(1S,2S,8R)-8-Acetoxy-9-(*tert*-butyldimethylsilyloxymethyl)-2,3,5,6,7,8-hexahydro-6,7-dimethyl-1,2-(*N*-methylaziridino)-5-oxo-1*H*-pyrrolo[1,2-*a*]indole (**49**).	^{13}C NMR	101
A 29	(1S,2S,6S,7S) and (1S,2S,6R,7R) (1S,2S,6S,7R) and (1S,2S,6R,7S)-9-(tert-Butyldimethylsilyloxymethyl)-5,8-dioxo-2,3,5,6,7,8-hexahydro-6,7-dimethyl-1,2-(N-methylaziridino)-1H-pyrrolo[1,2-a]indole (**51**)	^{1}H NMR	102
A 30	(1S,2S,6S,7S) and (1S,2S,6R,7R) (1S,2S,6S,7R) and (1S,2S,6R,7S)-9-(tert-Butyldimethylsilyloxymethyl)-5,8-dioxo-2,3,5,6,7,8-hexahydro-6,7-dimethyl-1,2-(N-methylaziridino)-1H-pyrrolo[1,2-a]indole (**51**)	^{13}C NMR	103
A 31	(1*S*,2*S*)-9-(*tert*-Butyldimethylsilyloxymethyl)-2,3-dihydro-6,7-dimethyl-1,2-(*N*-methylaziridino)-1*H*-pyrrolo[1,2-*a*]indole-5,8-dione (**52**).	^{1}H NMR	104
A 32	(1*S*,2*S*)-9-(*tert*-Butyldimethylsilyloxymethyl)-2,3-dihydro-6,7-dimethyl-1,2-(*N*-methylaziridino)-1*H*-pyrrolo[1,2-*a*]indole-5,8-dione (**52**).	^{13}C NMR	105
A 33	(1S,2S)-2,3-Dihydro-9-hydroxymethyl-6,7-dimethyl-1,2-(N-methylaziridino)-1H-pyrrolo[1,2-a]indole-5,8-dione (**53**).	^{1}H NMR	106
A 34	(1S,2S)-2,3-Dihydro-9-hydroxymethyl-6,7-dimethyl-1,2-(N-methylaziridino)-1H-pyrrolo[1,2-a]indole-5,8-dione (53).	^{13}C NMR	107
A 35	(1S,2S)-2,3-Dihydro-9-{9-fluorenylmethoxycarbonylcarbamoyloxymethyl)-6,7-dimethyl-1,2-(N-methylaziridino)-1H-pyrrolo[1,2-a]indole-5,8-dione (**54**).	^{1}H NMR	108
A 36	(1S,2S)-2,3-Dihydro-9-{9-fluorenylmethoxycarbonylcarbamoyloxymethyl)-6,7-dimethyl-1,2-(N-methylaziridino)-1H-pyrrolo[1,2-a]indole-5,8-dione (**54**).	^{13}C NMR	109
A 37	(1S,2S)-9-Carbamoyloxymethyl-2,3-dihydro-6-methyl-1,2-(N methylaziridino)-1H-pyrrolo[1,2-a]indole-5,8-dione (**3**).	^{1}H NMR	110
A 38	(1S,2S)-9-Carbamoyloxymethyl-2,3-dihydro-6-methyl-1,2-(N methylaziridino)-1H-pyrrolo[1,2-a]indole-5,8-dione (**3**).	^{13}C NMR	111

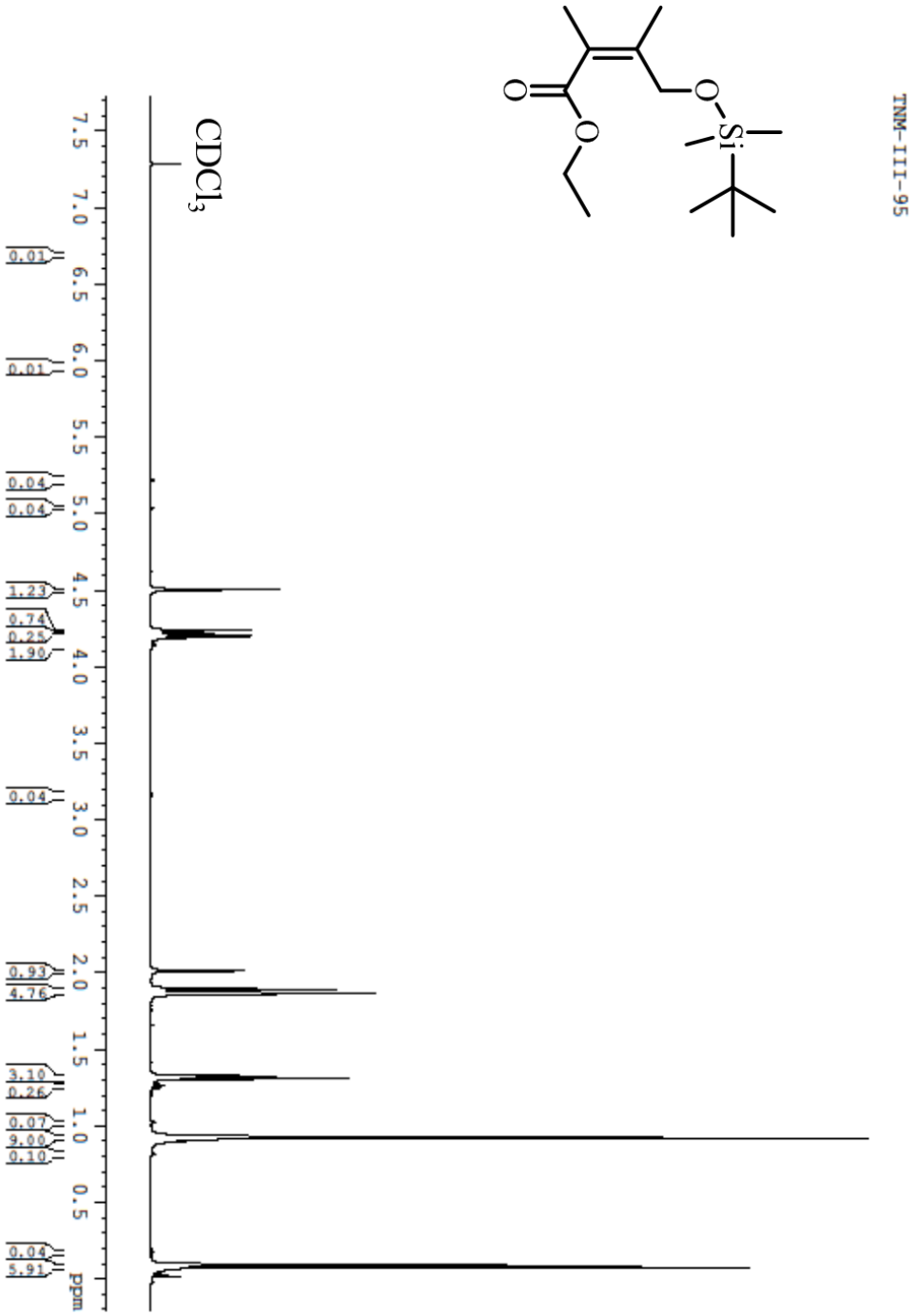

Figure A1. **^{1}H NMR spectrum of 4-(tert-Butyldimethylsilyloxy)-2, 3-dimethyl-2-butenoic acid ethyl ester (33).**

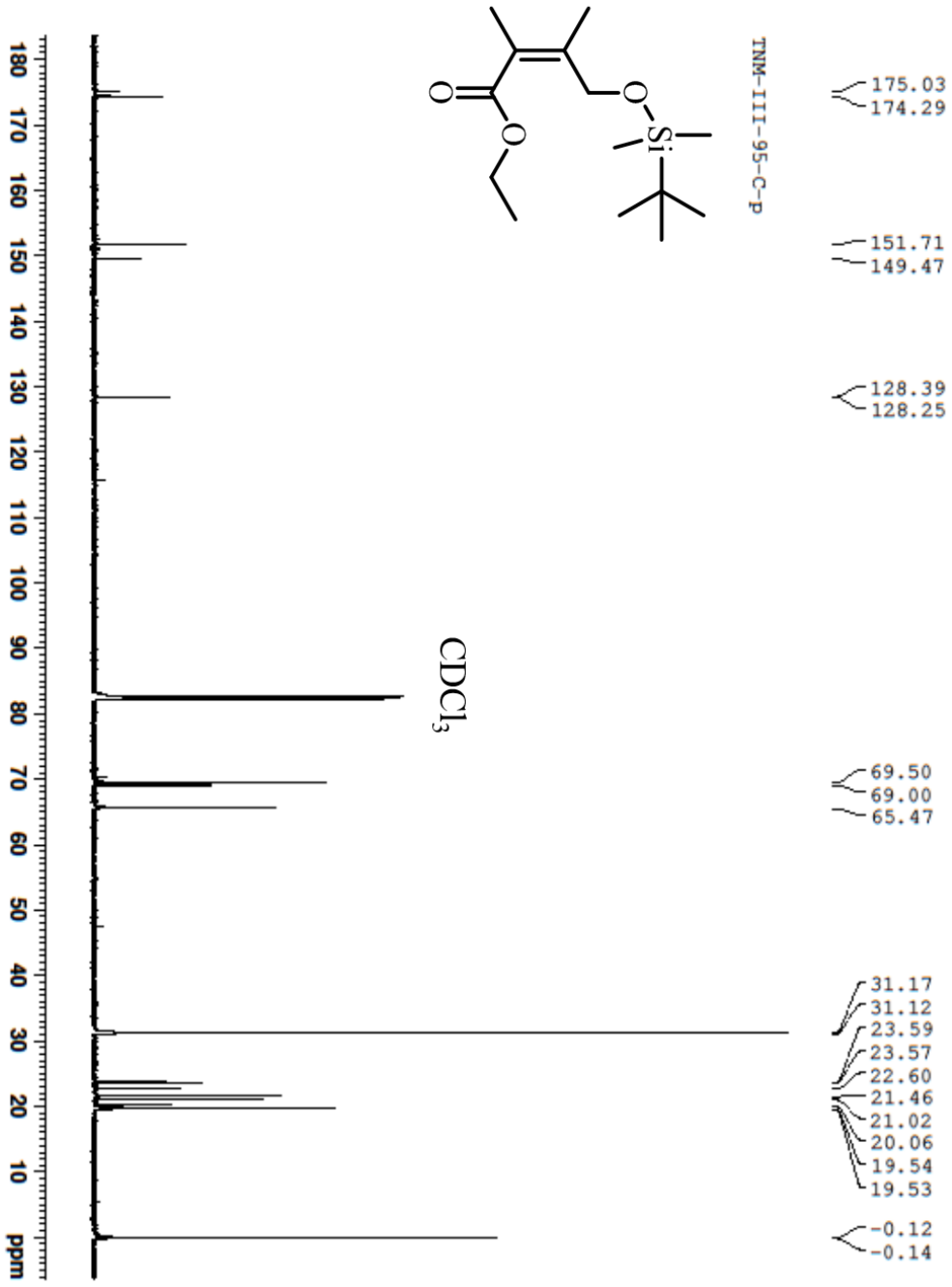

Figure A2. **^{13}C NMR of 4-(tert-Butyldimethylsilyloxy)-2, 3-dimethyl-2-butenoic acid ethyl ester (33).**

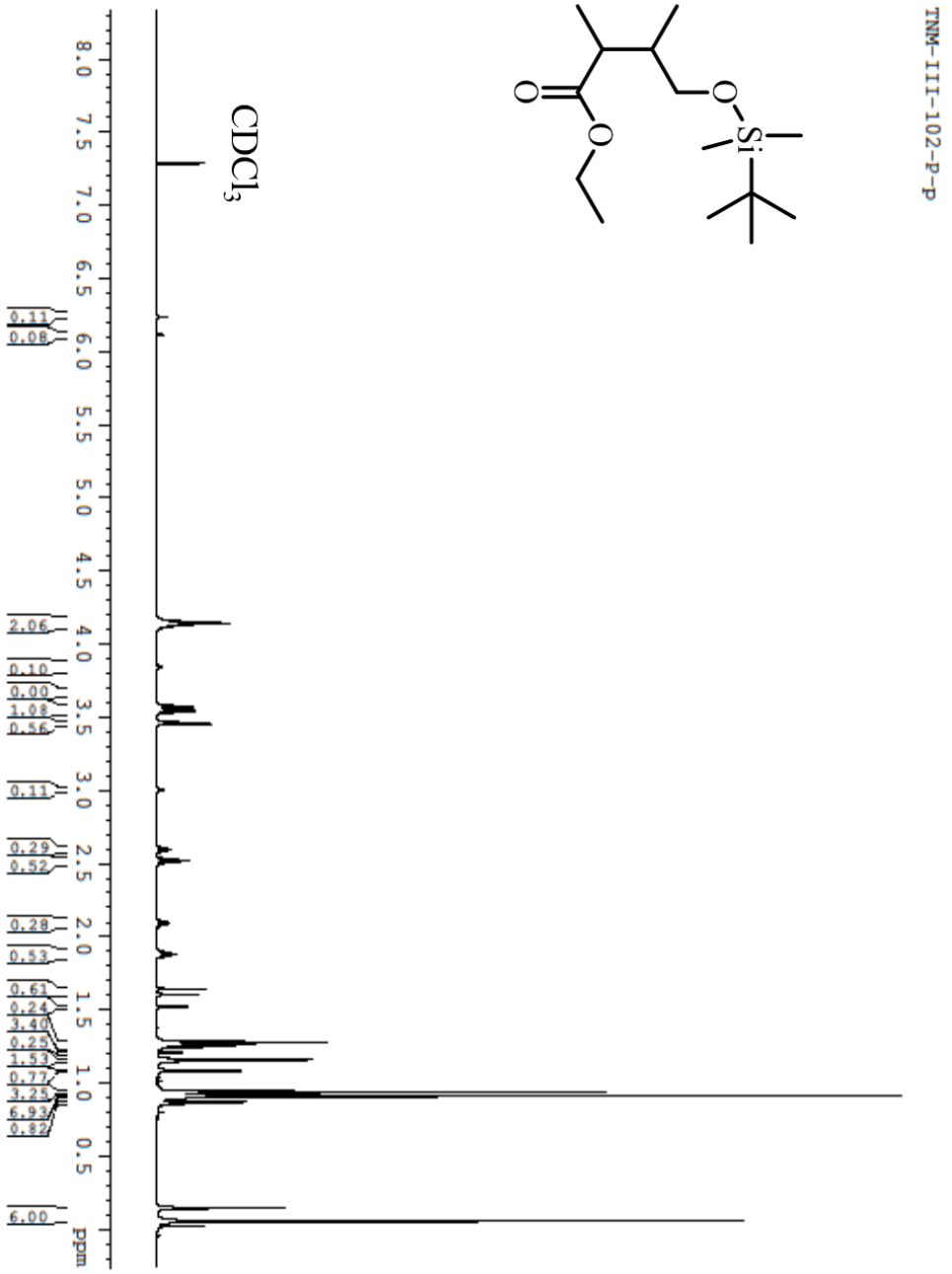

Figure A3. **^{1}H NMR spectrum of 4-(tert-Butyldimethylsilyloxy)-2, 3-dimethyl-butyric acid ethyl ester (34).**

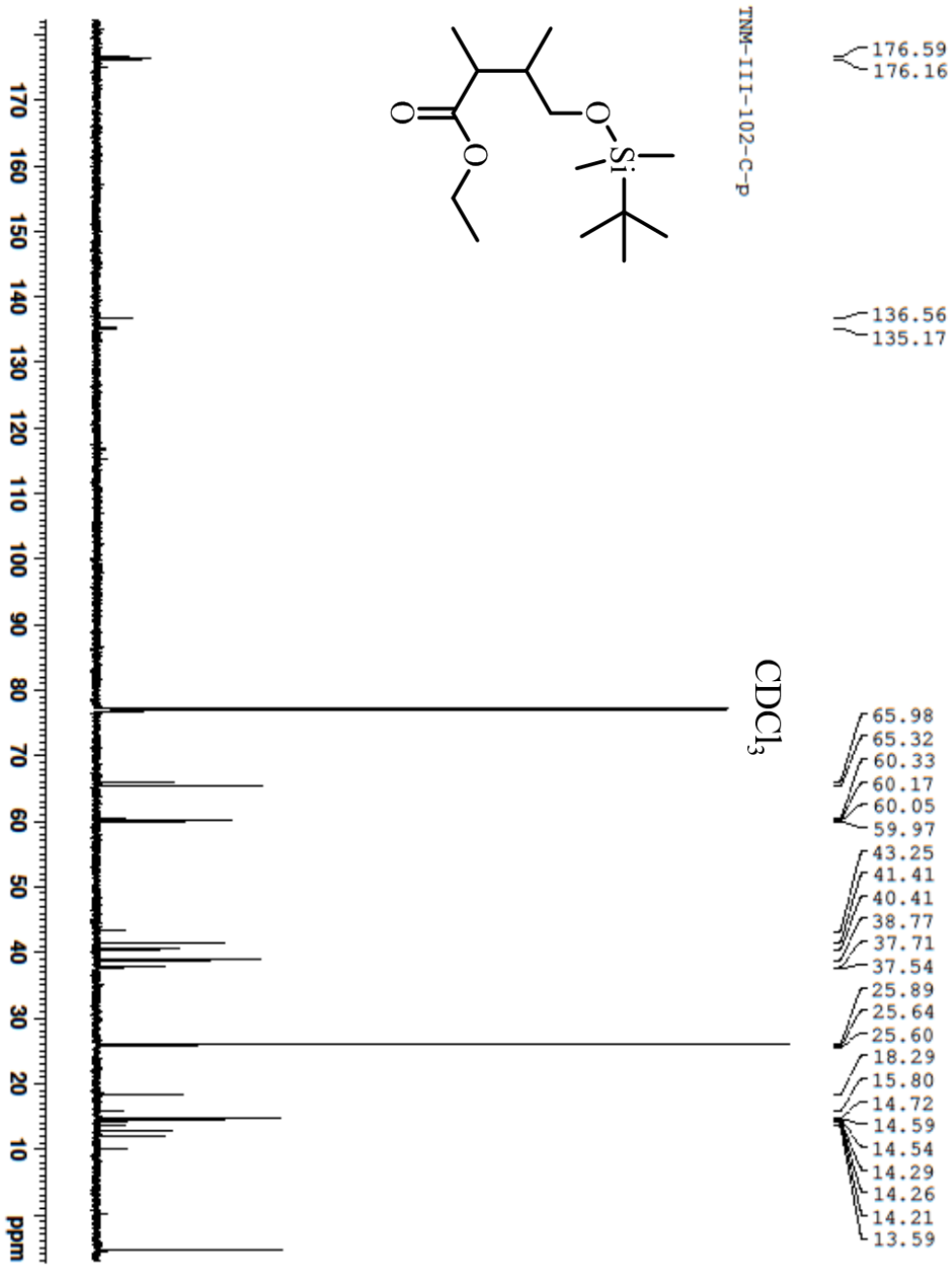

Figure A4. **^{13}C NMR spectrum of 4-(tert-Butyldimethylsilyloxy)-2, 3-dimethyl-butyric acid ethyl ester (34).**

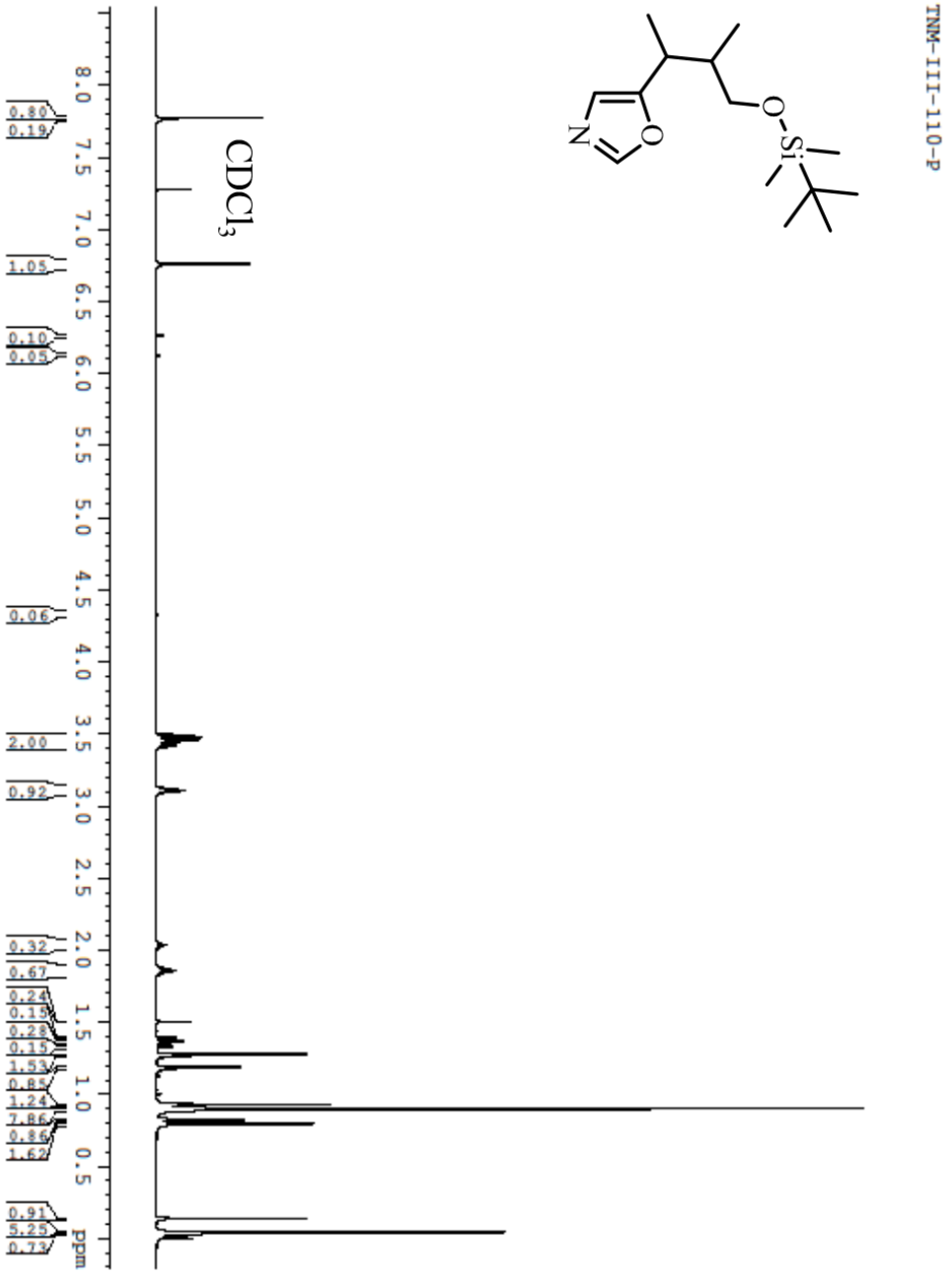

Figure A5. **^{1}H NMR spectrum of 5-[3-(tert-Butyldimethylsilyloxy)-1,2-dimethylpropyl]-oxazole (35).**

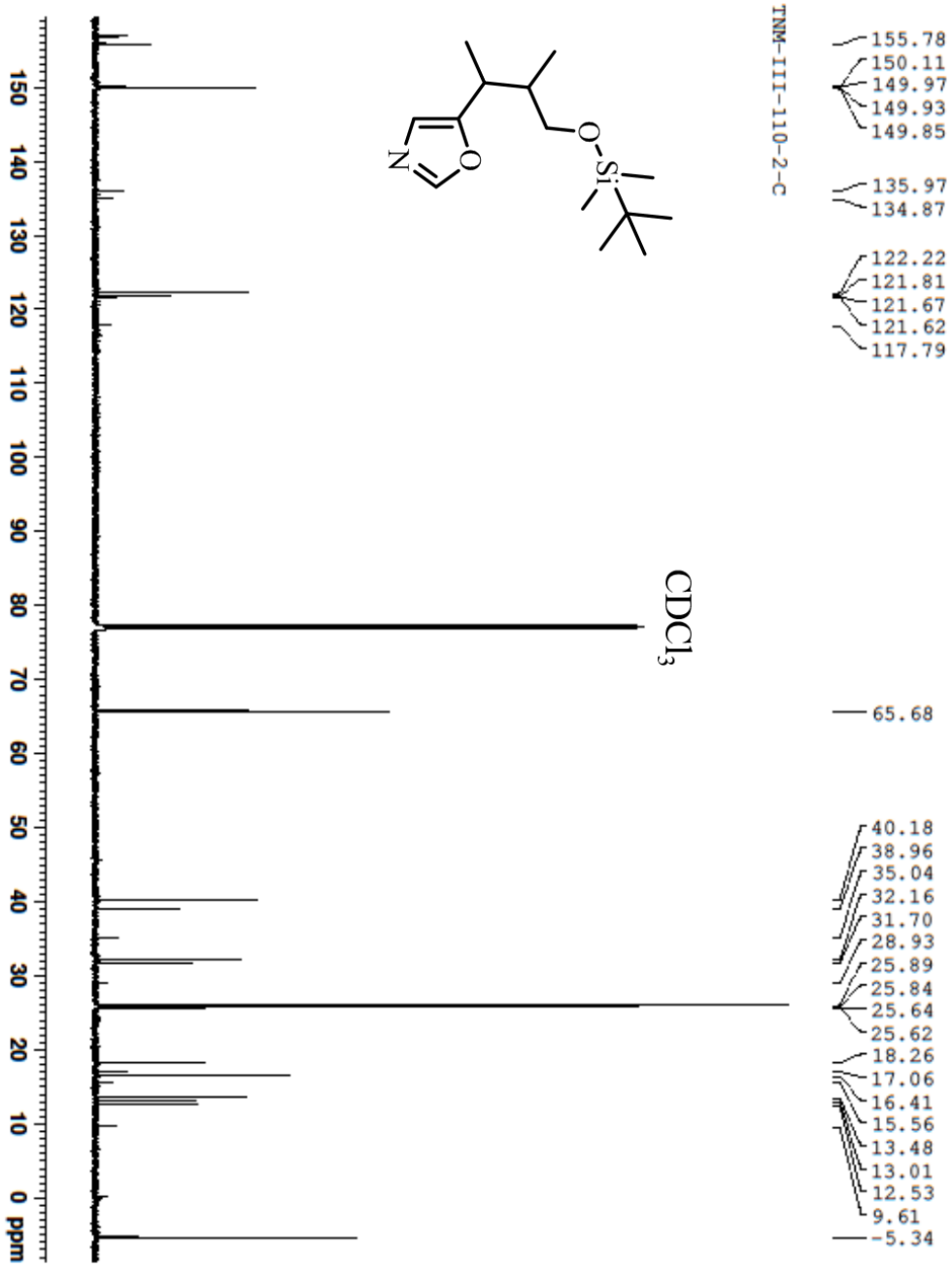

Figure A6. **^{13}C NMR of 5-[3-(tert-Butyldimethylsilyloxy)-1,2-dimethylpropyl]-oxazole (35).**

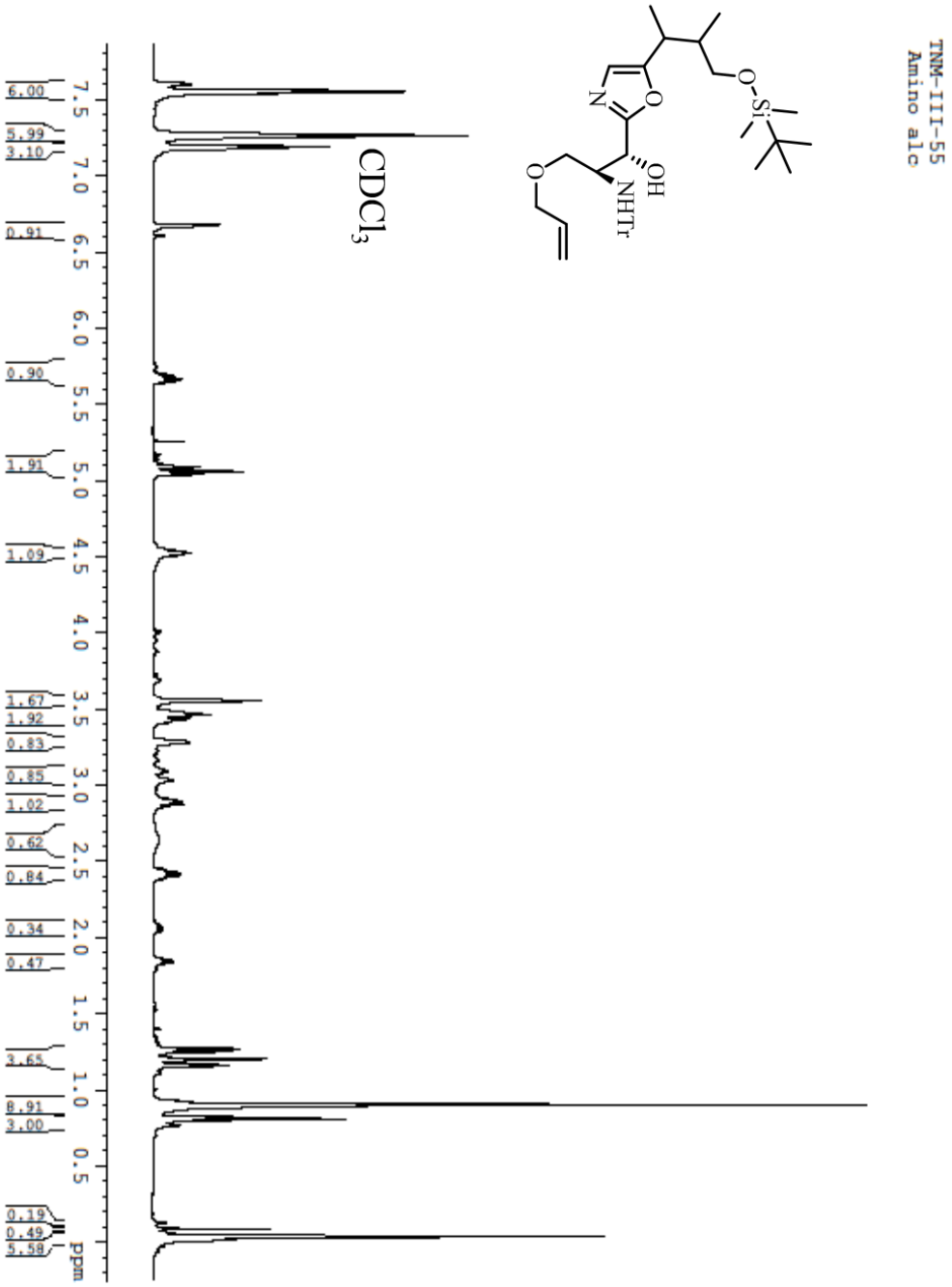

Figure A7. 1H NMR spectrum of 2-[(lR,2S) and (lS,2S)-3-Allyloxy-l-hydroxy-2-tritylaminopropyl)-5-[(1R) and (1S) , (2R) and (2S)- tert-butyldimethylsilyloxy-1,2-dimethylpropyl]oxazole (39)

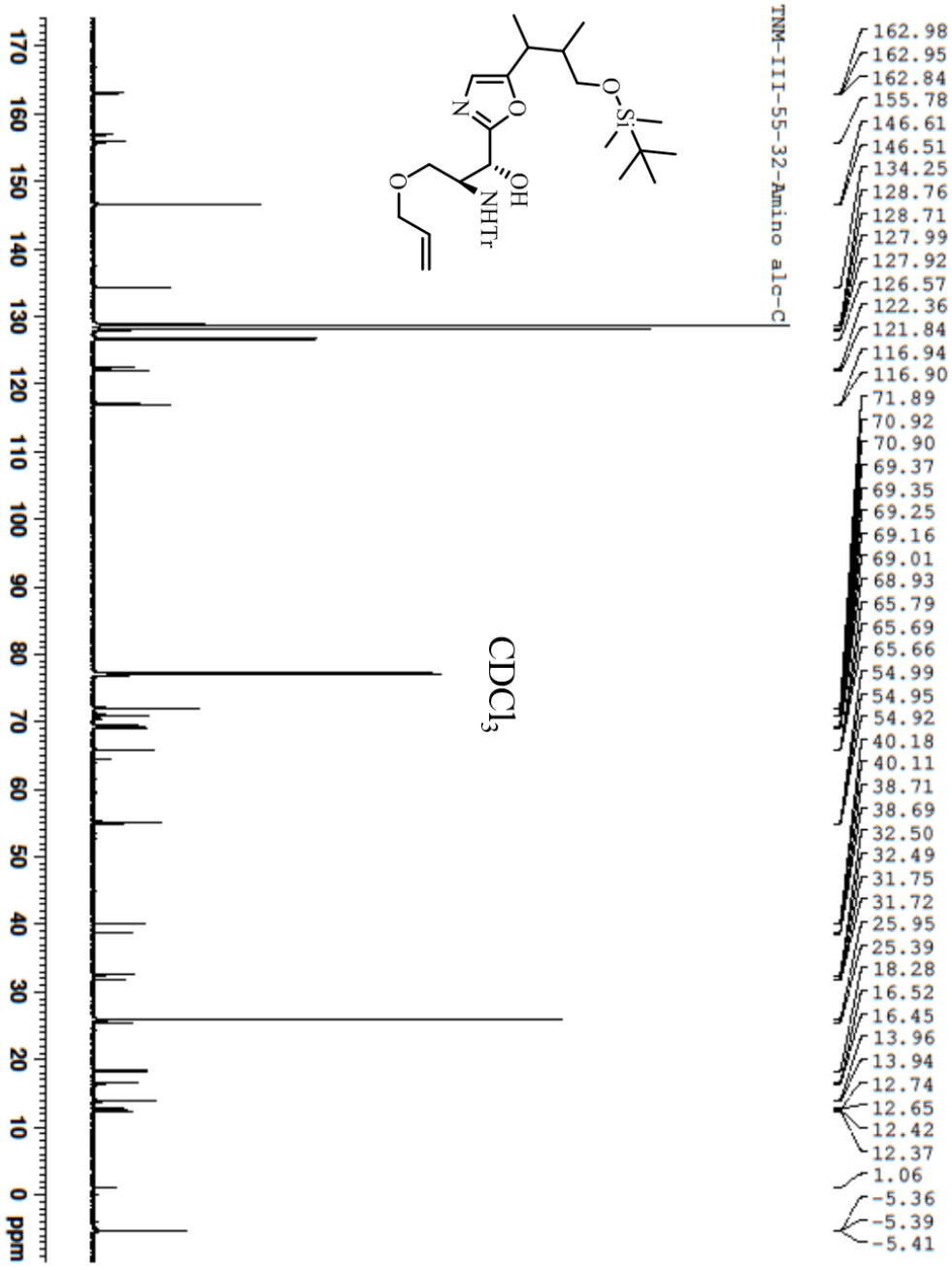

Figure A8. 13C NMR spectrum of 2-[(lR,2S) and (lS,2S)-3-Allyloxy-l-hydroxy-2-tritylaminopropyl)-5-[(1R) and (1S) , (2R) and (2S)- tert-butyldimethylsilyloxy-1,2-dimethylpropyl]oxazole (39)

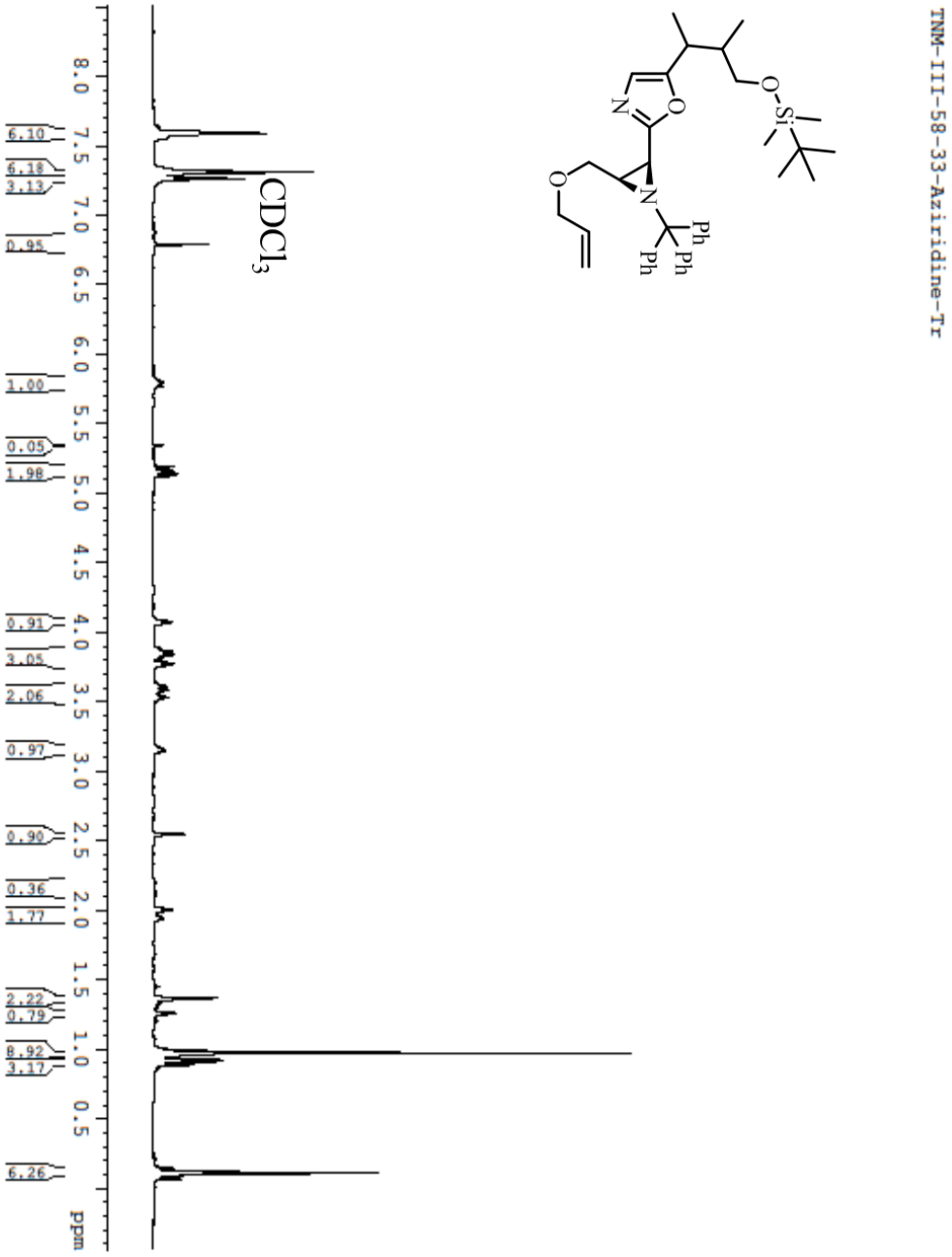

Figure A9. 1H NMR spectrum of 2-[(2S,3R)-3-Allyloxymethyl-1-trityl-aziridin-2-yl]-5-[(1R) and (1S) , (2R) and (2S)- tert-butyldimethylsilyloxy-1,2-dimethylpropyl]oxazole (40)

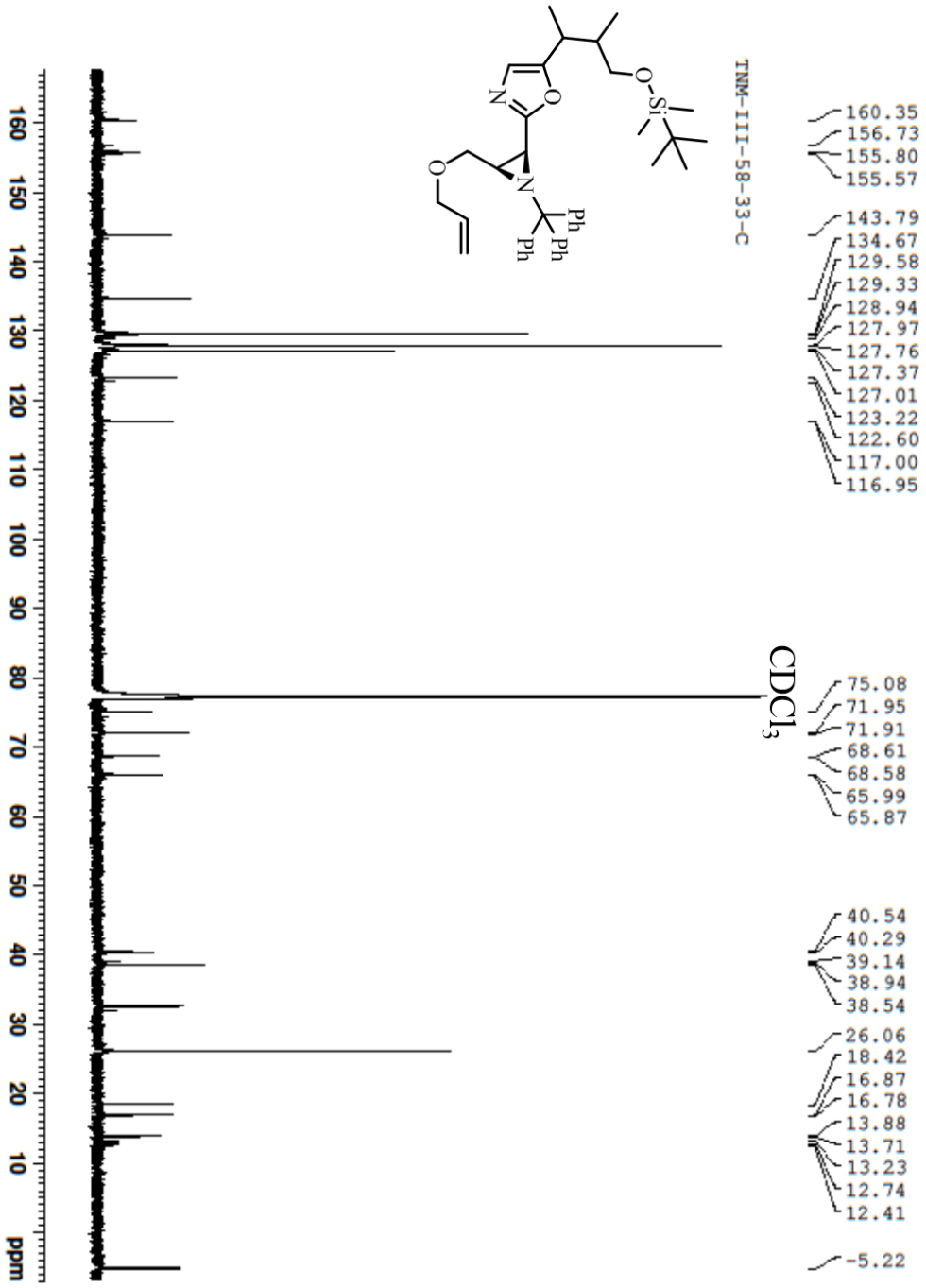

Figure A10. ^{13}C NMR spectrum of 2-[(2S,3R)-3-Allyloxymethyl-1-trityl-aziridin-2-yl]-5-[(1R) and (1S) , (2R) and (2S)- tert-butyldimethylsilyloxy-1,2-dimethylpropyl]oxazole (40)

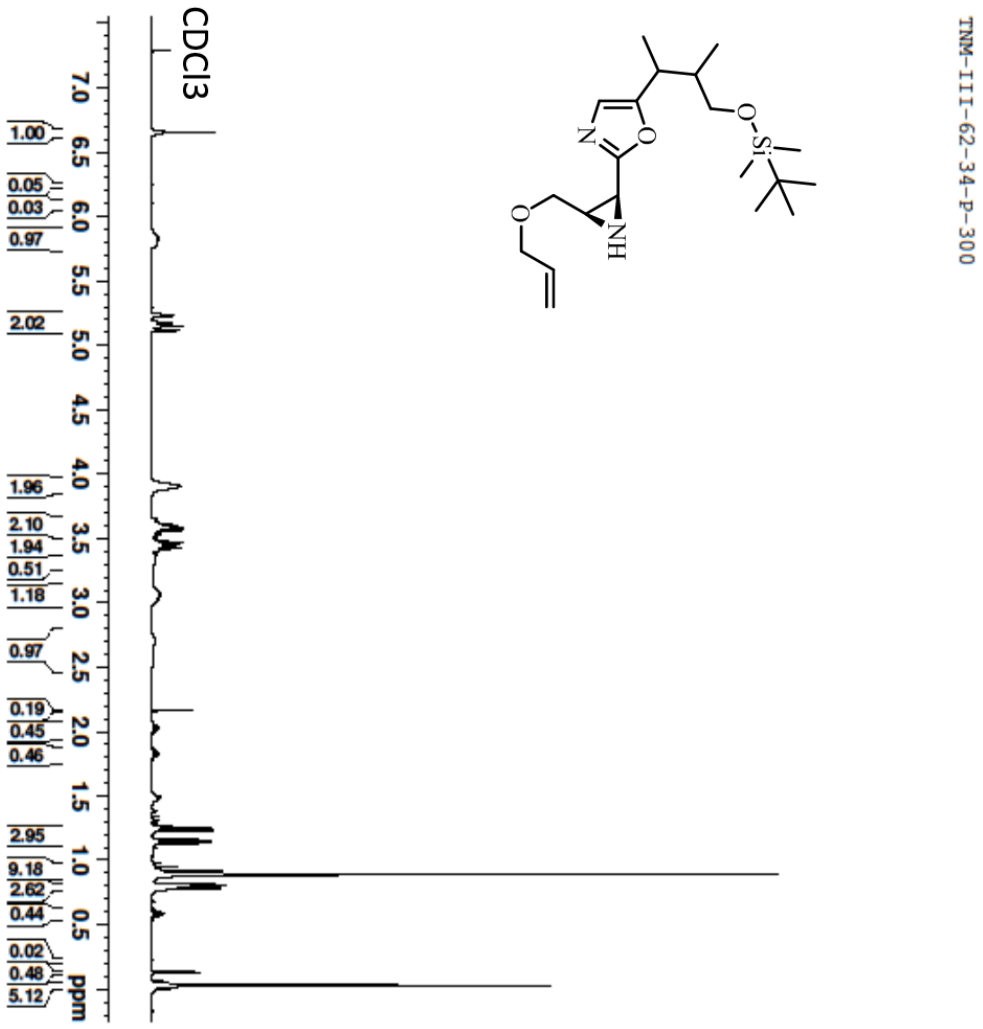

Figure A11. ^{1}H NMR spectrum of 2-[(2S,3R)-3-Allyloxymethylaziridin-2-yl]-5-[(1R) and (1S) , (2R) and (2S)- tert-butyldimethylsilyloxy-1,2-dimethylpropyl]oxazole (41).

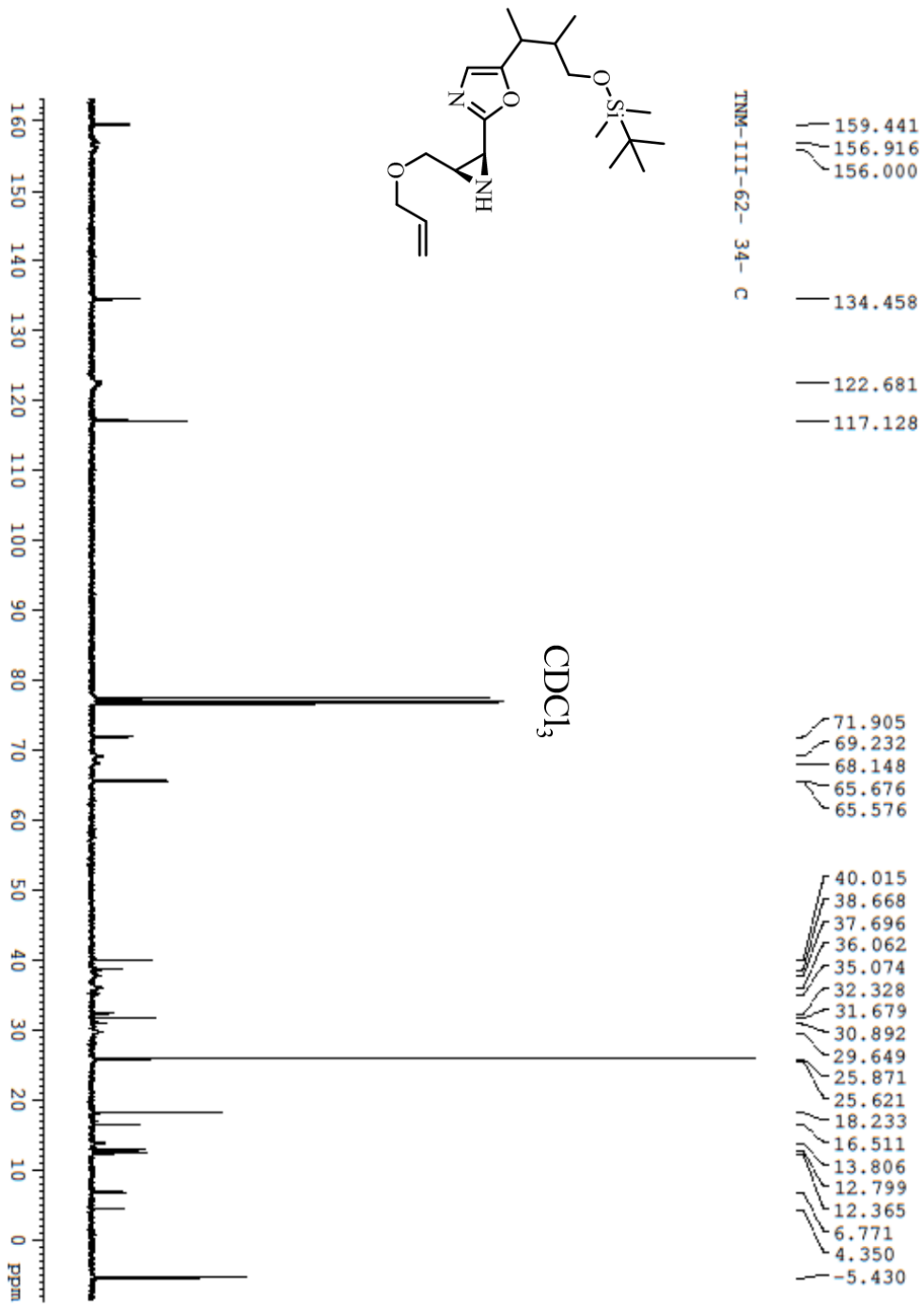

Figure A12. ^{13}C NMR spectrum of 2-[(2S,3R)-3-Allyloxymethylaziridin-2-yl]-5-[(1R) and (1S) , (2R) and (2S)- tert-butyldimethylsilyloxy-1,2-dimethylpropyl]oxazole (41).

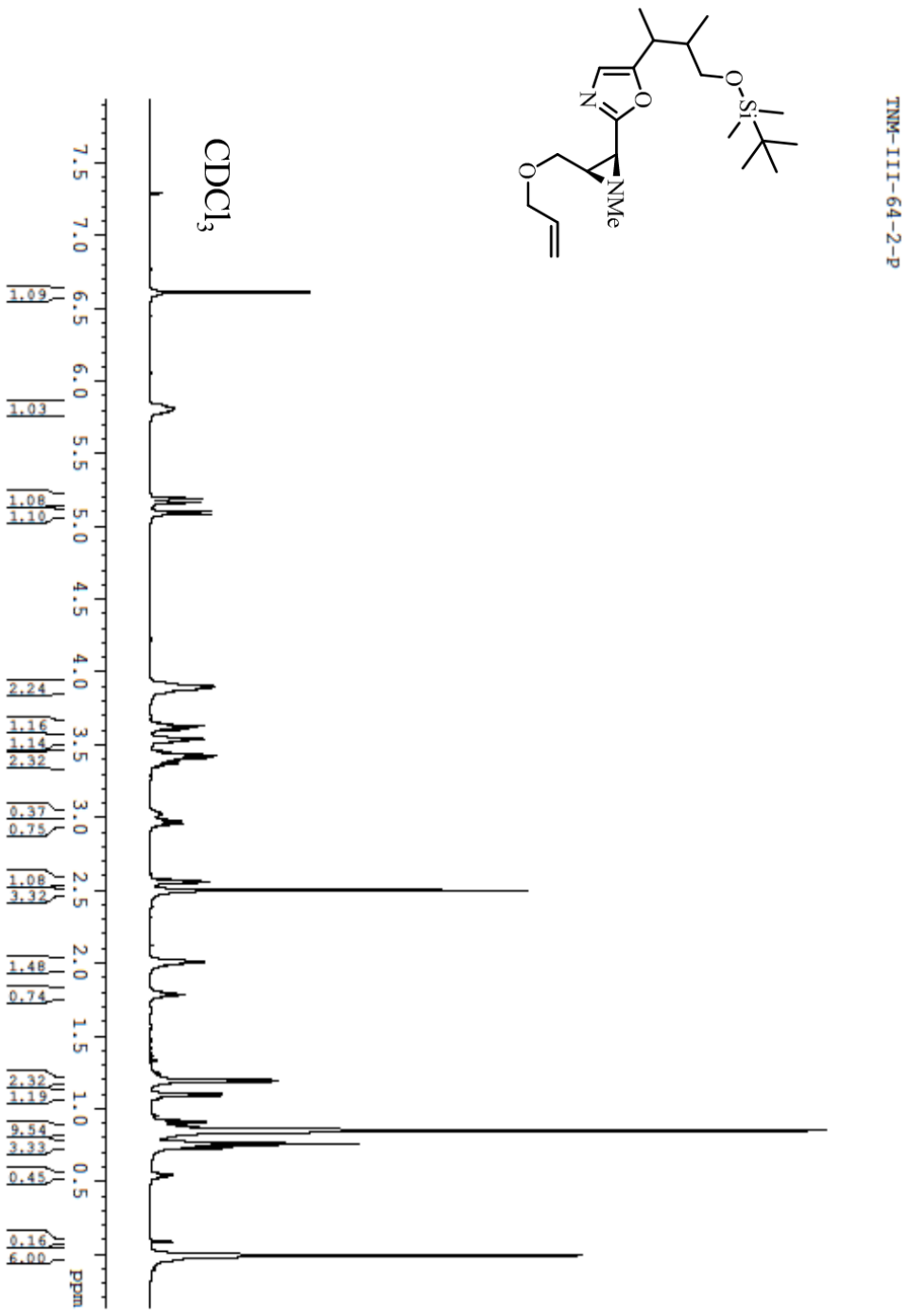

Figure A13. ^{1}H NMR spectrum of 2-[(2S,3R)-3-Allyloxymethyl-1-methyaziridin-2-yl]-5-[(1R) and (1S) , (2R) and (2S)- tert-butyldimethylsilyloxy-1,2-dimethylpropyl]oxazole (42).

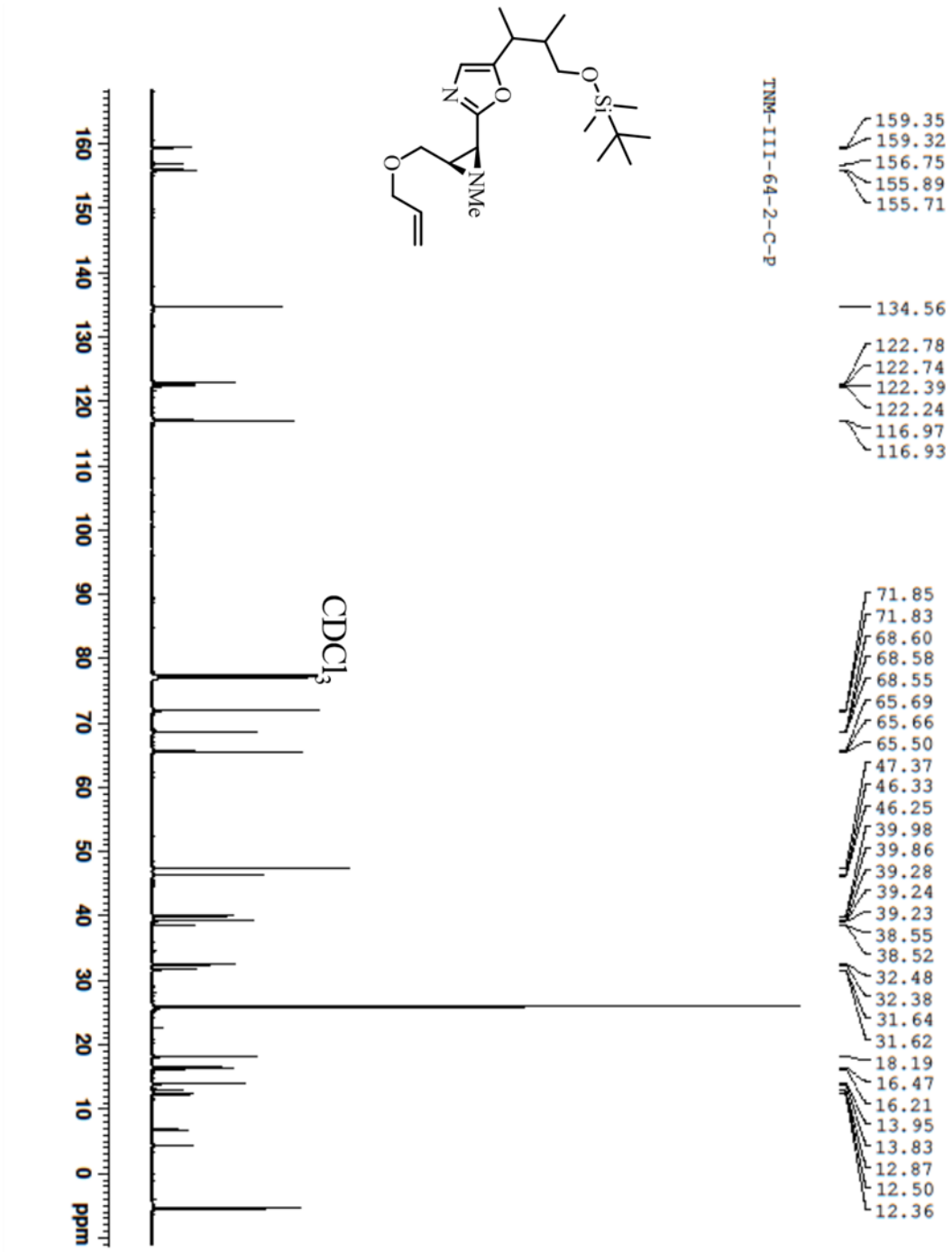

Figure A14. **^{13}C NMR spectrum of 2-[(2S,3R)-3-Allyloxymethyl-1-methyaziridin-2-yl]-5-[(1R) and (1S) , (2R) and (2S)- tert-butyldimethylsilyloxy-1,2-dimethylpropyl]oxazole (42).**

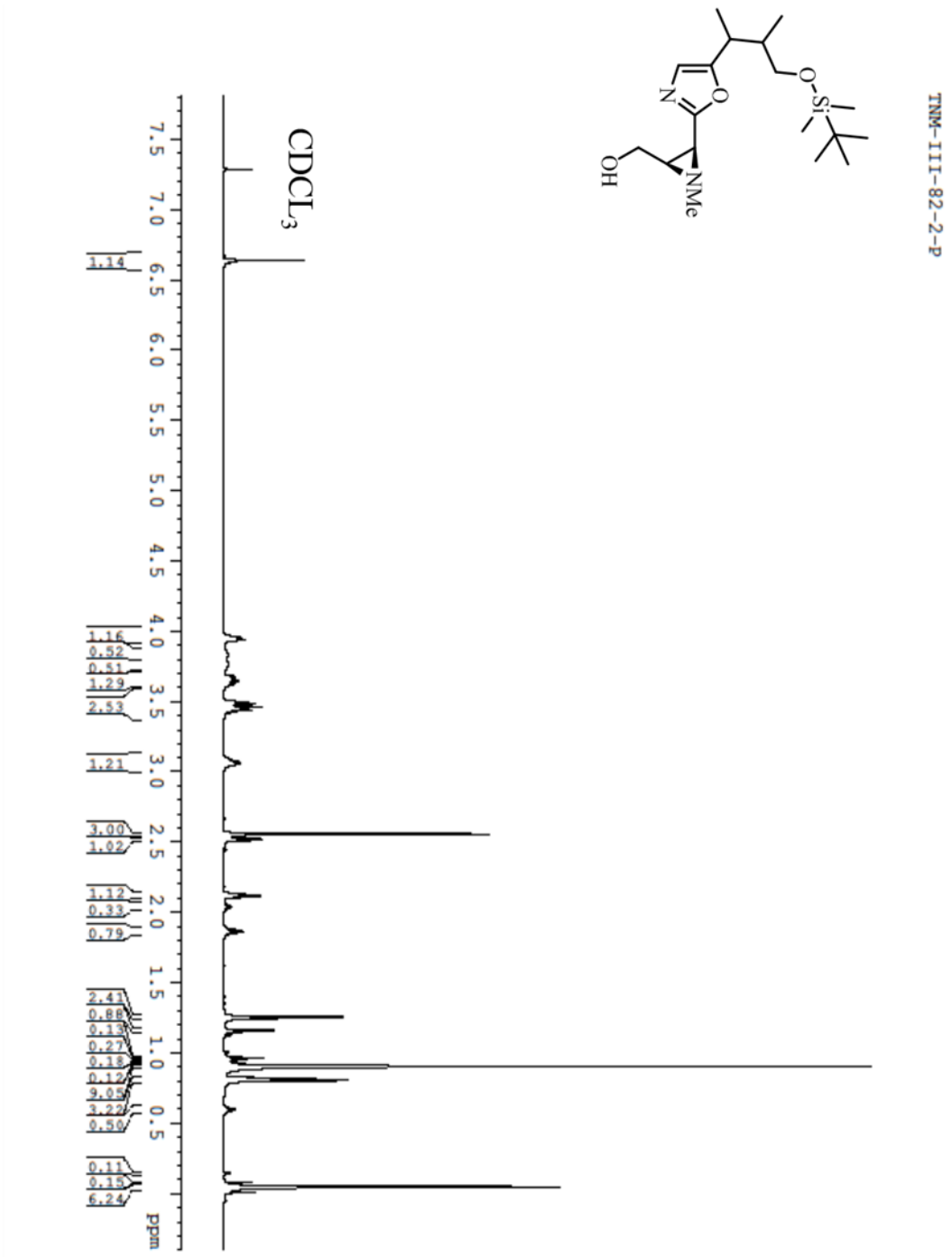

Figure A15. ^{1}H NMR spectrum of (2S,3R)-2-(5-[(1R) and (1S), (2R) and (2S)-3-tert-butyldimethylsilyloxy-1,2-dimethylpropyl]oxazol-2-yl)-3-hydroxymethyl-1-methylaziridine (43).

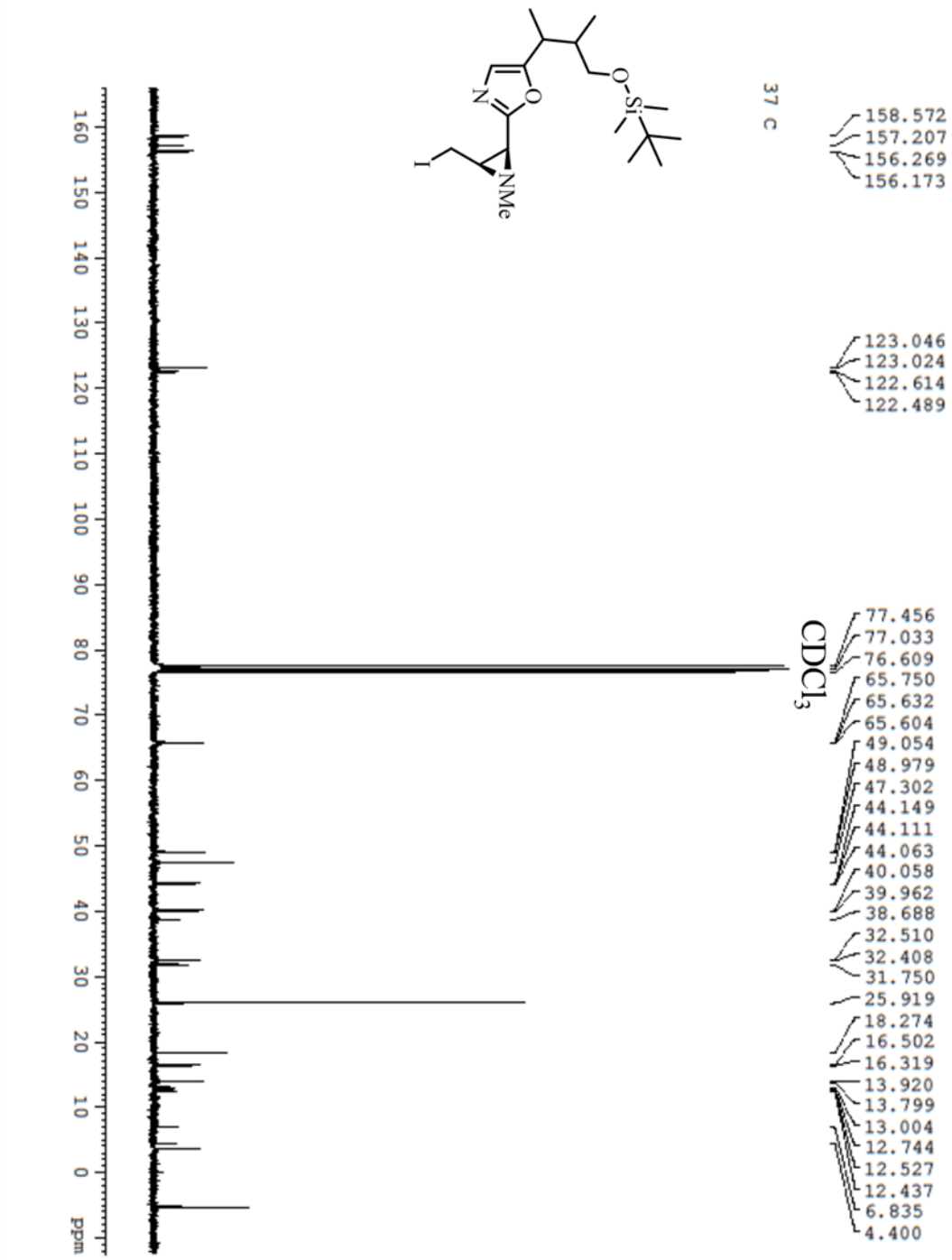

Figure A16. ^{13}C NMR spectrum of (2S,3R)-2-(5-[(1R) and (1S), (2R) and (2S)-3-tert-butyldimethylsilyloxy-1,2-dimethylpropyl]oxazol-2-yl)-3-hydroxymethyl-1-methylaziridine (43).

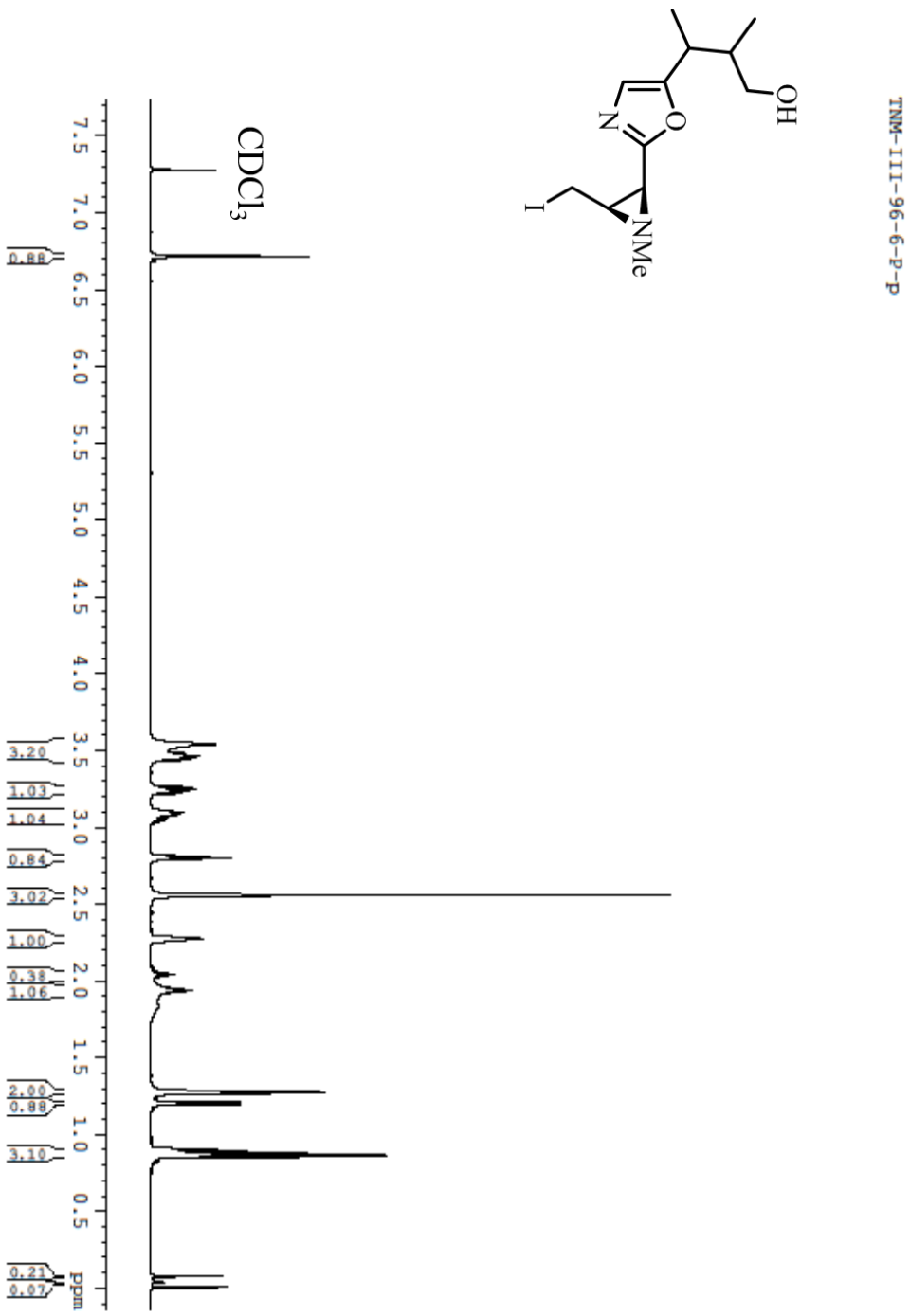

Figure A17. ^{1}H NMR spectrum of (2S,3R)-2-(5-[(1R) and (1S), (2R) and (2S) -3-tert-butyldimethylsilyloxy-1,2-dimethylpropyl]oxazol-2-yl)-3-iodomethyl-1-methylaziridine (44).

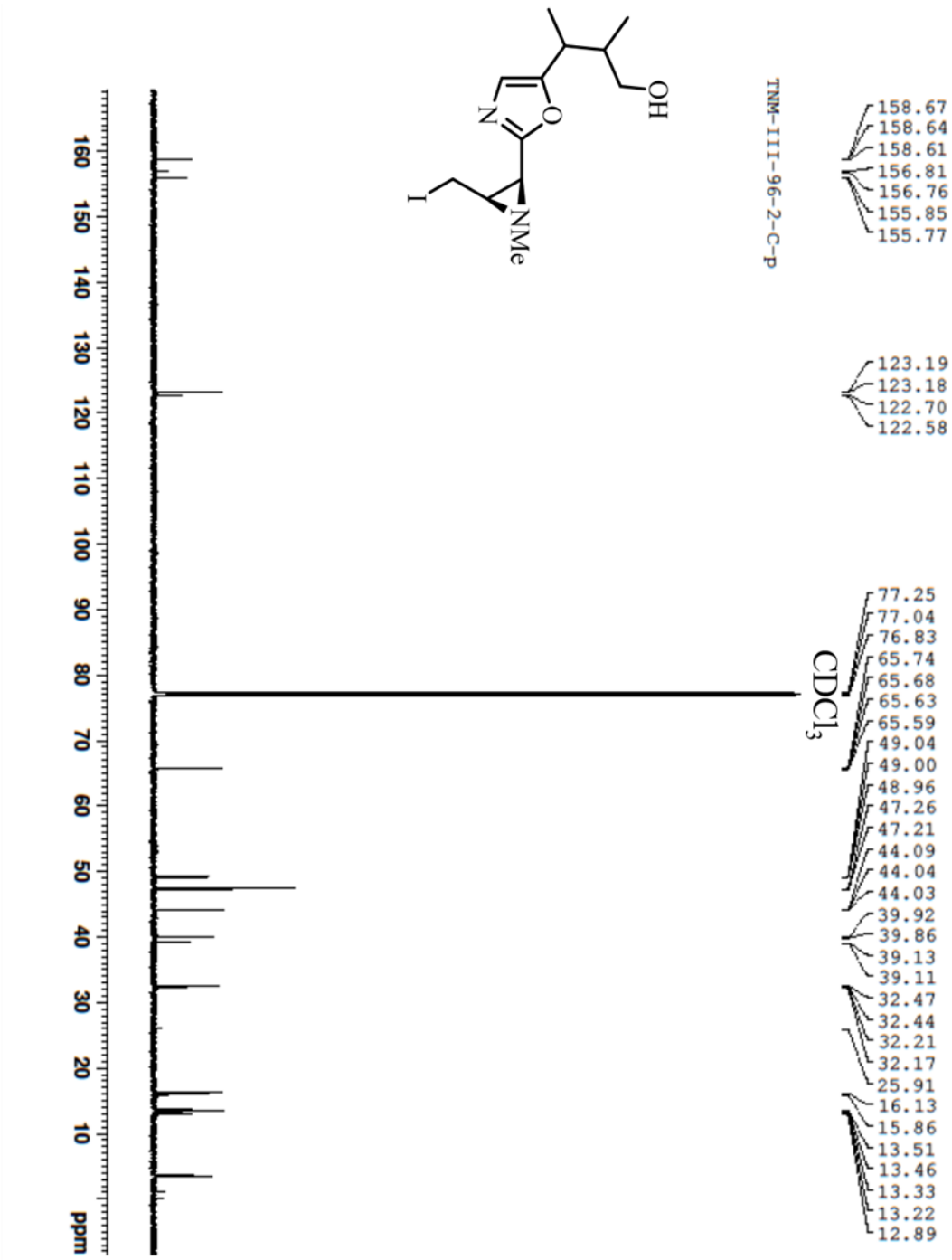

Figure A18. ^{13}C NMR spectrum of (2S,3R)-2-(5-[(1R) and (1S), (2R) and (2S) -3-tert-butyldimethylsilyloxy-1,2-dimethylpropyl]oxazol-2-yl)-3-iodomethyl-1-methylaziridine (44).

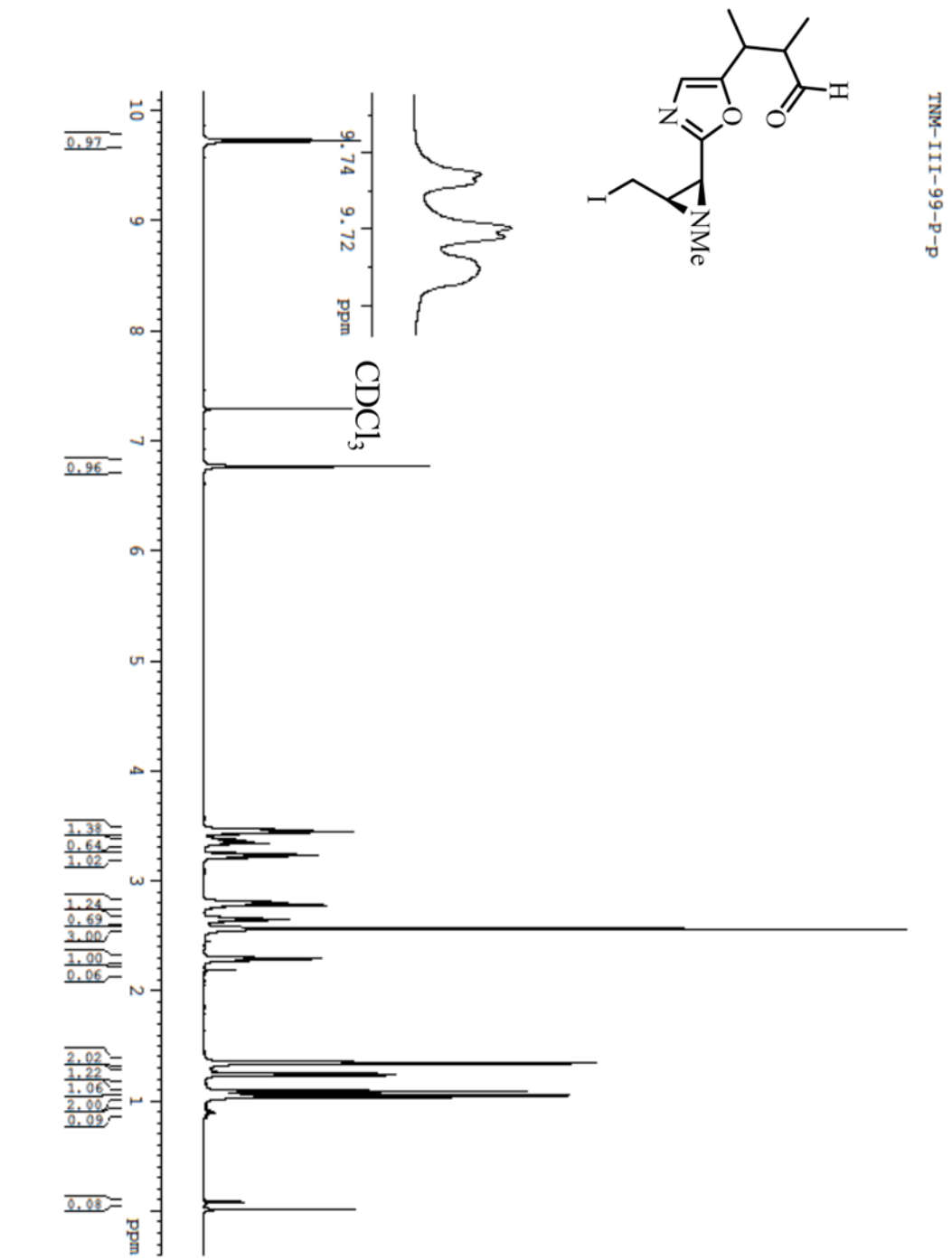

Figure A19. ^{1}H NMR spectrum of (2S,3R)-2-(5-[(1R) and (1S), (2R) and (2S) -3-hydroxy-1,2-dimethylpropyl]oxazol-2-yl)-3-iodomethyl-1-methylaziridine (45).

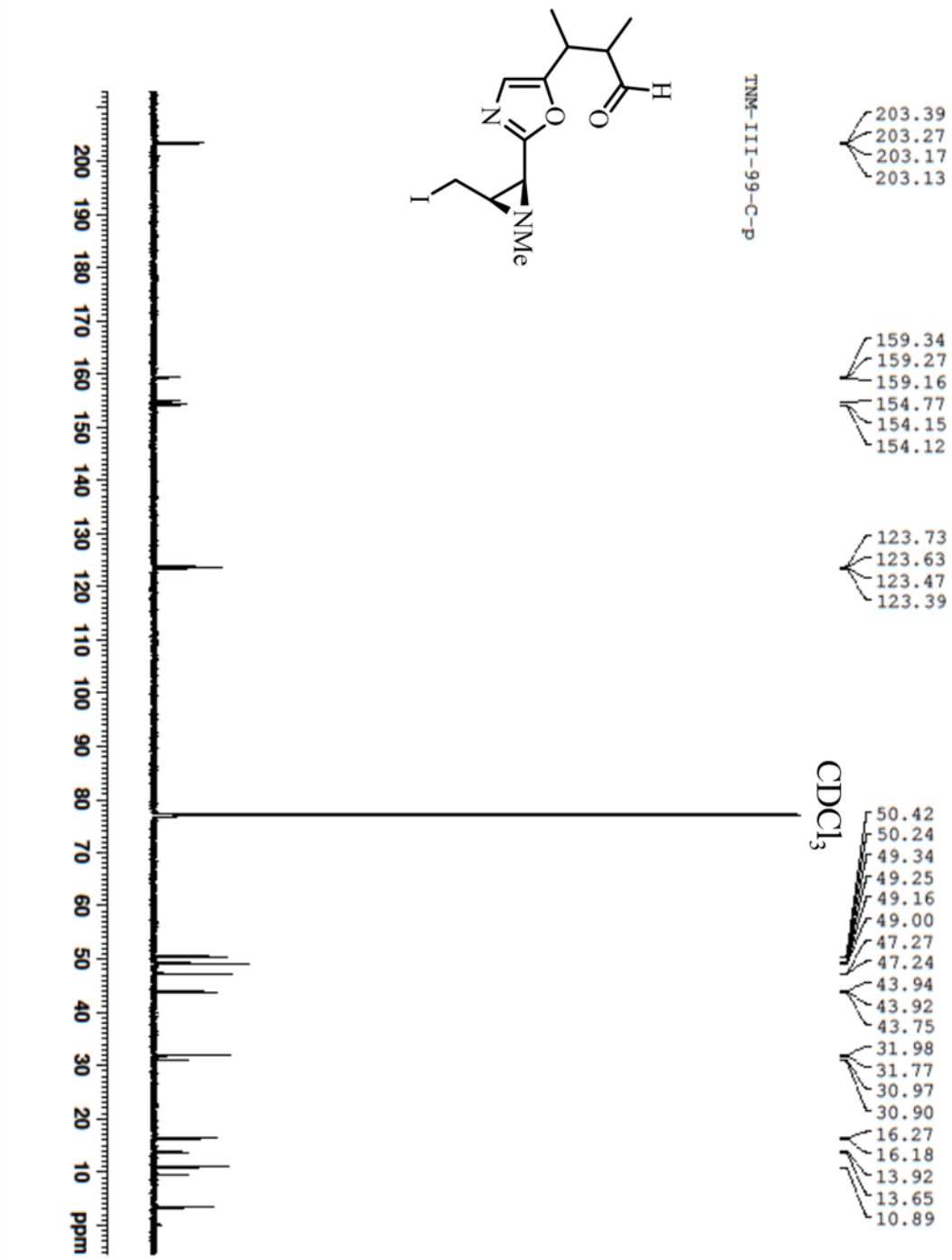

Figure A20. ^{13}C NMR spectrum of (2S,3R)-2-(5-[(1R) and (1S), (2R) and (2S) -3-hydroxy-1,2-dimethylpropyl]oxazol-2-yl)-3-iodomethyl-1-methylaziridine (45).

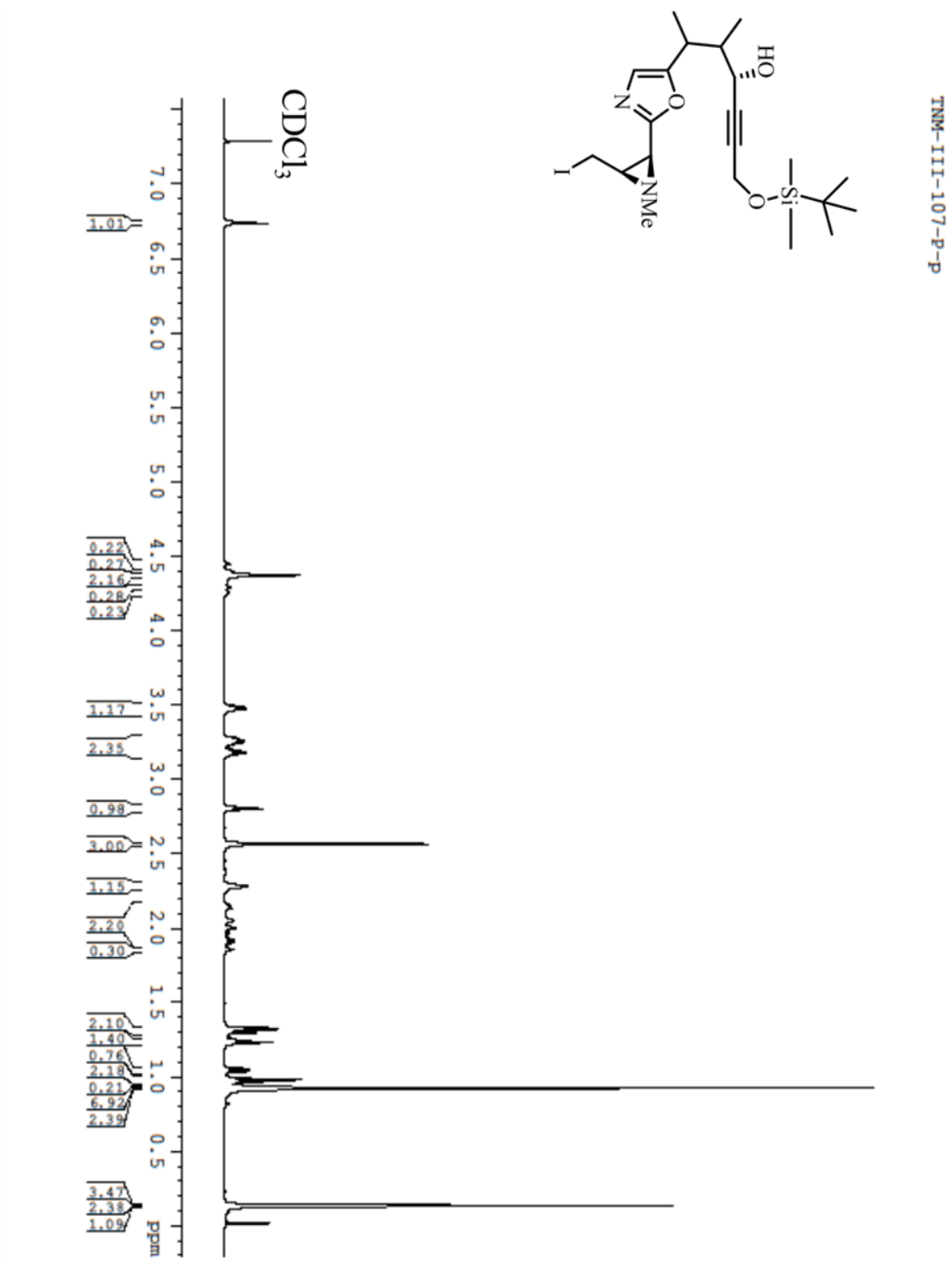

Figure A21. ^{1}H NMR spectrum of 2S,3R)-3-Iodomethyl-1-methyl-2-(5-[(1R) and (1S), (2R) and (2S) -1,2-dimethyl-3-oxopropyl]oxazol-2-yl)aziridine (46).

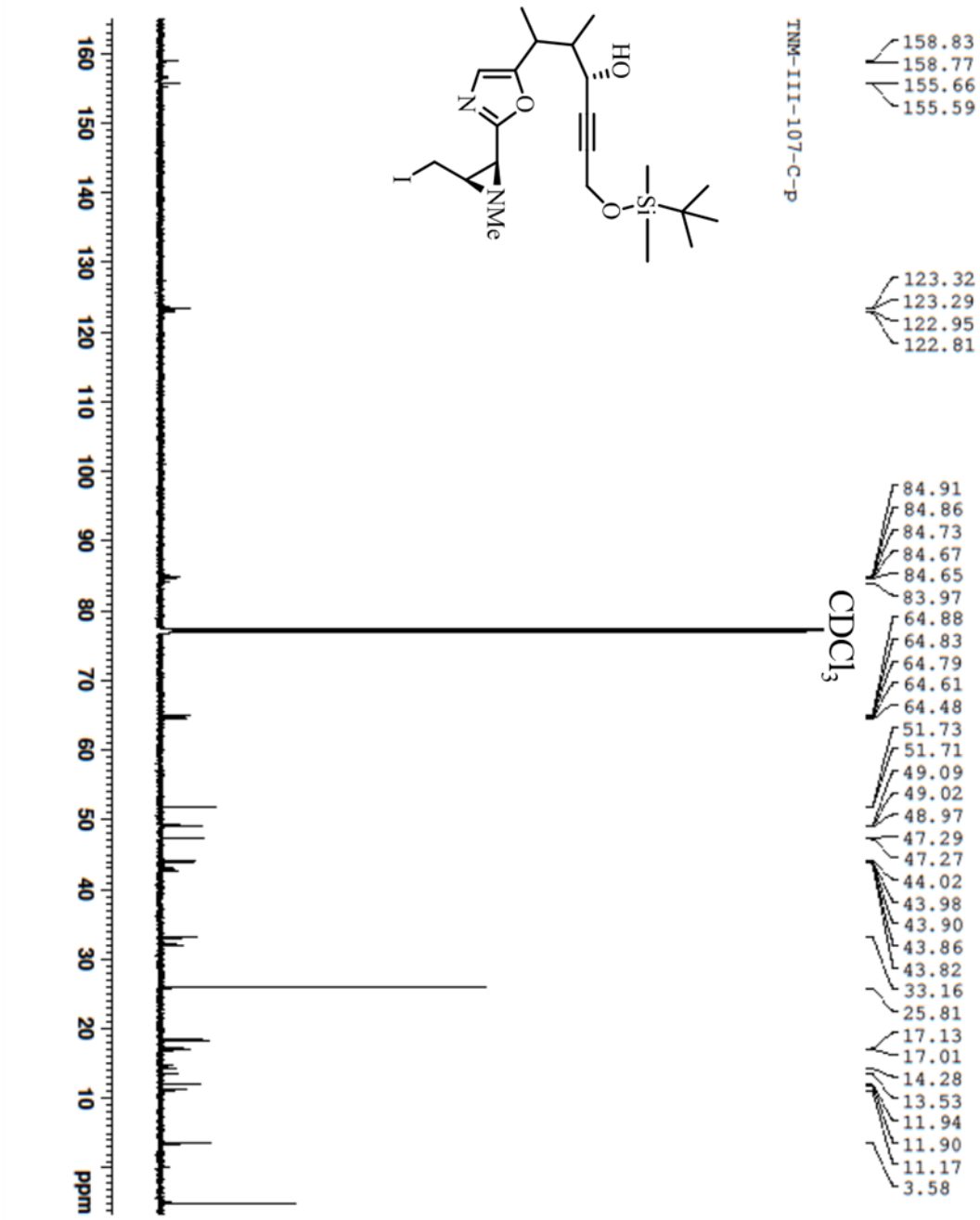

Figure A22. ^{13}C NMR spectrum of 2S,3R)-3-Iodomethyl-1-methyl-2-(5-[(1R) and (1S), (2R) and (2S) -1,2-dimethyl-3-oxopropyl]oxazol-2-yl)aziridine (46).

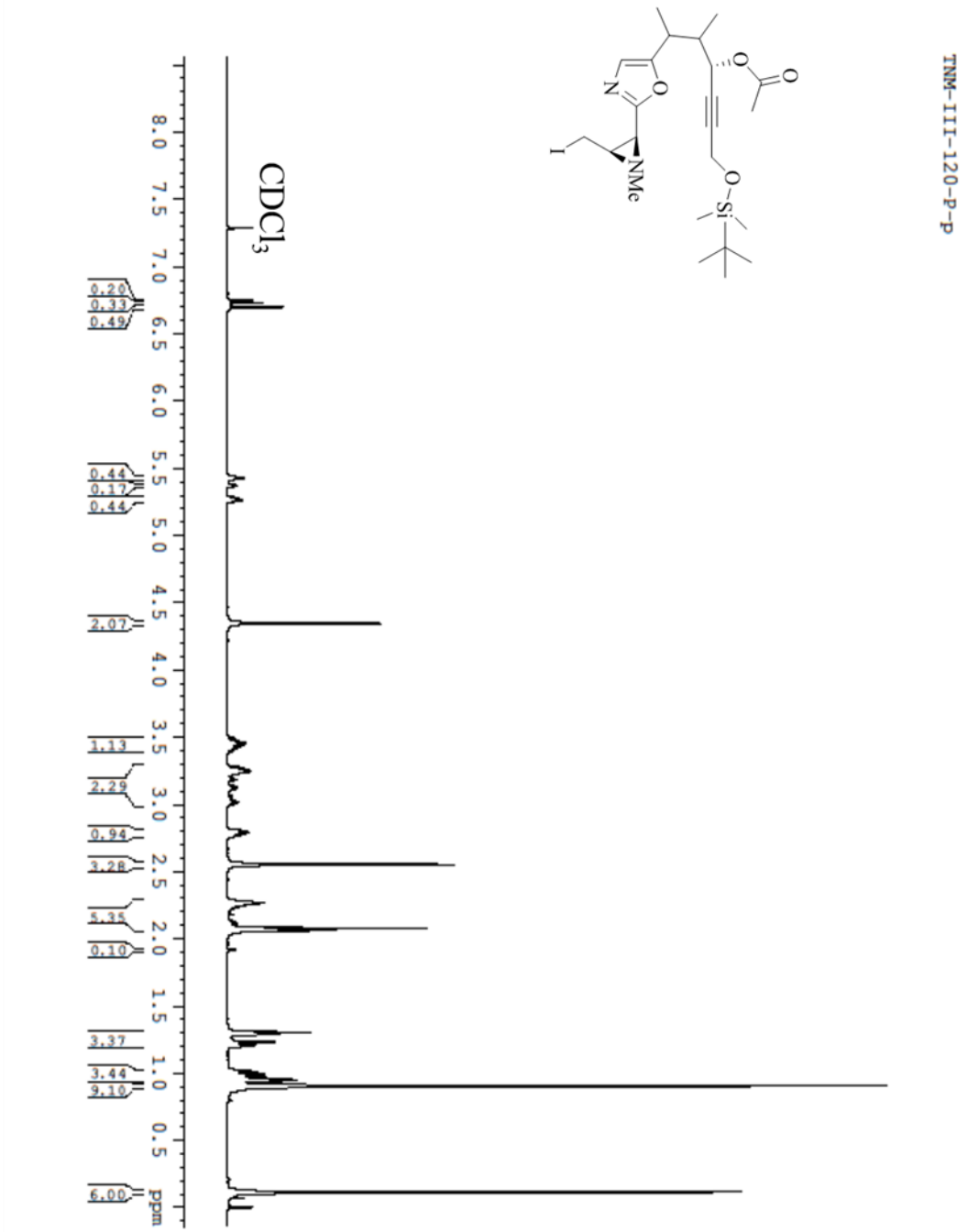

Figure A23. ^{1}H NMR spectrum of (2S,3R)-2-[5-[(1R,2R,3R), (1R,2R,3S), (1R,2S3R) ,((1S,2R,3R), (1S,2S,3S) (1R,2S,3S), (!R,2R,3S),(1S,2S,3R)-3-hydroxy-1,2-dimethyl-6-tert-butyldimethylsilyloxy-4-hexynyl]oxazol-2-yl]-3-iodomethyl-1-methylaziridine (47)

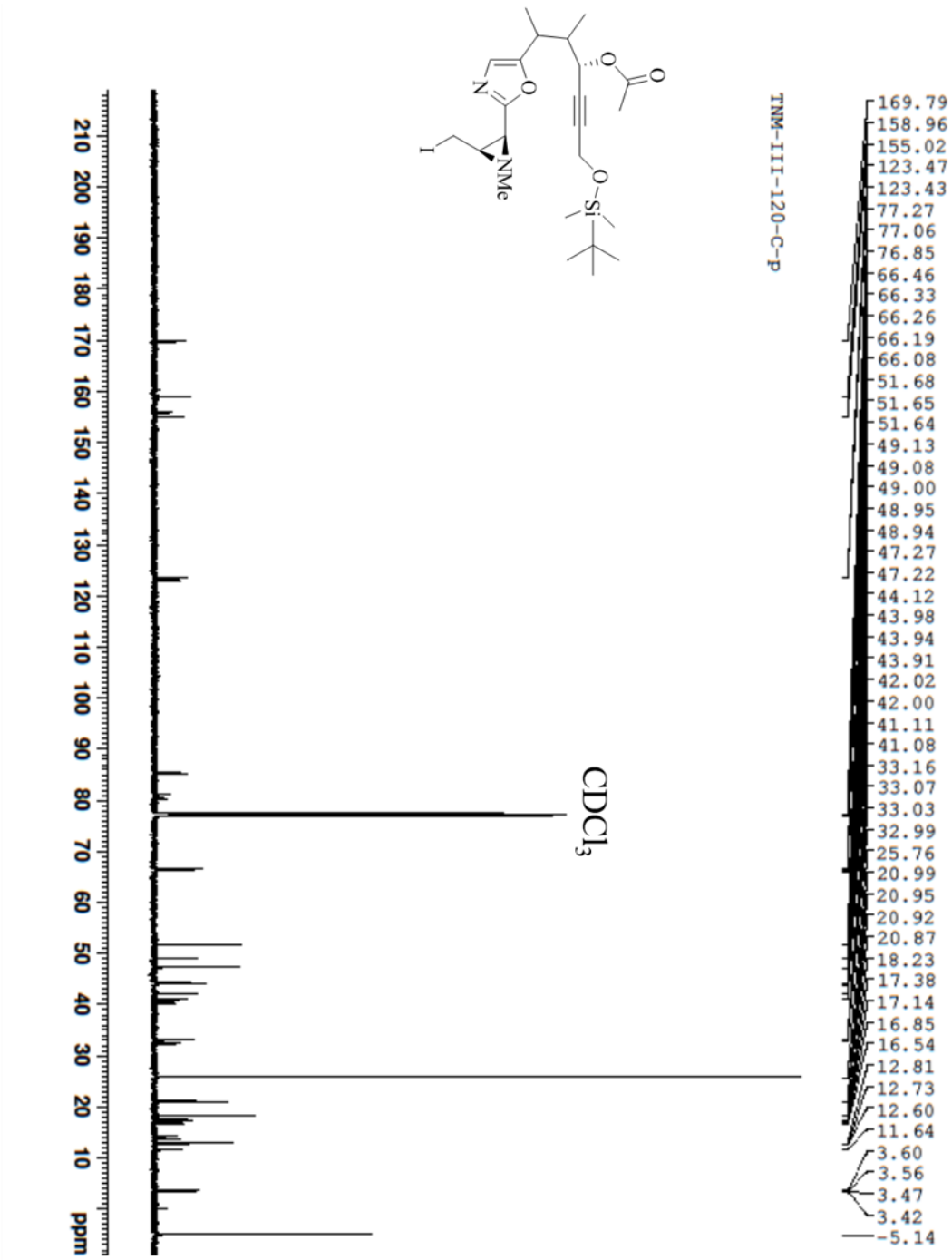

Figure A24. ^{13}C NMR spectrum of (2S,3R)-2-[5-[(1R,2R,3R), (1R,2R,3S), (1R,2S3R) ,((1S,2R,3R), (1S,2S,3S) (1R,2S,3S), (!R,2R,3S),(1S,2S,3R)-3-hydroxy-1,2-dimethyl-6-tert-butyldimethylsilyloxy-4-hexynyl]oxazol-2-yl]-3-iodomethyl-1-methylaziridine (47).

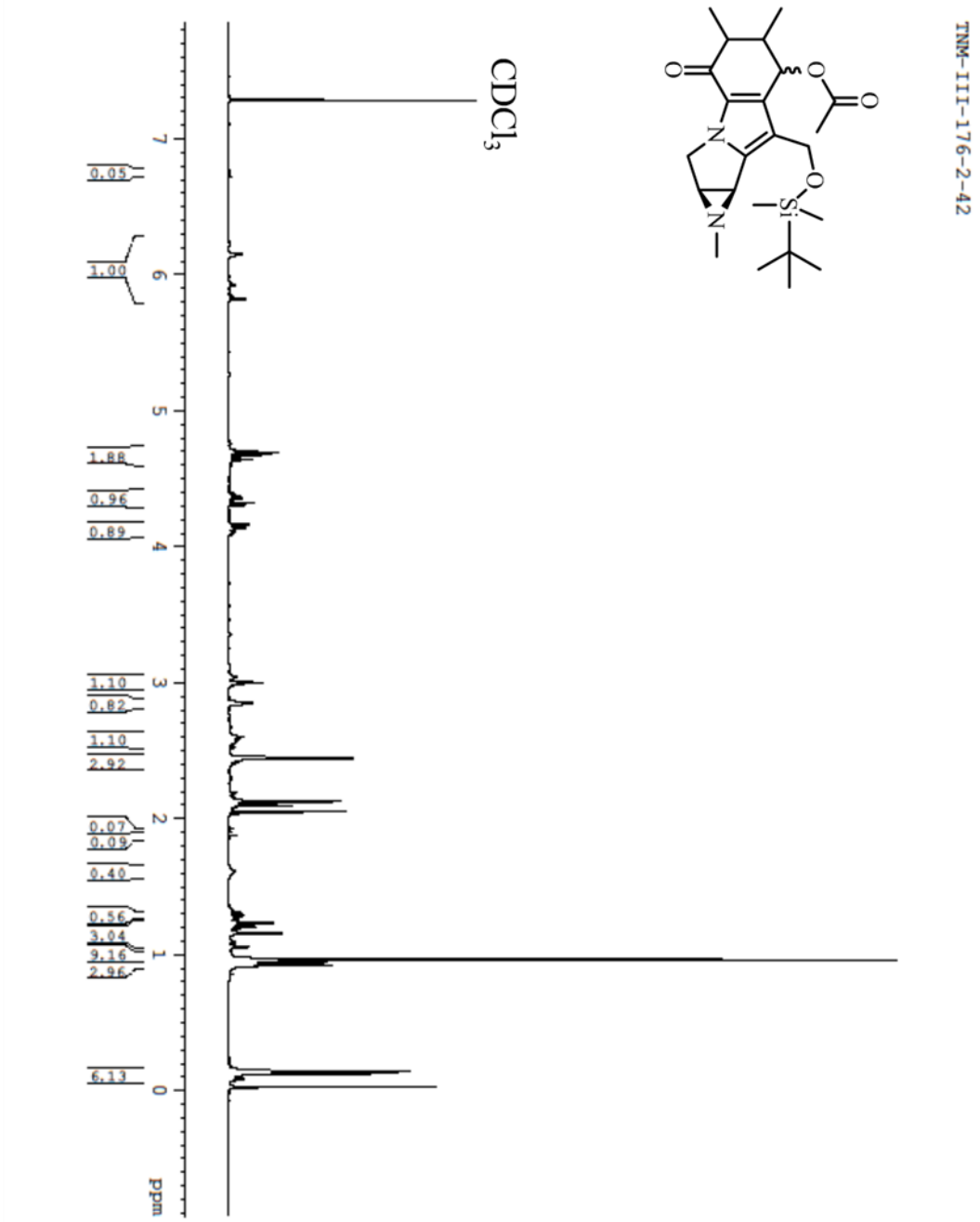

Figure A25. ^{1}H NMR spectrum of 2S,3R)-2-[5-[(1R,2R,3R), (1R,2R,3S), (1R,2S3R), ((1S,2R,3R), (1S,2S,3S) (1R,2S,3S), (1R,2R,3S),(1S,2S,3R)-3-Acetoxy-1,2-dimethyl-6-tert-butyldimethylsilyloxy-4-hexynyl]oxazol-2-yl]-3-iodomethyl-1-methylaziridine (48).

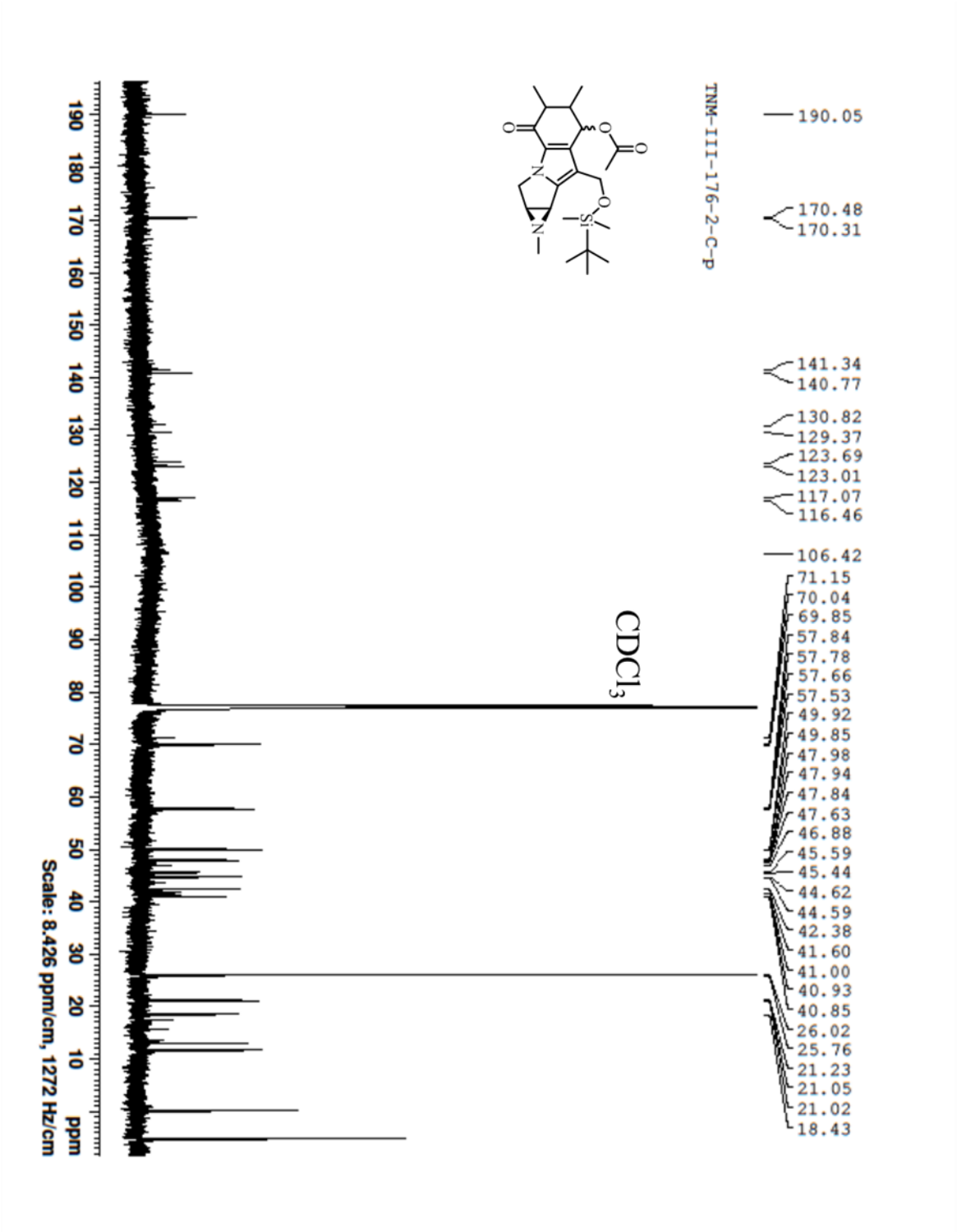

Figure A26. **^{13}C NMR spectrum of 2S,3R)-2-[5-[(1R,2R,3R), (1R,2R,3S), (1R,2S3R), ((1S,2R,3R), (1S,2S,3S) (1R,2S,3S), (1R,2R,3S),(1S,2S,3R)-3-Acetoxy-1,2-dimethyl-6-tert-butyldimethylsilyloxy-4-hexynyl]oxazol-2-yl]-3-iodomethyl-1-methylaziridine (48).**

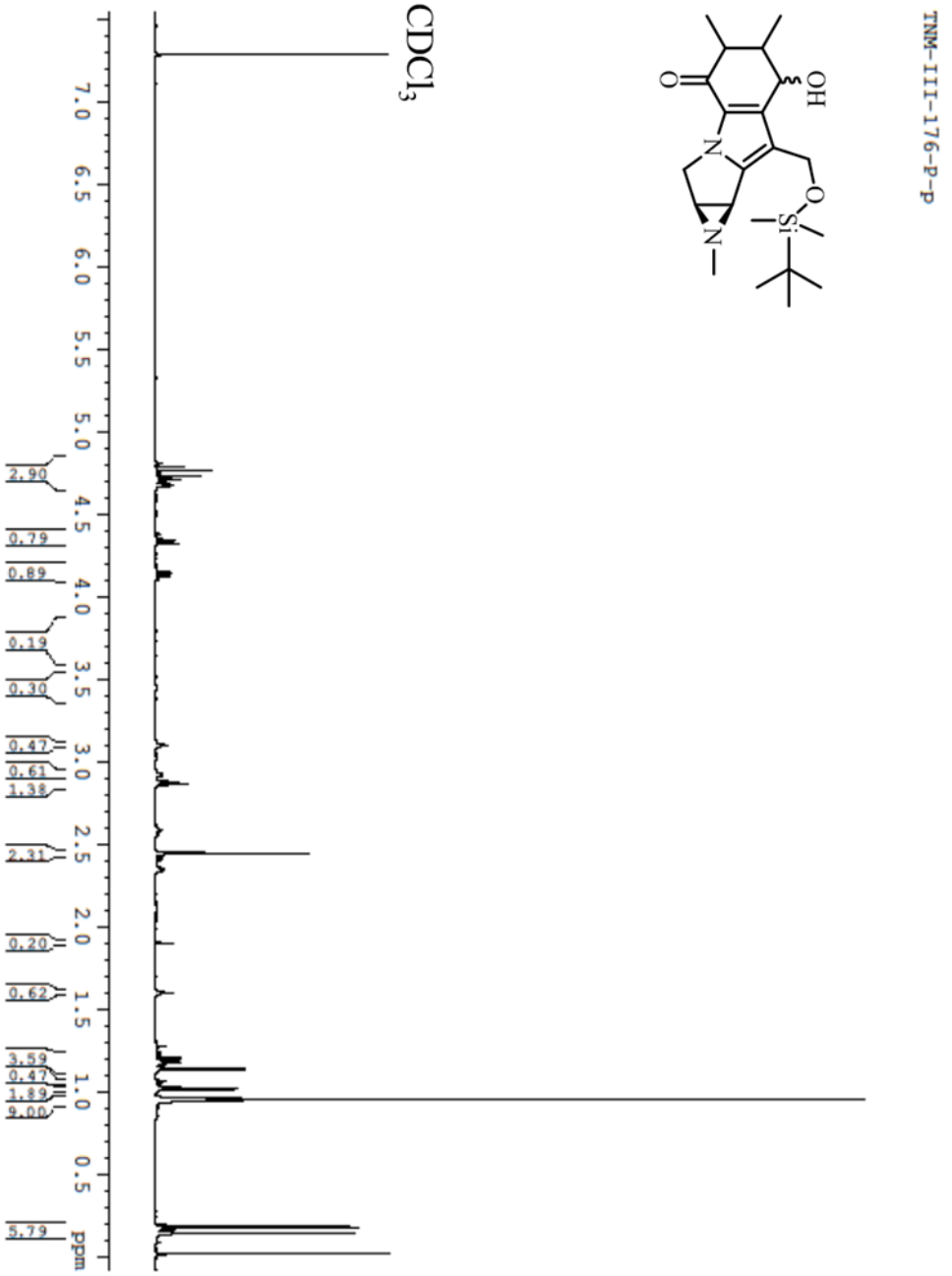

Figure A27. ^{1}H NMR spectrum of (1S,2S, -[(1R,2R,8R), (1R,2R,8S), (1R,2S,8R) ,((1S,2R,8R), (1S,2S,8S) (1R,2S,8S), (1R,2R,8S),(1S,2S,8R)-8-Acetoxy-9-(tert-butyldimethylsilyloxymethyl)-2,3,5,6,7,8-hexahydro-6,7-dimethyl-1,2-(N-methylaziridino)-5-oxo-1H-pyrrolo[1,2-a]indole (49).

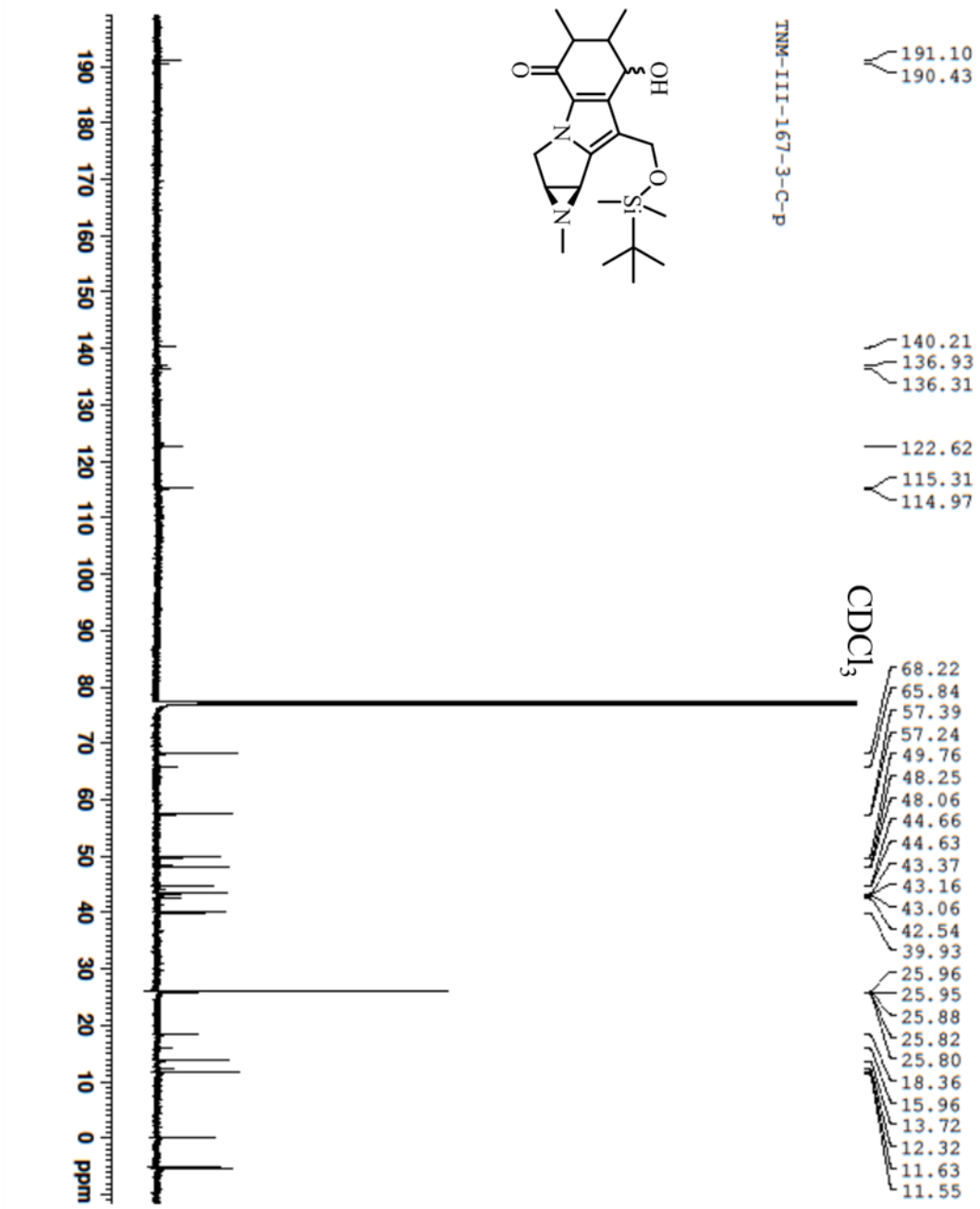

Figure A28. ^{13}C NMR spectrum of (1S,2S, -[(1R,2R,8R), (1R,2R,8S), (1R,2S,8R) ,((1S,2R,8R), (1S,2S,8S) (1R,2S,8S), (1R,2R,8S),(1S,2S,8R)-8-Acetoxy-9-(tert-butyldimethylsilyloxymethyl)-2,3,5,6,7,8-hexahydro-6,7-dimethyl-1,2-(N-methylaziridino)-5-oxo-1H-pyrrolo[1,2-a]indole (49).

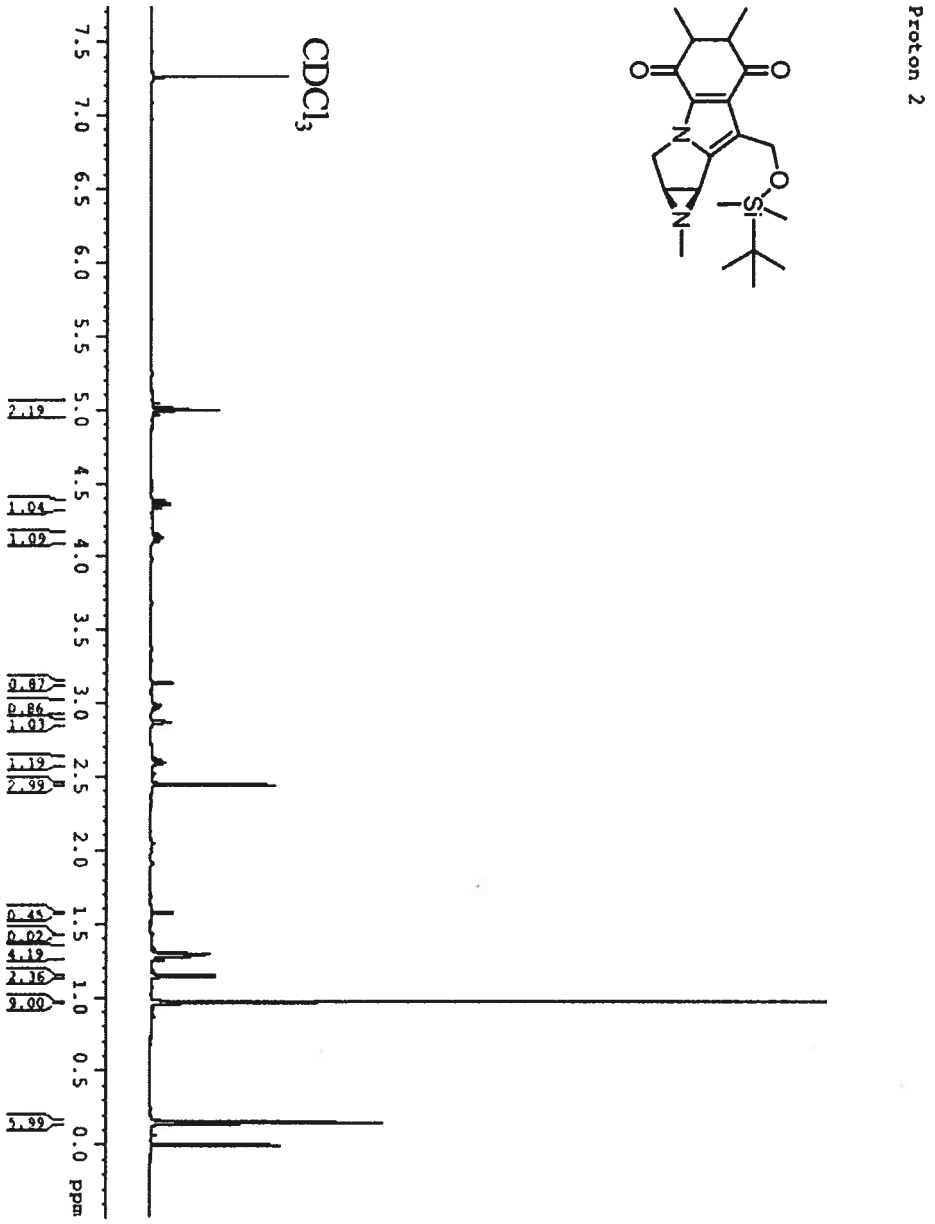

Figure A29. ^{1}H **NMR spectrum of (1S,2S,6S,7S) and (1S,2S,6R,7R) (1S,2S,6S,7R) and (1S,2S,6R,7S)-9-(tert-Butyldimethylsilyloxymethyl)-5,8-dioxo-2,3,5,6,7,8-hexahydro-6,7-dimethyl-1,2-(N-methylaziridino)-1H-pyrrolo[1,2-a]indole (51)**

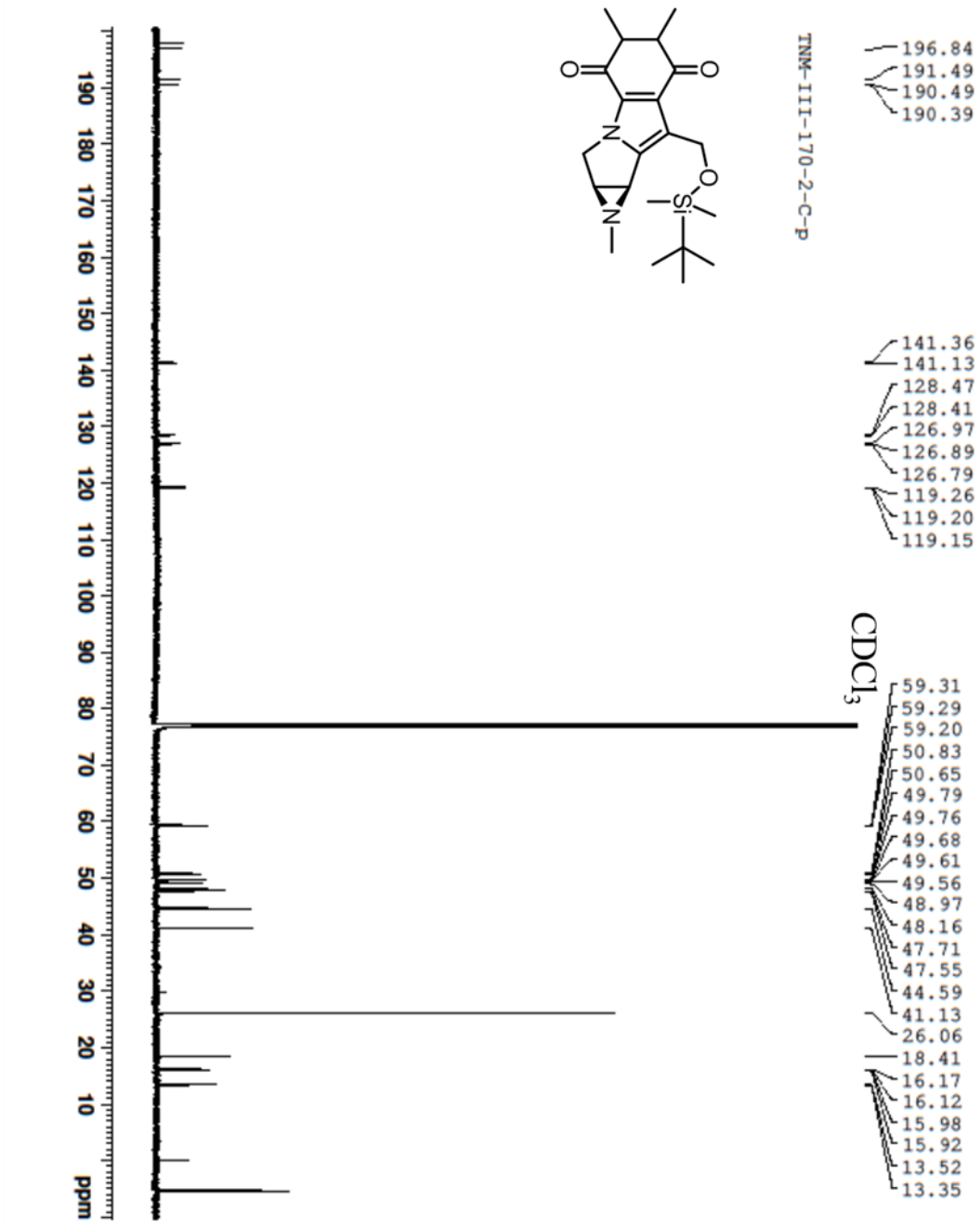

Figure A30. ^{3}C NMR spectrum of (1S,2S,6S,7S) and (1S,2S,6R,7R) (1S,2S,6S,7R) and (1S,2S,6R,7S)-9-(tert-Butyldimethylsilyloxymethyl)-5,8-dioxo-2,3,5,6,7,8-hexahydro-6,7-dimethyl-1,2-(N-methylaziridino)-1H-pyrrolo[1,2-a]indole (51)

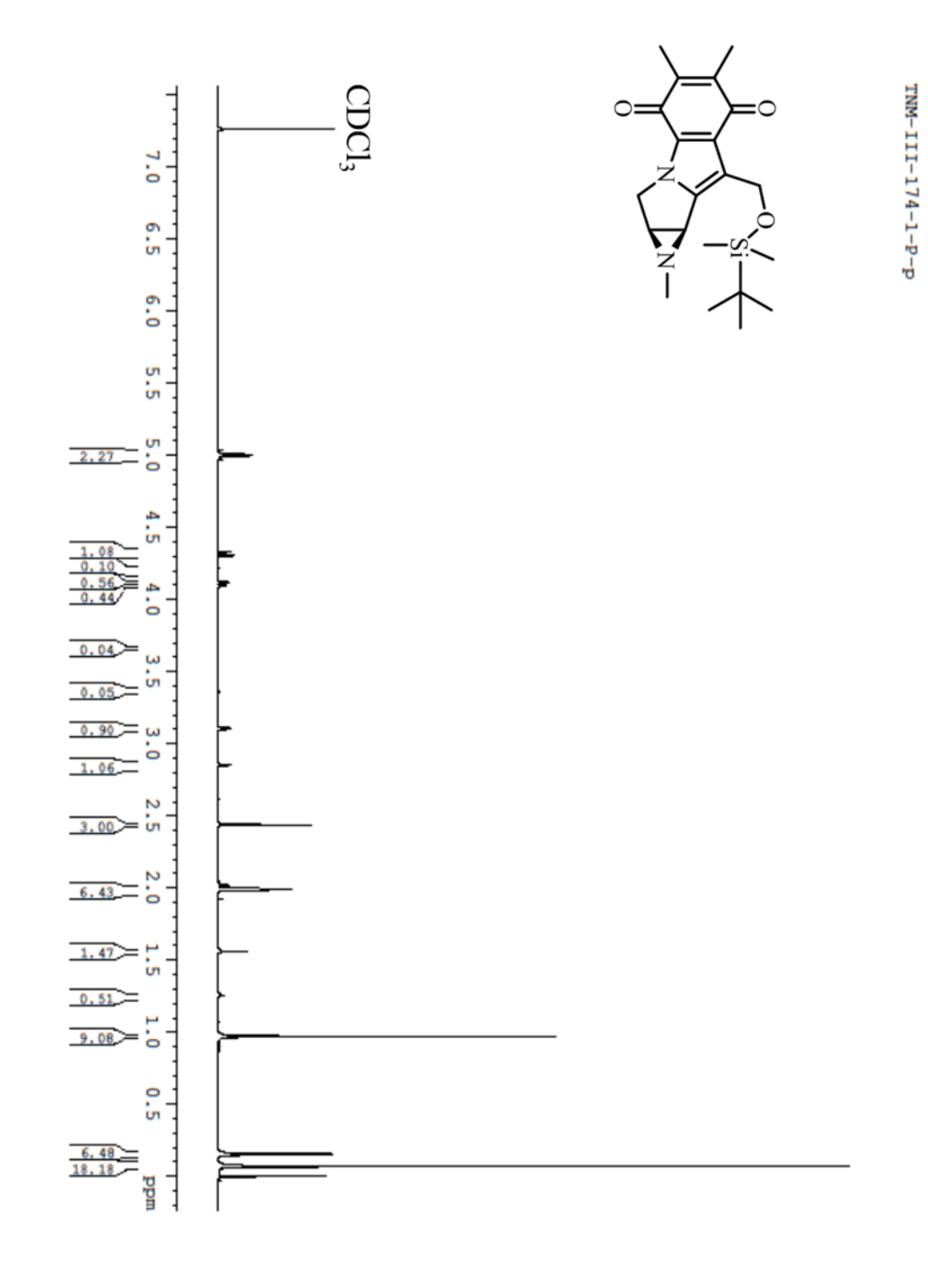

Figure A31. ^{1}H NMR spectrum of (1S,2S)-9-(tert-Butyldimethylsilyloxymethyl)-2,3-dihydro-6,7-dimethyl-1,2-(N-methylaziridino)-1H-pyrrolo[1,2-a]indole-5,8-dione (52).

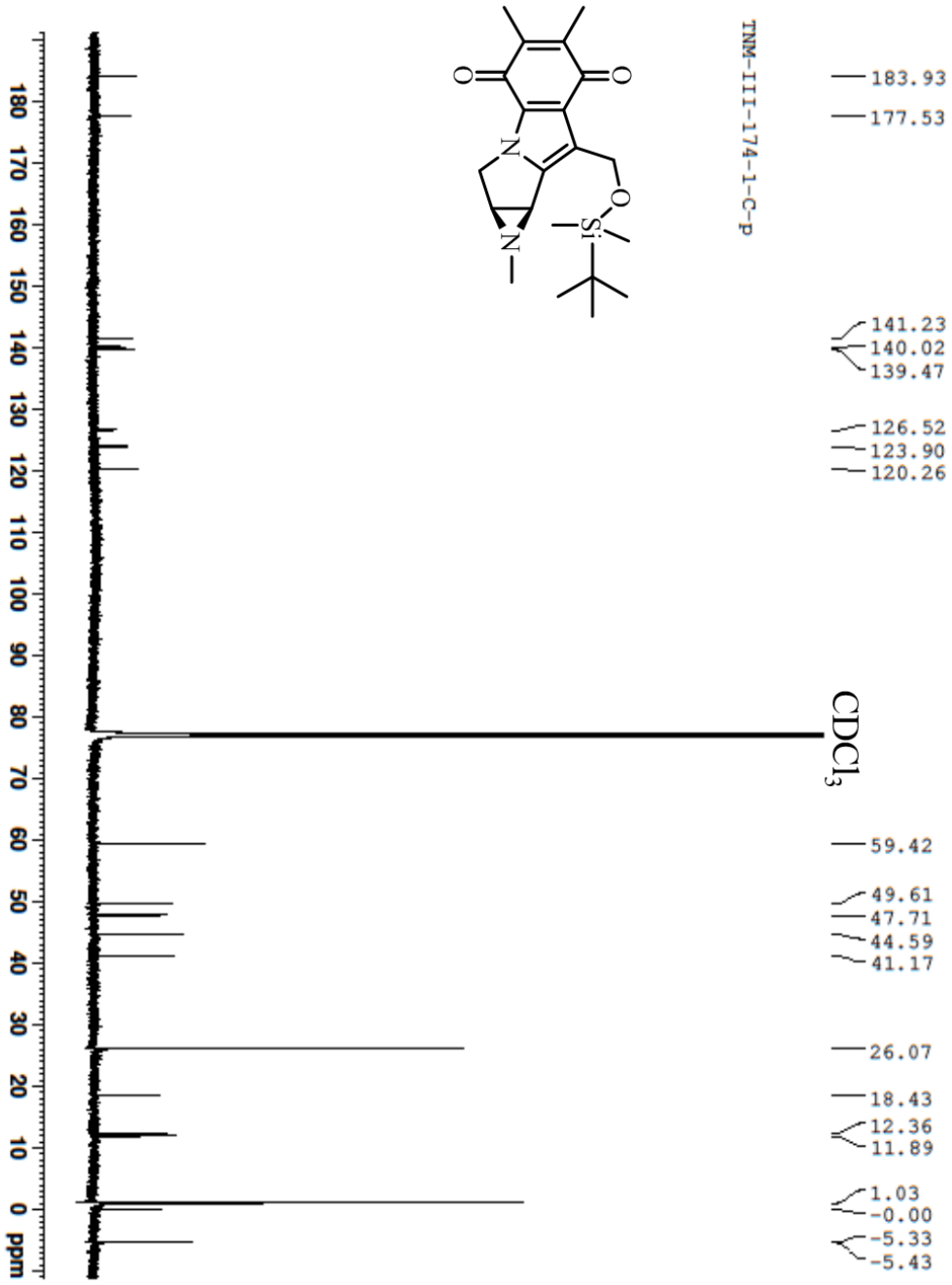

Figure A32. ^{13}C NMR spectrum of (1S,2S)-9-(tert-Butyldimethylsilyloxymethyl)-2,3-dihydro-6,7-dimethyl-1,2-(N-methylaziridino)-1H-pyrrolo[1,2-a]indole-5,8-dione (52).

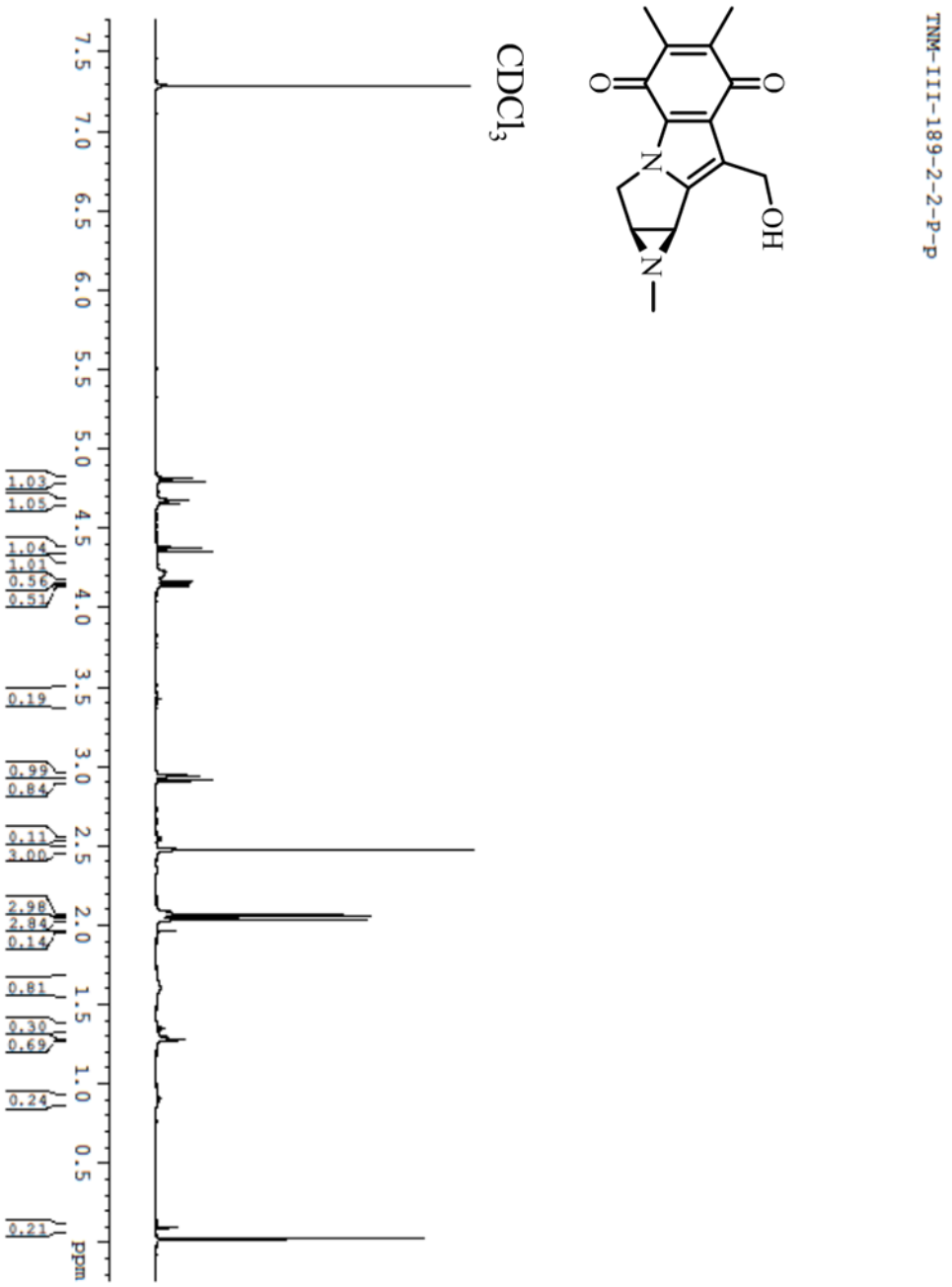

Figure A33. ^{1}H NMR spectrum of (1S,2S)-2,3-Dihydro-9-hydroxymethyl-6,7-dimethyl-1,2-(N-methylaziridino)-1H-pyrrolo[1,2-a]indole-5,8-dione (53).

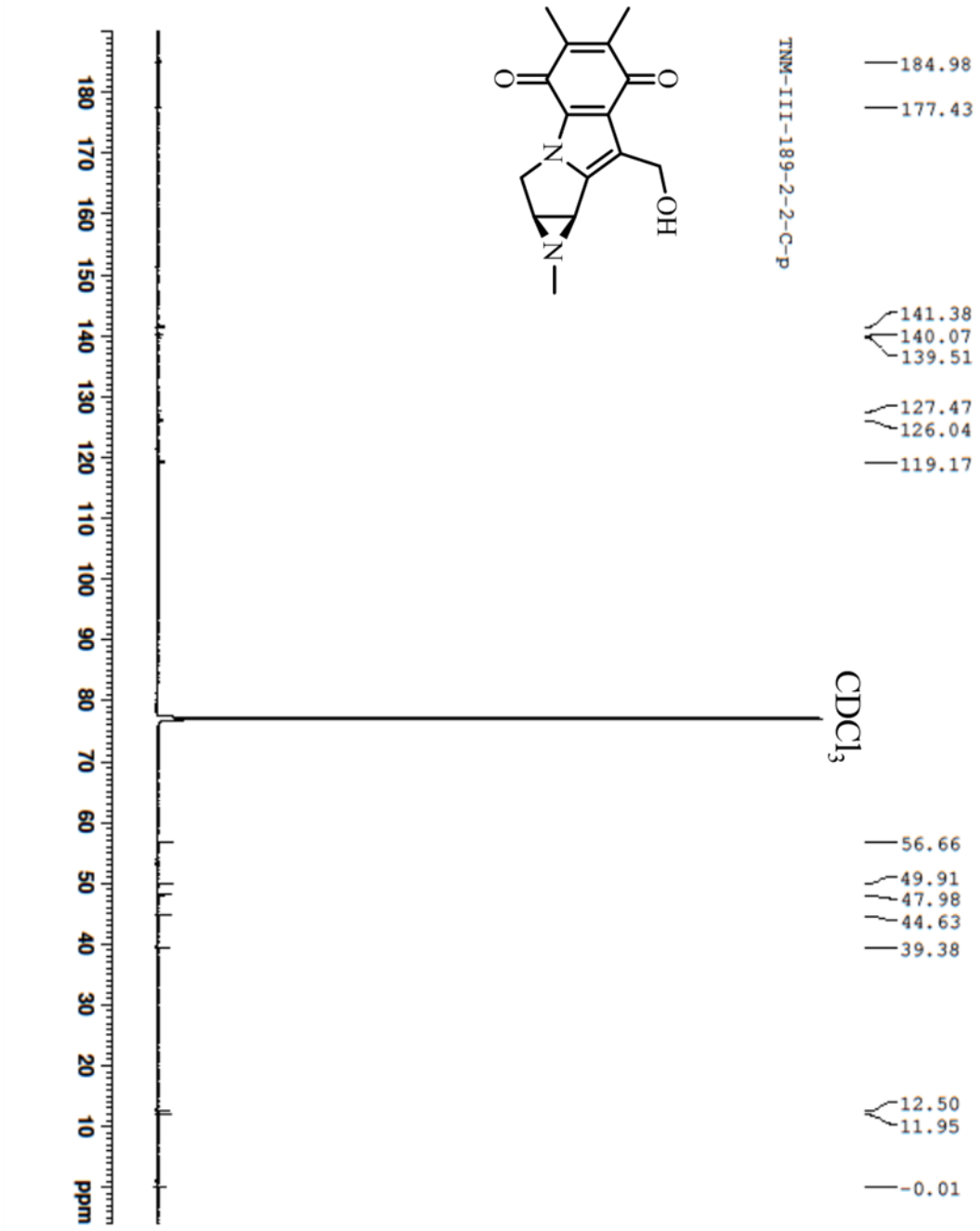

Figure A34. ^{13}**C NMR spectrum of (1S,2S)-2,3-Dihydro-9-hydroxymethyl-6,7-dimethyl-1,2-(N-methylaziridino)-1H-pyrrolo[1,2-a]indole-5,8-dione (53).**

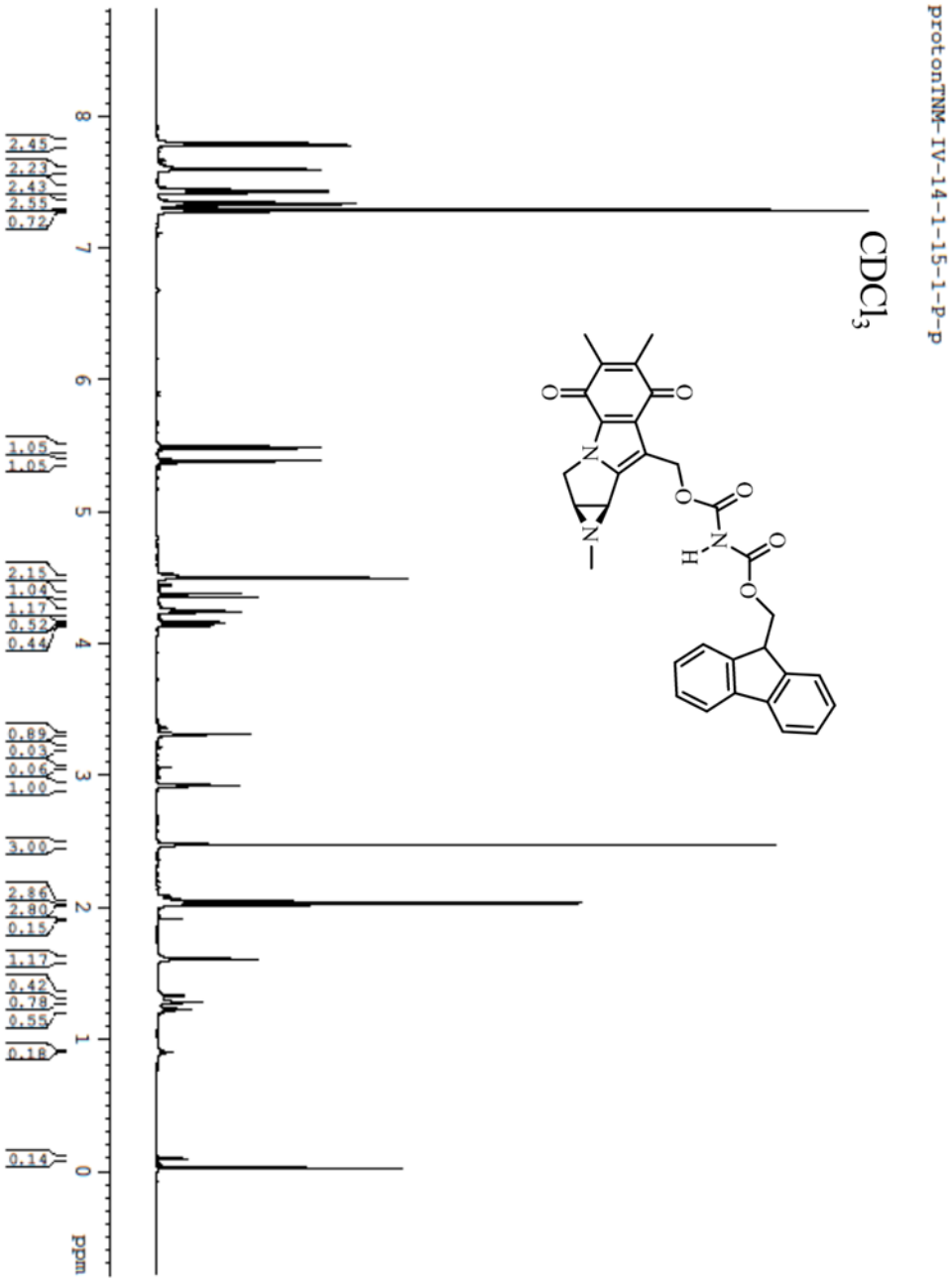

Figure A35. ^{1}H NMR spectrum of (1S,2S)-2,3-Dihydro-9-{9-fluorenylmethoxycarbonylcarbamoyloxymethyl)-6,7-dimethyl-1,2-(N-methylaziridino)-1H-pyrrolo[1,2-a]indole-5,8-dione (54).

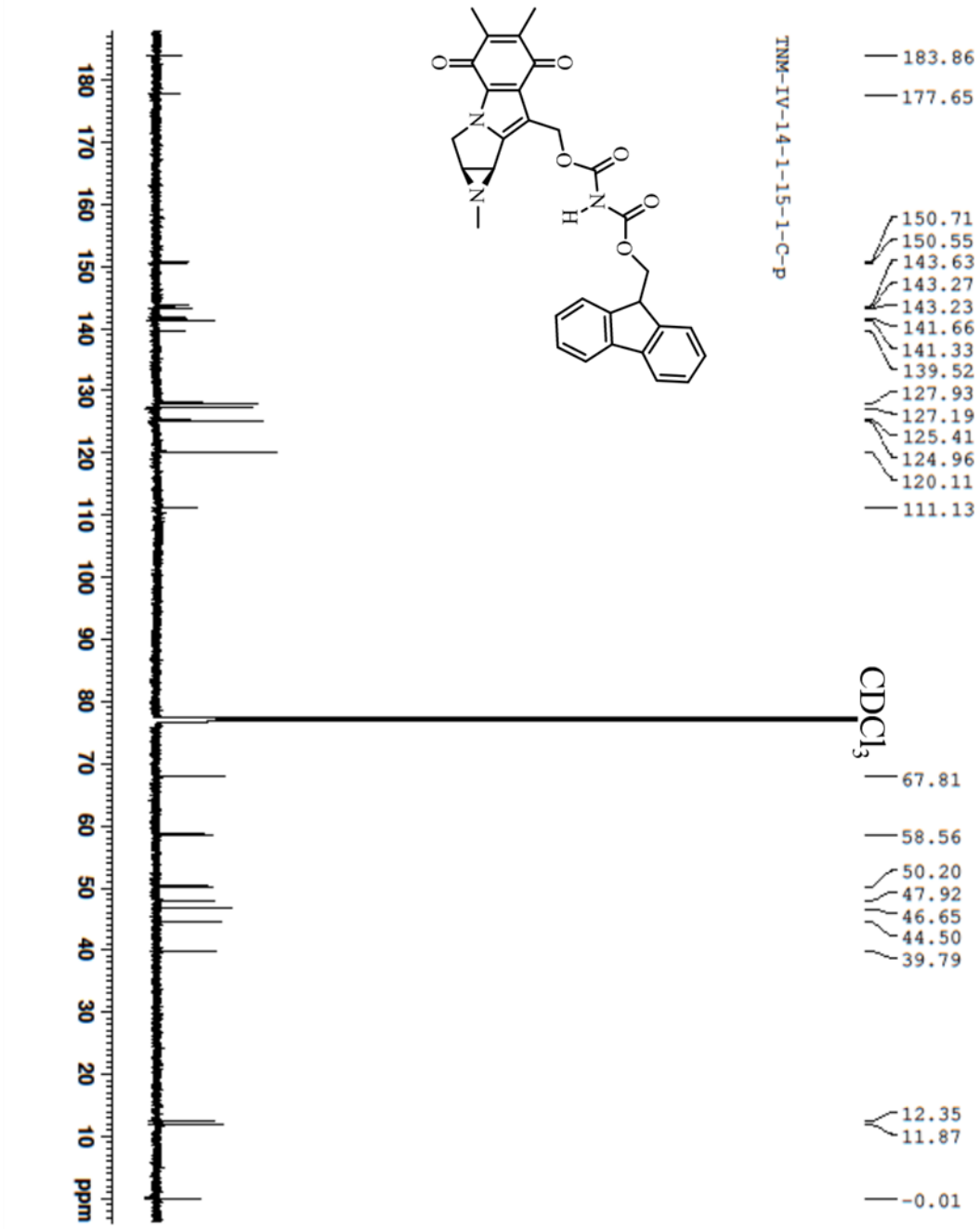

Figure A36. ^{13}C NMR spectrum of (1S,2S)-2,3-Dihydro-9-{9-fluorenylmethoxycarbonylcarbamoyloxymethyl)-6,7-dimethyl-1,2-(N-methylaziridino)-1H-pyrrolo[1,2-a]indole-5,8-dione (54).

Figure A4. ^{13}C NMR spectrum of

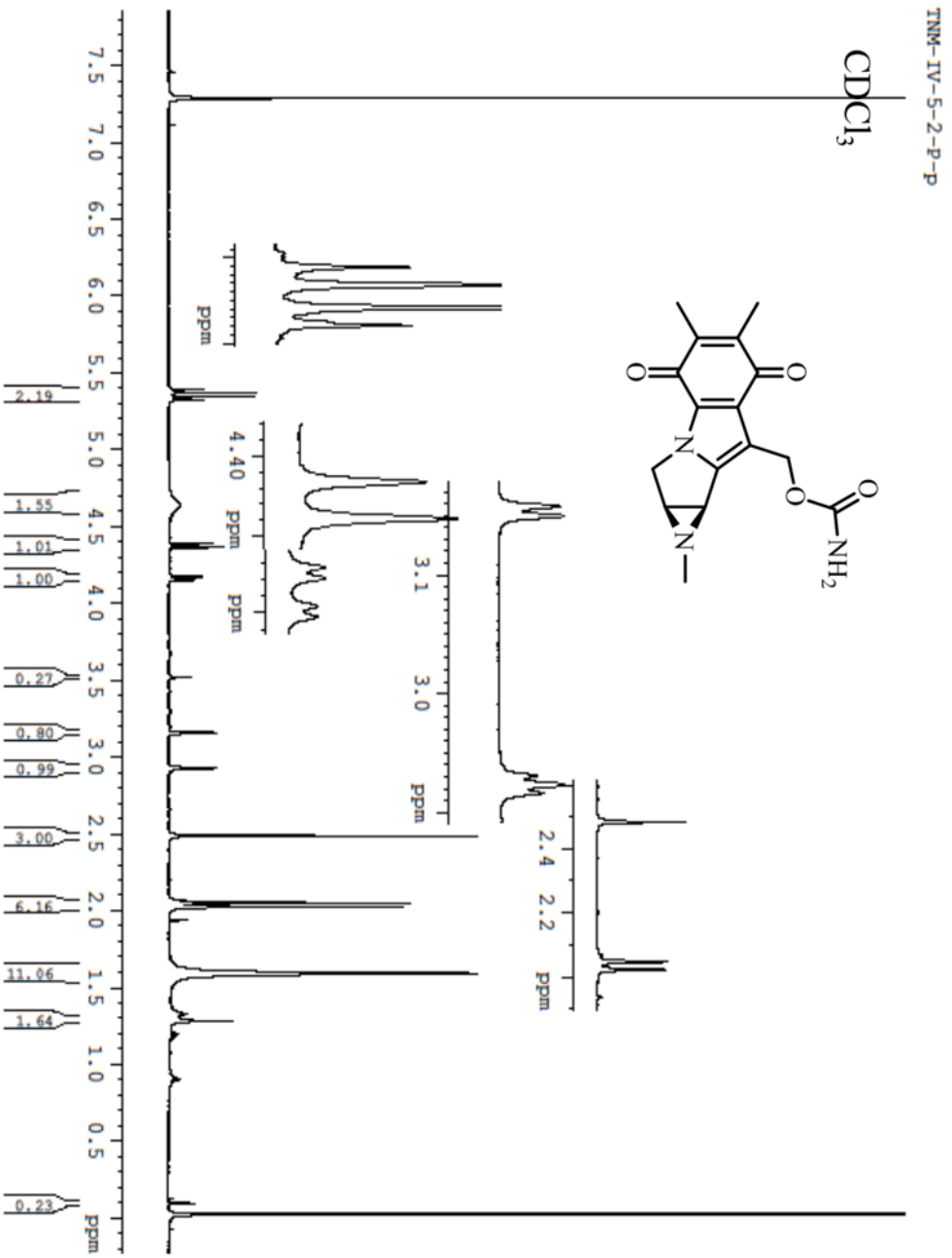

Figure A37. ^{1}H NMR spectrum of (1S,2S)-9-Carbamoyloxymethyl-2,3-dihydro-6-methyl-1,2-(N methylaziridino)-1H-pyrrolo[1,2-a]indole-5,8-dione (3).

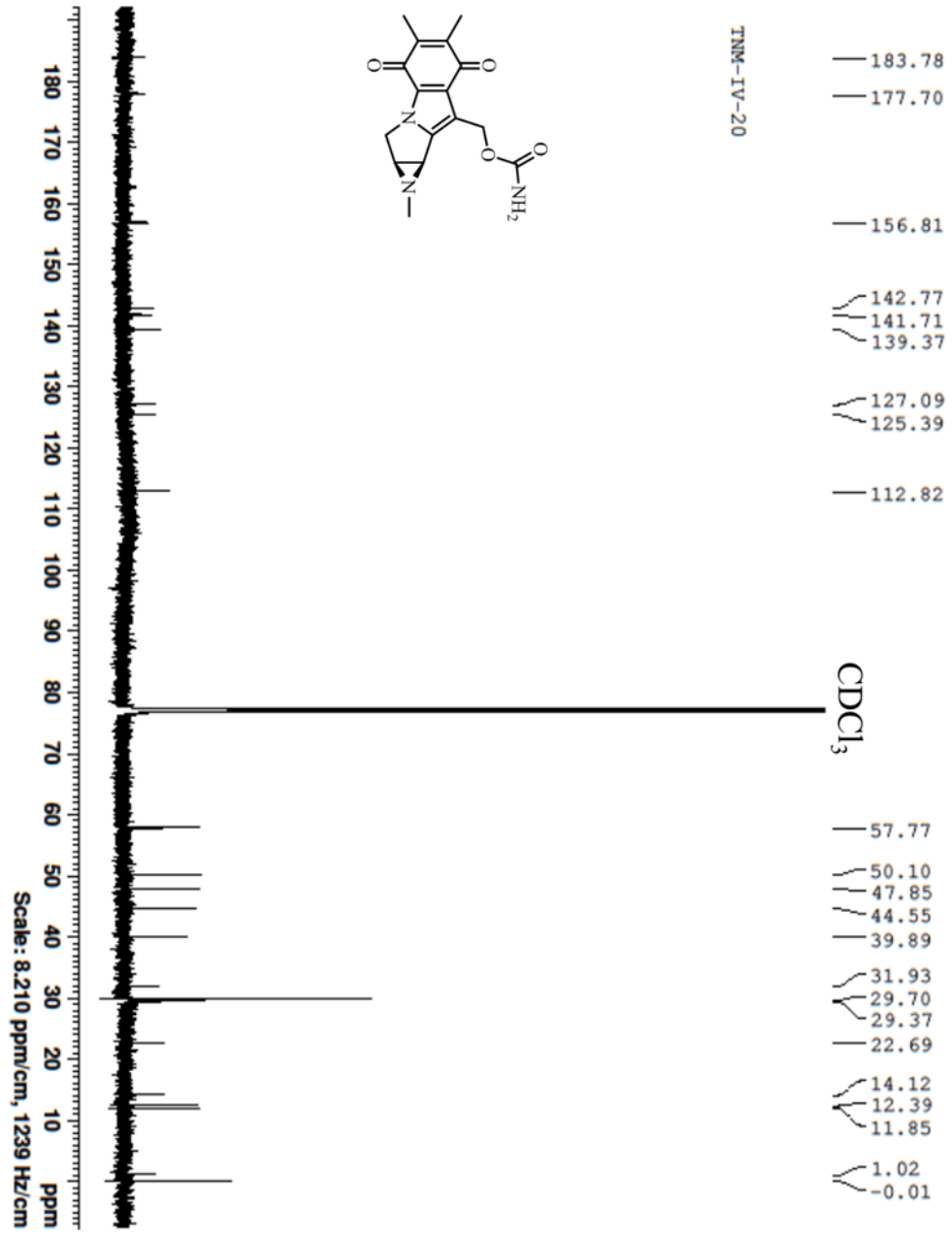

Figure A38. **^{13}C NMR spectrum of (1S,2S)-9-Carbamoyloxymethyl-2,3-dihydro-6-methyl-1,2-(N methylaziridino)-1H-pyrrolo[1,2-a]indole-5,8-dione (3).**

APPENDIX B

UV Spectra

Figure Number	Methanolysis of Aziridinomitosene **3**	Page Number
B1……..	UV-Vis spectrum of Methanolysis of AZM **3** at pH 6.0 over 4500 Minutes	113
B2……..	UV-Vis spectrum of methanolysis of AZM **3** at pH 7.0 over 4500 Minutes	114
B3……..	UV-Vis absorbance at 480 nm over 4500 minutes (methanolysis of AZM **3** at pH 7.0)	115
B4……..	UV-Vis spectrum of methanolysis of AZM **3** at pH 8.7 over 300 Minutes	116

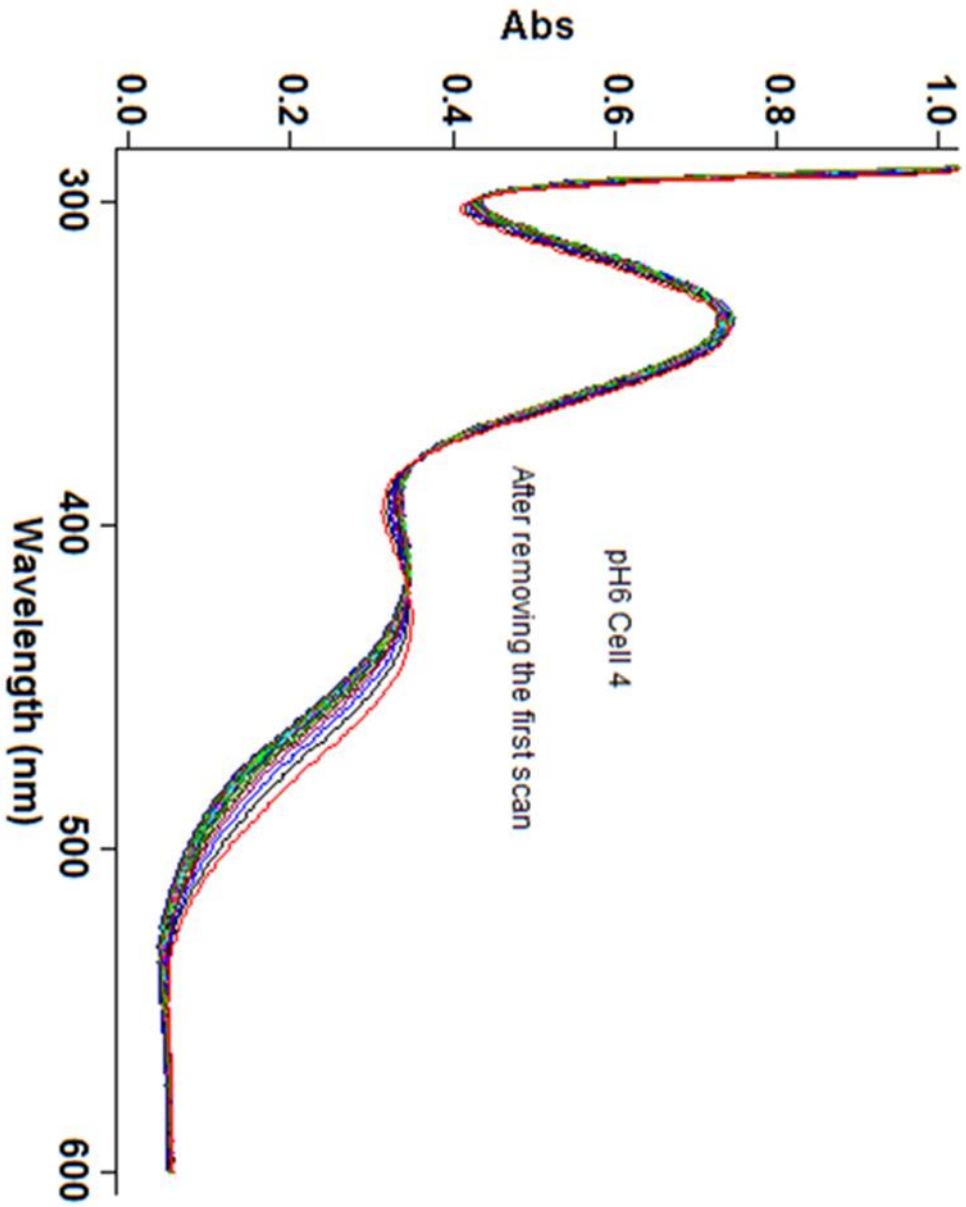

Figure B1. UV-Vis spectrum of Methanolysis of AZM 3 at pH 6.0 over 4500 Minutes

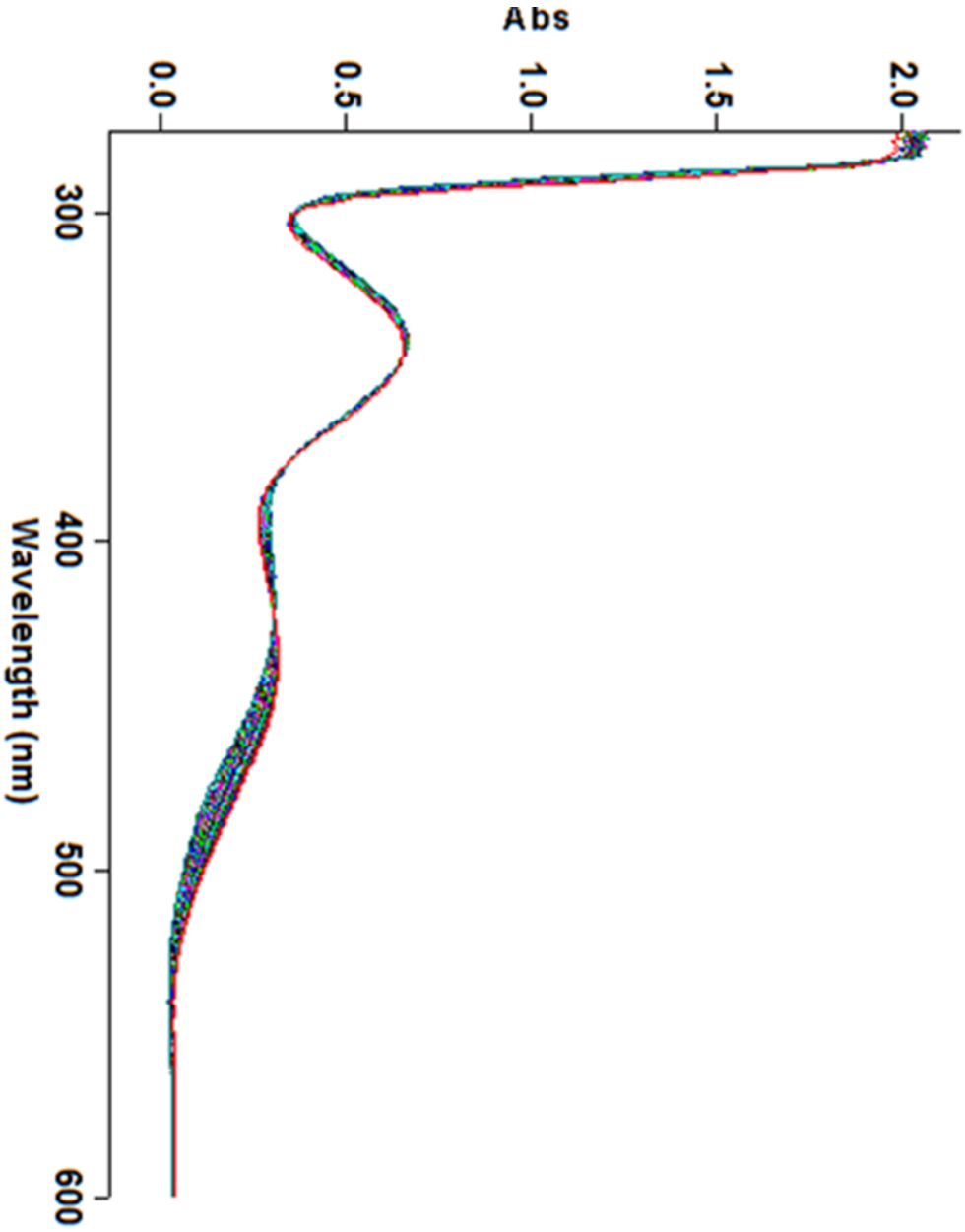

Figure B2. UV-Vis spectrum of methanolysis of AZM 3 at pH 7.0 over 4500 Minutes

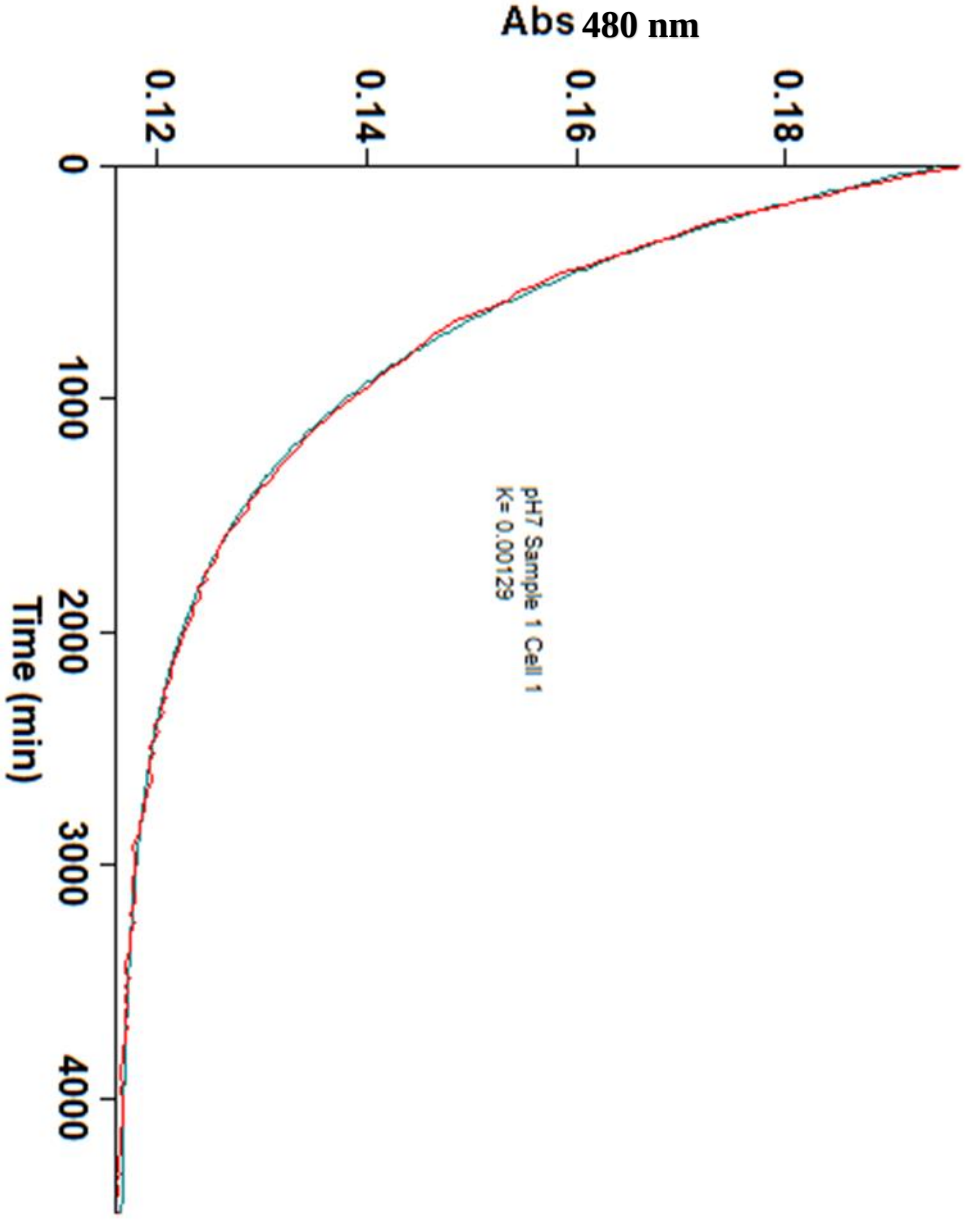

Figure B3. UV-Vis absorbance at 480 nm over 4500 minutes (methanolysis of AZM 3 at pH 7.0)

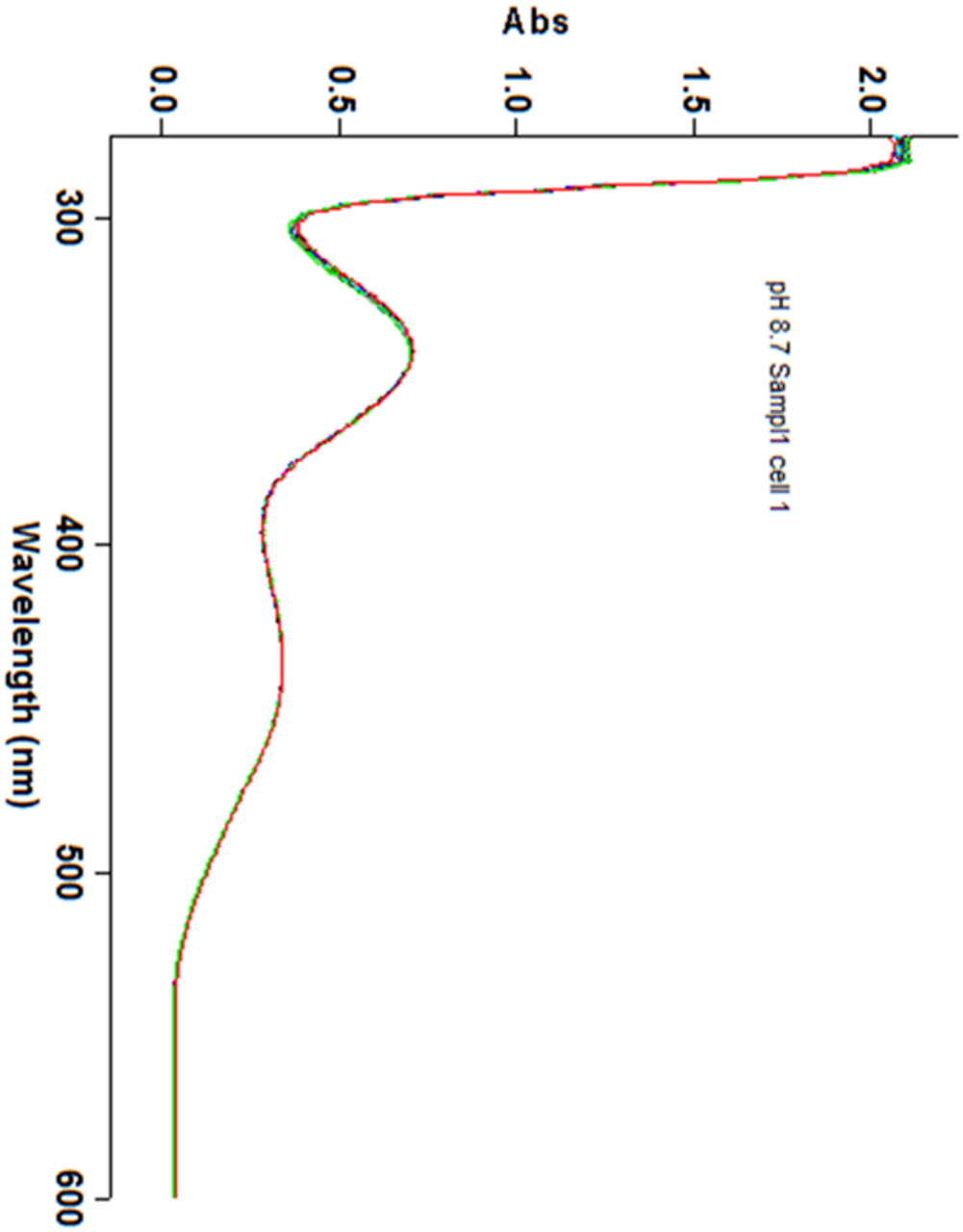

Figure B4. UV-Vis spectrum of methanolysis of AZM 3 at pH 8.7 over 300 Minutes